TECHNICAL REPORT STANDARD TITLE PAGE

1. Report No.	2. Government Accession No.	3. Recipient's Catalog No.
FHWA/TX-87/461-1F		

4. Title and Subtitle	5. Report Date
DEVELOPMENT OF GUARDRAIL TO BRIDGE RAIL TRANSITION	June 1988
	6. Performing Organization Code

7. Author(s)	8. Performing Organization Report No.
Roger P. Bligh, Dean L. Sicking, & Hayes E. Ross, Jr.	Research Report 461-1F

9. Performing Organization Name and Address	10. Work Unit No.
Texas Transportation Institute Texas A&M University System College Station, Texas 77843	11. Contract or Grant No. Research Study 2-8-86-461
	13. Type of Report and Period Covered
12. Sponsoring Agency Name and Address Texas State Department of Highways and Public Transportation Transportation Planning Division P. O. Box 5051, Austin, Texas 78763	Final Report Sept. 1985 - August 1987
	14. Sponsoring Agency Code

15. Supplementary Notes

Research performed in cooperation with DOT, FHWA.

16. Abstract

This report describes the development and testing of a guardfence-to-rigid bridge rail transition. The transition consists of a tubular W-beam supported on 7 inch diameter round wood posts. It is designed to transition to a vertical wall or to the concrete safety shaped barrier. It can be used on new construction or as a retrofit for existing installations. Based on a full-scale vehicular crash test program, the design was judged to be in compliance with recommended impact performance criteria as presented in NCHRP Report 230.

Also described is a tentative design for approach guardfence at bridge ends near an abutting roadway. The design consists of short radius, curved guardrail supported on weakened round wood posts. Tubular W-beam and nested W-beam elements were examined and both appear to offer acceptable performance for a design impact speed of approximately 40 mph.

17. Key Words	18. Distribution Statement
Bridge Rail, Approach Rail, Guardrail, Transition, Computer Simulation, Crash Tests	No restriction. This document is available to the public through the National Technical Information Service 5285 Port Royal Road. Springfield, Virginia 22161

19. Security Classif. (of this report)	20. Security Classif. (of this page)	21. No. of Pages	22. Price
Unclassified	Unclassified	131	

Form DOT F 1700.7 (8-69)

DEVELOPMENT OF GUARDRAIL TO BRIDGE RAIL TRANSITION

by

Roger P. Bligh
Engineering Research Associate

Dean L. Sicking
Assistant Research Engineer

and

Hayes E. Ross, Jr.
Research Engineer

Research Report 461-1F

on

Research Study No. 2-8-86-461
Guardrail / Bridge Rail Transitions

Sponsored by

Texas State Department of Highways and Public Transportation

in cooperation with

The U.S. Department of Transportation
Federal Highway Administration

June 1988

Texas Transportation Institute
Texas A&M University
College Station, Texas

METRIC CONVERSION FACTORS

Approximate Conversions to Metric Measures

Symbol	When You Know	Multiply by	To Find	Symbol
		LENGTH		
in	inches	*2.5	centimeters	cm
ft	feet	30	centimeters	cm
yd	yards	0.9	meters	m
mi	miles	1.6	kilometers	km
		AREA		
in^2	square inches	6.5	square centimeters	cm^2
ft^2	square feet	0.09	square meters	m^2
yd^2	square yards	0.8	square meters	m^2
mi^2	square miles	2.6	square kilometers	km^2
	acres	0.4	hectares	ha
		MASS (weight)		
oz	ounces	28	grams	g
lb	pounds	0.45	kilograms	kg
	short tons (2000 lb)	0.9	tonnes	t
		VOLUME		
tsp	teaspoons	5	milliliters	ml
Tbsp	tablespoons	15	milliliters	ml
fl oz	fluid ounces	30	milliliters	ml
c	cups	0.24	liters	l
pt	pints	0.47	liters	l
qt	quarts	0.95	liters	l
gal	gallons	3.8	liters	l
ft^3	cubic feet	0.03	cubic meters	m^3
yd^3	cubic yards	0.76	cubic meters	m^3
		TEMPERATURE (exact)		
°F	Fahrenheit temperature	5/9 (after subtracting 32)	Celsius temperature	°C

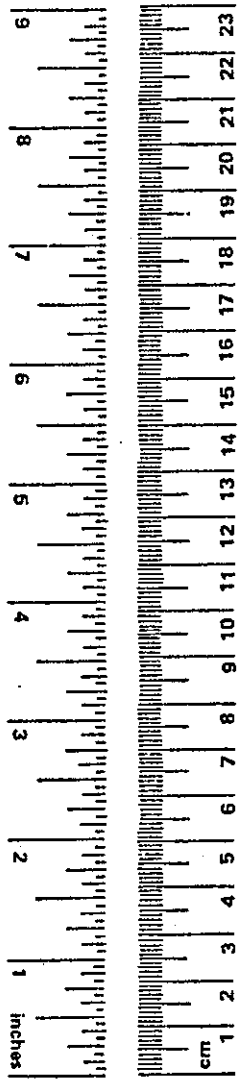

*1 in = 2.54 (exactly). For other exact conversions and more detailed tables, see NBS Misc. Publ. 286, Units of Weights and Measures, Price $2.25, SD Catalog No. C13.10:286.

Approximate Conversions from Metric Measures

Symbol	When You Know	Multiply by	To Find	Symbol
		LENGTH		
mm	millimeters	0.04	inches	in
cm	centimeters	0.4	inches	in
m	meters	3.3	feet	ft
m	meters	1.1	yards	yd
km	kilometers	0.6	miles	mi
		AREA		
cm^2	square centimeters	0.16	square inches	in^2
m^2	square meters	1.2	square yards	yd^2
km^2	square kilometers	0.4	square miles	mi^2
ha	hectares (10,000 m^2)	2.5	acres	
		MASS (weight)		
g	grams	0.035	ounces	oz
kg	kilograms	2.2	pounds	lb
t	tonnes (1000 kg)	1.1	short tons	
		VOLUME		
ml	milliliters	0.03	fluid ounces	fl oz
l	liters	2.1	pints	pt
l	liters	1.06	quarts	qt
l	liters	0.26	gallons	gal
m^3	cubic meters	35	cubic feet	ft^3
m^3	cubic meters	1.3	cubic yards	yd^3
		TEMPERATURE (exact)		
°C	Celsius temperature	9/5 (then add 32)	Fahrenheit temperature	°F

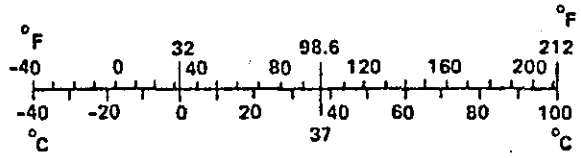

DISCLAIMER

The contents of this report reflect the views of the authors who are responsible for the opinions, findings, and conclusions presented herein. The contents do not necessarily reflect the official views or policies of the Texas State Department of Highways and Public Transportation or the Federal Highway Administration. This report does not constitute a standard, specification, or regulation.

KEY WORDS

Bridge Rail, Approach Rail, Guardrail, Transition, Computer Simulation, Crash Tests

ACKNOWLEDGEMENTS

This research study was conducted under a cooperative program between the Texas Transportation Institute (TTI), the Texas State Department of Highways and Public Transportation (SDHPT), and the Federal Highway Administration (FHWA). John Panak, Harold Cooner, and Mark Marek of the SDHPT worked closely with the researchers and provided valuable input to this study. The authors are very appreciative of their comments and suggestions.

IMPLEMENTATION STATEMENT

The tubular W-beam transition developed in this study is recommended for immediate incorporation into the SDHPT standard specifications. Field performance of the new design should be monitored to identify any potential problems with construction or safety performance.

The short-radius guardrail treatment utilizing a nested W-beam guardrail is recommended for immediate incorporation at sites where low speeds and traffic volumes warrant such a design.

ABSTRACT

This report describes the development and testing of a guardfence-to-rigid bridge rail transition. The transition consists of a tubular W-beam supported on 7 inch diameter round wood posts. It is designed to transition to a vertical wall or to the concrete safety shaped barrier. It can be used on new construction or as a retrofit for existing installations. Based on a full-scale vehicular crash test program, the design was judged to be in compliance with recommended impact performance criteria as presented in NCHRP Report 230.

Also described is a tentative design for approach guardfence at bridge ends near an abutting roadway. The design consists of short radius, curved guardrail supported on weakened round wood posts. Tubular W-beam and nested W-beam elements were examined and both appear to offer acceptable performance for a design impact speed of approximately 40 mph.

TABLE OF CONTENTS

LIST OF FIGURES

LIST OF TABLES

I. INTRODUCTION AND OBJECTIVES

A bridge rail is a longitudinal barrier whose primary function is to prevent errant vehicles from going over the side of the bridge. Most bridge rails are of either rigid or semi-rigid construction in order to limit dynamic deflections during impact. This prevents the wheels of the impacting vehicle from falling between the bridge rail and the edge of the bridge deck, and allows the vehicle to be safely contained and redirected. The most common types of bridge rails are reinforced concrete walls or metal rails on concrete parapets. In recent years, the concrete safety shaped barrier (CSSB) has been used on a large percentage of new bridges. A major problem associated with the use of the CSSB and other rigid bridge rails is the manner in which they are terminated. If left untreated, the exposed ends of these bridge rails present a serious safety hazard.

In most instances, an approach roadside barrier is used to shield the exposed bridge end and to prevent errant vehicles from getting behind the bridge and encountering underlying hazards. These approach guardrails are typically much more flexible than the bridge rails or parapets to which they are attached. The more flexible system is believed to induce fewer injuries and is far less costly than a rigid barrier system. However, these flexible barriers can deflect sufficiently to allow an errant vehicle to impact or "snag" on the end of the rigid barrier, even when the two barriers are securely attached. Therefore, a transition section is required whenever there is a significant change in lateral stiffness and strength from the approach barrier to the bridge rail.

Guardrail/Bridge Rail Transitions

A large number of bridge-involved accidents occur in this transition zone every year, making it a critical element in roadside barrier design. The purpose of the transition is to provide continuity of protection where the guardrail joins the bridge rail. The lateral stiffness of the transition zone should increase smoothly and continuously from the more flexible to the less flexible system. Special emphasis must be placed on the avoidance of vehicle snagging or excessive deflections in the transition zone. Such pocketing or snagging of the vehicle can lead to excessive vehicle decelerations or other unacceptable results.

Since the need for a transition zone increases as the difference in guardrail/bridge rail stiffness increases, a critical condition exists where W-beam approach rail transitions into a rigid concrete bridge rail such as the CSSB. At present, the most widely used treatment of this problem involves carrying the W-beam approach rail onto the bridge and reducing the post spacing on the 25 ft. section just upstream of the bridge end. Post spacing in the transition region is typically half of the standard 6 ft.-3 in. post spacing used on most W-beam guardfence. Standard Texas W-beam guardfence

incorporates 7 in. round wood posts and the attachment of the rail to the bridge end is provided by a terminal connector or "Michigan end shoe." Figure 1 shows the typical SDHPT transition to a vertical concrete bridge rail.

Figure 2 shows a widely used transition that is very similar to the standard Texas system. In this system, the W-beam rail is blocked out from 6 in. X 8 in. timber posts. The post spacing is the same as that for the Texas system described above. For certain impact conditions, this transition design has been shown to be unable to prevent severe snagging on the end of a rigid concrete barrier (1). When this system was crash tested, the vehicle came to an abrupt stop after severely snagging on the end of the rigid bridge rail. The severity of the impact caused a 9 in. translation of the simulated concrete wingwall which was sufficient to cause a tensile failure in the W-beam approach rail. Figure 3 shows the extensive damage to the vehicle and transition region observed during this test.

Based on the similarities between standard Texas transitions and tested systems as described above, it is evident that current SDHPT transition designs will not meet recommended performance standards (2). Current SDHPT designs permit too much deflection in the transition region, allowing the vehicle to pocket and snag on the bridge rail end.

Only a limited number of studies have addressed the guardrail/bridge rail transition problem and, consequently, very few standards exist for transitioning a flexible barrier system to a rigid concrete bridge rail. Several acceptable guardrail-to-bridge rail transition designs utilizing two sets of reduced post spacing near the bridge end were recently developed by Bronstad (1). These transition designs use 6 in. x 8 in. wood posts with blockouts and a 12 ft.-6 in. section of W-beam rub-rail adjacent to the bridge end. The first four posts upstream of the bridge end are spaced at 1 ft.-6 3/4 in. with the following four spaces at 3 ft.-1 1/2 in. Although these designs have exhibited good impact performance, the tight post spacing may present a problem when used on bridges designed to drain water near the end of the railing. The maximum clear distance between posts in these designs is only 12 in. and is inadequate for most bridge end drain designs. These problems are especially acute when the new transitions are used to retrofit existing bridge sites. Use of these designs in a retrofit situation would require the drainage system to be modified or redesigned.

Other acceptable transition designs were recently developed by Post (3). These systems are composed of oversized posts, nested W-beam or Thrie-beam rails, and flared bridge rail ends. Problems associated with the implementation of these designs include inventory and repair problems arising from the use of a non-standard guardrail post in the transition and high costs of flaring bridge rail ends during retrofit operations.

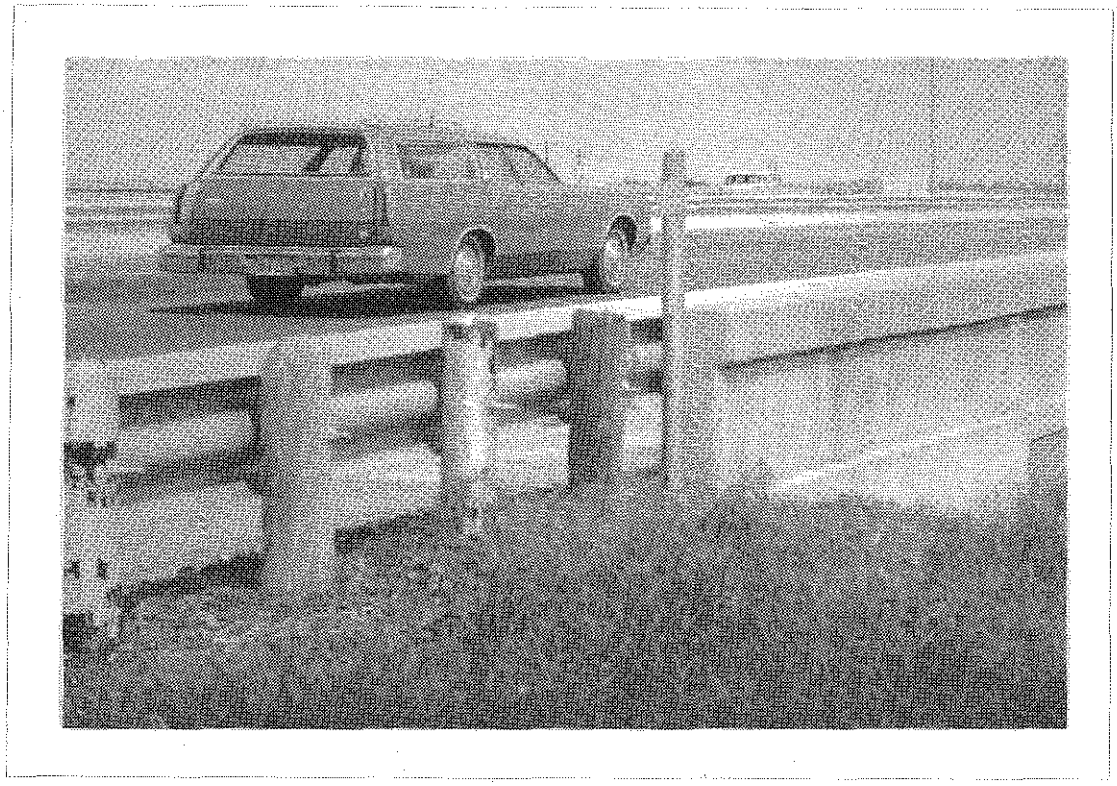

FIGURE 1. STANDARD TEXAS SDHPT TRANSITION TO RIGID WALL

FIGURE 2. TYPICAL TRANSITION TO RIGID WALL. TEST LA-1

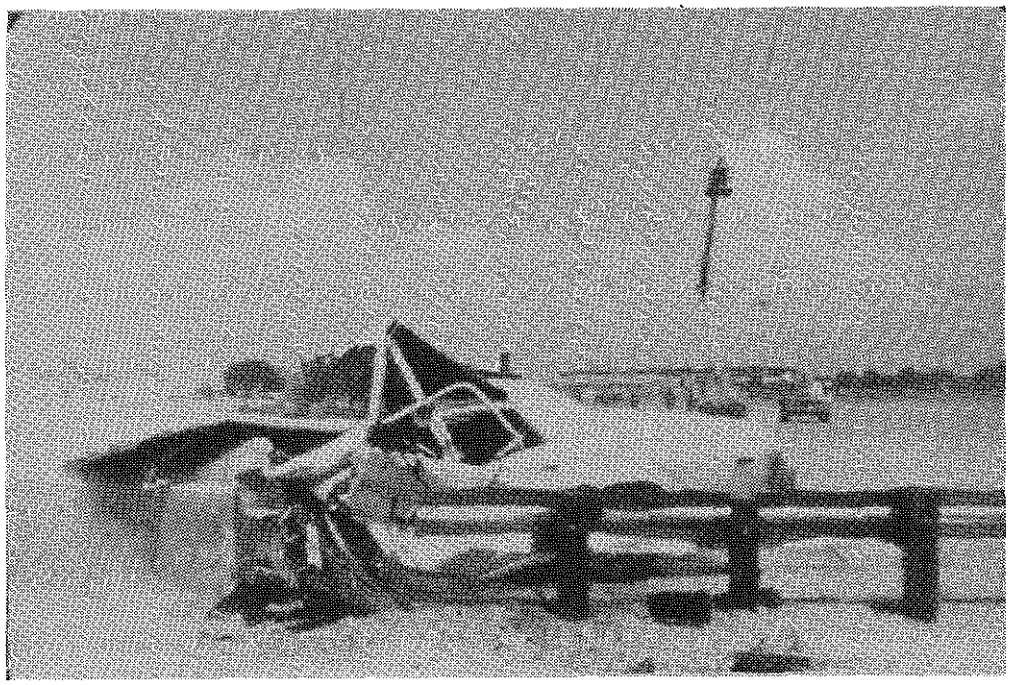

FIGURE 3. VEHICLE AND BARRIER DAMAGE AFTER TEST LA-1

Short-Radius Guardrail Treatments

An approach rail that presents a unique set of problems is the short-radius guardrail. Whenever a side road or driveway intersects a main roadway in close proximity to a bridge end, the approach rail cannot be terminated by extending it along the roadway past the length of need. Under these conditions, the approach guardrail must be curved on a tight radius and extended along the secondary roadway.

There are no existing national standards for short radius guardrail treatments. In Texas, the W-beam approach rail is typically curved from the main roadway to the secondary roadway with standard 7 in. diameter wood posts spaced at 6 ft.-3 in. around the curve. A new short radius guardrail treatment was recently developed under an FHWA study (1). The system consists of a W-beam rail curved to a 8 ft.-6 in. radius and terminated with a modified break-away cable terminal (BCT) 25 ft. down the secondary roadway. Weakened posts spaced at 6 ft.-3 in. were used along the curved section of rail.

This system exhibited only marginal impact performance during full-scale crash testing. Although a 4500 lb. vehicle was contained, the deflections of the system were excessive. Therefore, this treatment may not be acceptable when vehicle travel is strictly limited due to terrain conditions or other hazards.

Objectives

In view of the general lack of acceptable guardrail-to-bridge rail transitions and short-radius guardrail treatments, the study described herein was undertaken to:

(1) Develop a new transition design with the following characteristics:

   a) provide for easy retrofit of existing installations,
   b) provide sufficient post spacing to allow implementation where bridge end drains are required,
   c) designed for use with either vertical concrete parapets or concrete safety shaped barriers,
   d) meet nationally recognized safety standards.

(2) Develop recommendations for short-radius guardrail treatments.

II. TRANSITION DESIGN APPROACH

The interaction of an automobile with a barrier system is difficult to analyze. Dynamic effects, large displacements, and inelastic behavior must all be considered. The complexity of this dynamic interaction limits the number of approaches that can adequately analyze the transition problem. There are only two practical alternatives, full-scale crash testing and computer simulation. The use of full scale crash testing for the evaluation of numerous designs and modifications is cost prohibitive. On the other hand, computer simulation provides a relatively inexpensive and effective alternative for determining the impact performance of various barrier systems. The first phase of this study involved selecting and validating a computer simulation program for use in analyzing the vehicle/transition impacts. Several sophisticated finite element simulation programs were candidates for this purpose, including Barrier VII, GUARD, and HVOSM (4,5,6). Barrier VII was chosen as the most appropriate simulation program for use in this study. A discussion of available simulation programs and the reason Barrier VII was selected is presented in Appendix A.

Although Barrier VII has been well validated for use as a design tool in the development of a variety of flexible barriers, its use in simulating impacts near the transition zone from a flexible to a rigid barrier has been somewhat limited. The task of validating Barrier VII for analysis of impacts in the transition region was, therefore, the first step taken in the development process. This validation study is described in Appendix B.

The next task of the study was to identify the specific deficiencies in the impact performance of current transition designs. With the aid of the simulation program, design changes addressing these deficiencies were then developed and evaluated. Barrier VII was then used to conduct a parametric study of transition design. All simulations were strength type impacts with a full size vehicle traveling 60 mph and contacting the rail at an angle of 25 degrees. This impact condition simulates test designation 30 (2) which is the recommended test for evaluating the performance of a transition. Design parameters investigated include guardrail beam strength, post spacing, and post size.

Design charts were then developed based on the results of this parametric study. These charts can be used to determine the barrier deflection that could be expected for various transition configurations. Selection guidelines were then developed to aid in the selection of a final design. Some important selection criteria used in choosing a final design include: (1) ability to retrofit existing bridge rail installations, (2) adequate post spacing to allow bridge end drainage, (3) use of standard hardware, (4) ease of field installation, and (5) aesthetics. These guidelines were developed to help insure acceptance and implementation of the final

design.

Connections and other details of the final design were then resolved and a full scale prototype of the transition was constructed. The design was then further evaluated for impact performance through a full-scale crash testing program in accordance with nationally accepted guidelines (2).

III. TRANSITION DEVELOPMENT

As evident from the test results shown in Figure 3, current SDHPT transition designs to rigid concrete parapets do not meet nationally recognized safety standards (2). Under certain impact conditions, the current systems permit too much deflection in the transition region, allowing the vehicle to pocket and snag on the bridge rail end. In order to correct this problem, the dynamic deflection of the rail had to be limited to an acceptable value. The design parameters that were investigated to accomplish this task include: increasing guardrail beam strength, reducing post spacing, and increasing post size. Considering the widespread application of the W-beam transition to both the vertical concrete parapet and CSSB, it was desirable that any new design be able to retrofit these existing systems as well as have new construction applications.

The critical impact point for testing guardrail-to-bridge rail transitions is the point which the potential for snagging on the end of the rigid barrier is maximized. Note that this critical impact point changes with the stiffness of the approach barrier. Stiff approach barriers redirect impacting vehicles more quickly and, therefore, have a critical impact point nearer to the rigid barrier than do more flexible approach rails. A vehicle impacting the transition further upstream from the critical impact point has more time to begin redirection before the end of the bridge rail is reached, and thus the potential for snagging is reduced. A vehicle impacting closer to the bridge rail end can clear the transition zone before guardrail deflections become large enough to allow snagging or pocketing behind the bridge end.

It was determined in reference 1, that the critical impact point for moderately stiff transition designs is approximately 112 in. upstream from the end of the bridge rail. This critical impact point was verified with the Barrier VII simulation program and was, thereafter, used for all simulation and testing of transitions to rigid barriers. Further, Barrier VII analysis indicated that the critical impact location on standard strong post guardrails was approximately 125 in. from the end of the intermediate barrier. Therefore, analysis and testing of impacts on standard guardrails was conducted using an impact point 125 in. upstream from the start of the transition.

Design Curves

Barrier VII, was used to conduct a parametric study of designs for transitions to rigid barriers. All simulations involved impacts with a 4500 lb vehicle traveling 60 mph and contacting the rail 112 inches upstream of the rigid barrier end at an angle of 25 degrees. The basic transition design consisted of a standard strong post W-beam approach rail with modified post spacing and beam strength over

the last 25 ft. before the bridge rail. The bridge rail was modeled as a straight vertical concrete parapet. A typical set of Barrier VII input is given in Appendix C.

The major design parameters investigated include guardrail beam strength, post spacing, and post size. The two post sizes investigated were a standard 7 in. diameter wood post and a "double strength" post. A double strength post was defined as a post that would develop twice the dynamic lateral resistance of the standard post. This increased post strength can be achieved by increasing the embedment depth and/or post section modulus. When determining the properties of such a post, it should be ensured that the full lateral capacity of the post can be developed. That is, failure should result from yielding of the surrounding soil rather than by fracture of the post. When a post fails quickly through fracturing, much of the energy absorbing capacity of the system is lost, and guardrail deflections may increase. Examples of double strength posts are: an 8 in. X 8 in. wood post embedded approximately 48 in. and a 10 in. X 10 in. wood post with an embedment of 40 in.

Figures 4 and 5 show predicted maximum dynamic deflections for various transition configurations using the two different post sizes that were studied. These figures were used to determine barrier deflections that could be expected for a wide range of beam strengths and post spacings. It should be noted that 6 in. X 8 in. wood posts and W 6X9 steel posts have been shown to have a dynamic lateral capacity approximately the same as a 7 in. round post. Thus, although Figure 4 was developed for a 7 in. round post, either of these other posts could be substituted as the "standard post" for transition design.

Deflection Design Criteria

As discussed previously, barrier deflection is believed to be a good indicator of the probability of a vehicle snagging on a rigid barrier end. Twelve full scale crash tests from reference 1 were reviewed in an effort to determine a maximum allowable barrier deflection. Figure 6 shows a plot of barrier deflection for each of the tests conducted in the referenced study. As shown in this figure, for unflared bridge rail ends, the approach guardrail can be allowed to deflect no more than 12 inches before significant vehicle snagging becomes a potential problem.

In support of the crash test data, a series of simulation runs were made for the purpose of tracking wheel position past the wingwall end. It was observed that for deflections in excess of 12 in., the wheel followed a trajectory through the end of the concrete barrier (see Figure 7). This behavior is indicative of severe vehicle snagging and poor safety performance. However, for barrier deflections less than 12 in., the wheel followed a path safely outside of the bridge rail end (see Figure 8). These results

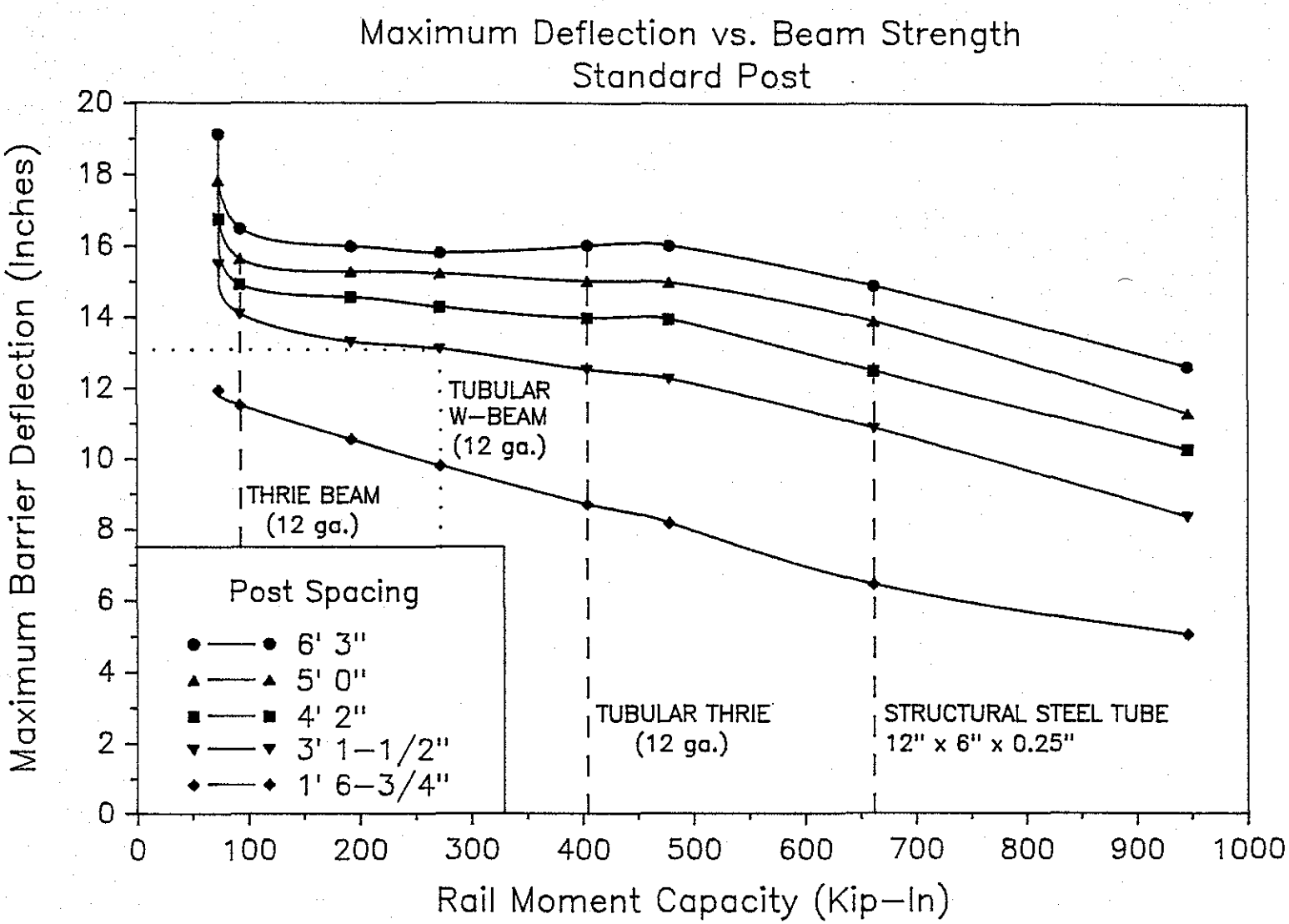

FIGURE 4. DESIGN CURVES FOR STANDARD POST TRANSITIONS

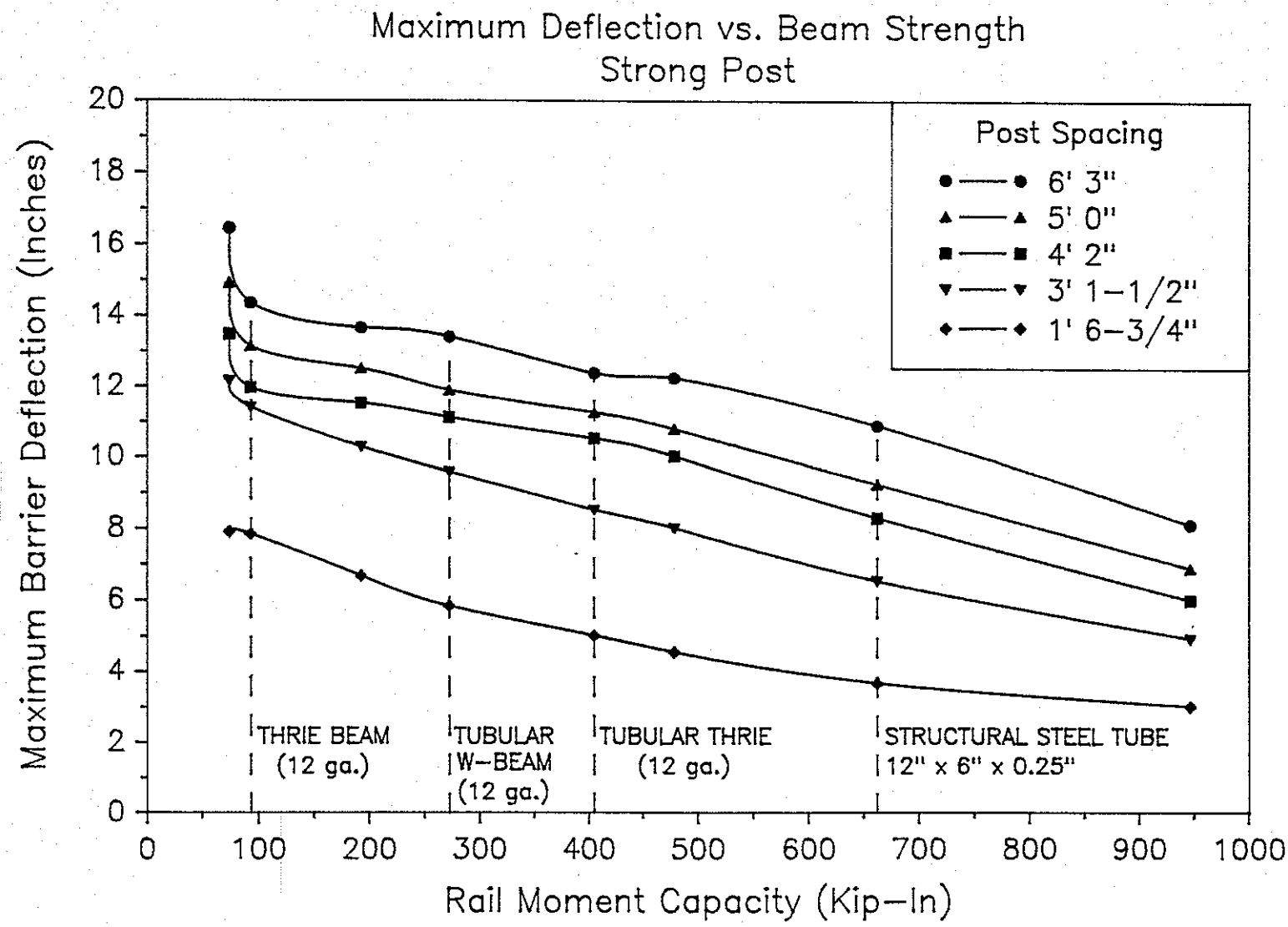

FIGURE 5. DESIGN CURVES FOR DOUBLE STRENGTH POST TRANSITIONS

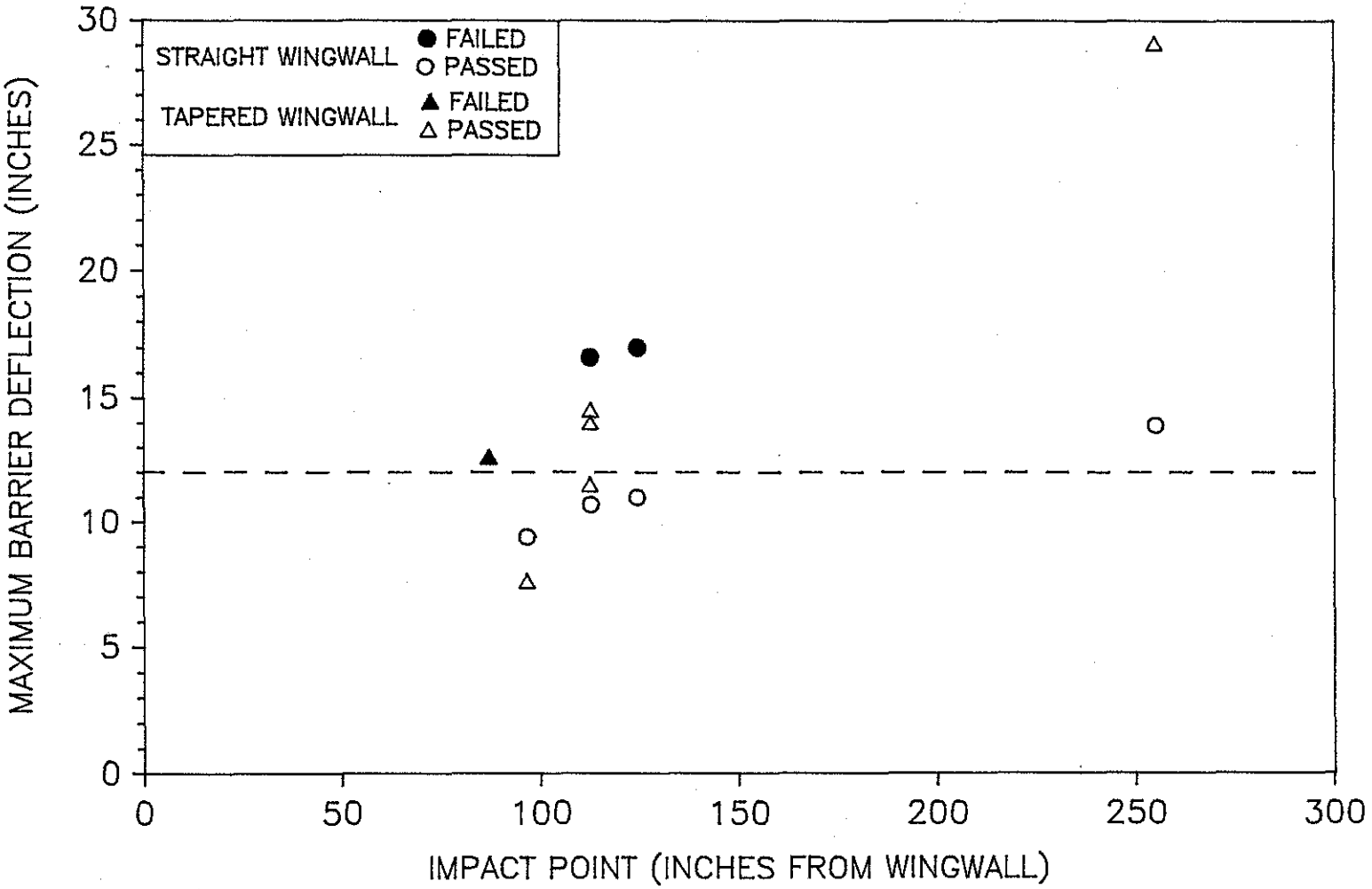

FIGURE 6. MAXIMUM DEFLECTION FROM TRANSITION CRASH TESTS

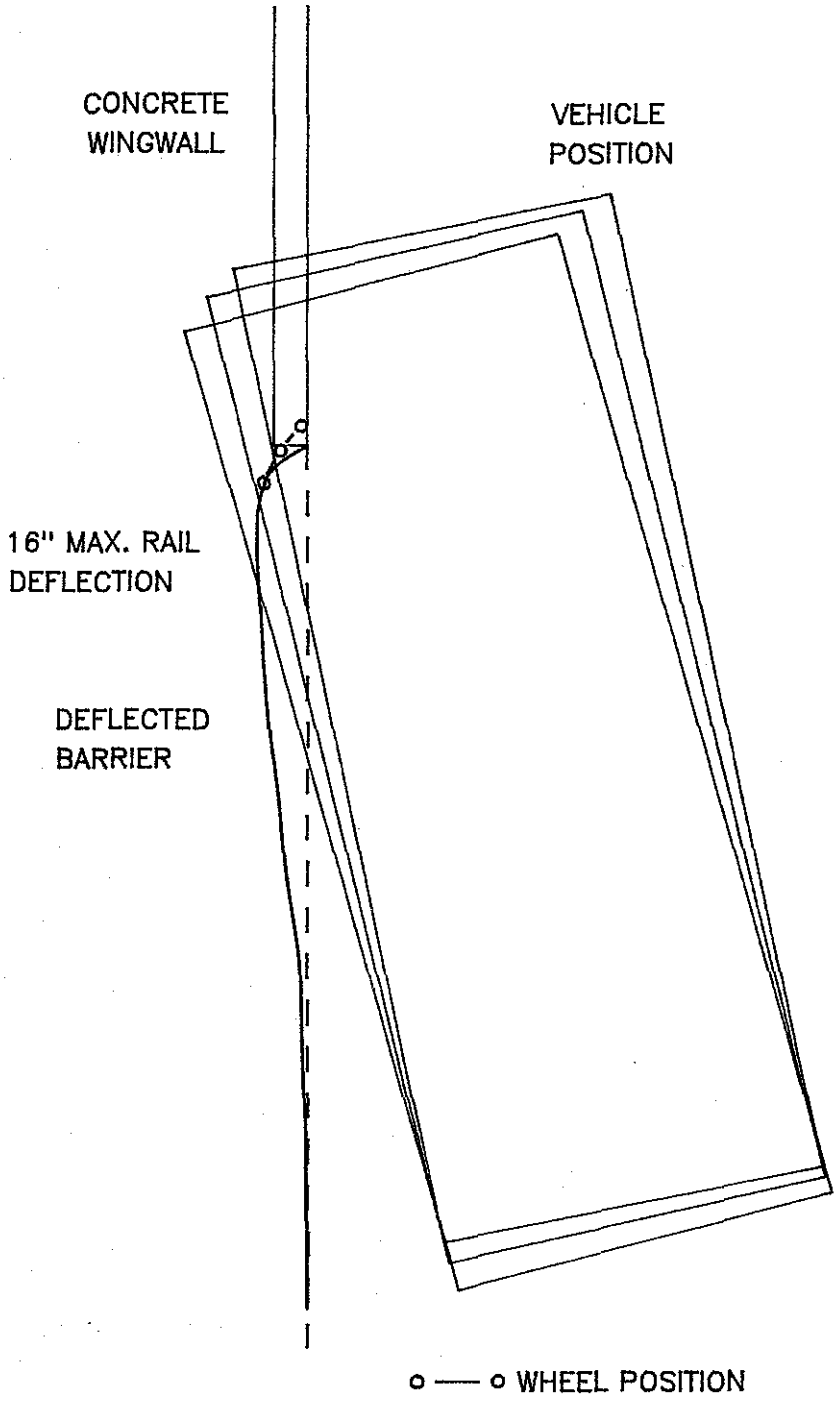

FIGURE 7. WHEEL TRAJECTORY, 16 IN. DEFLECTION

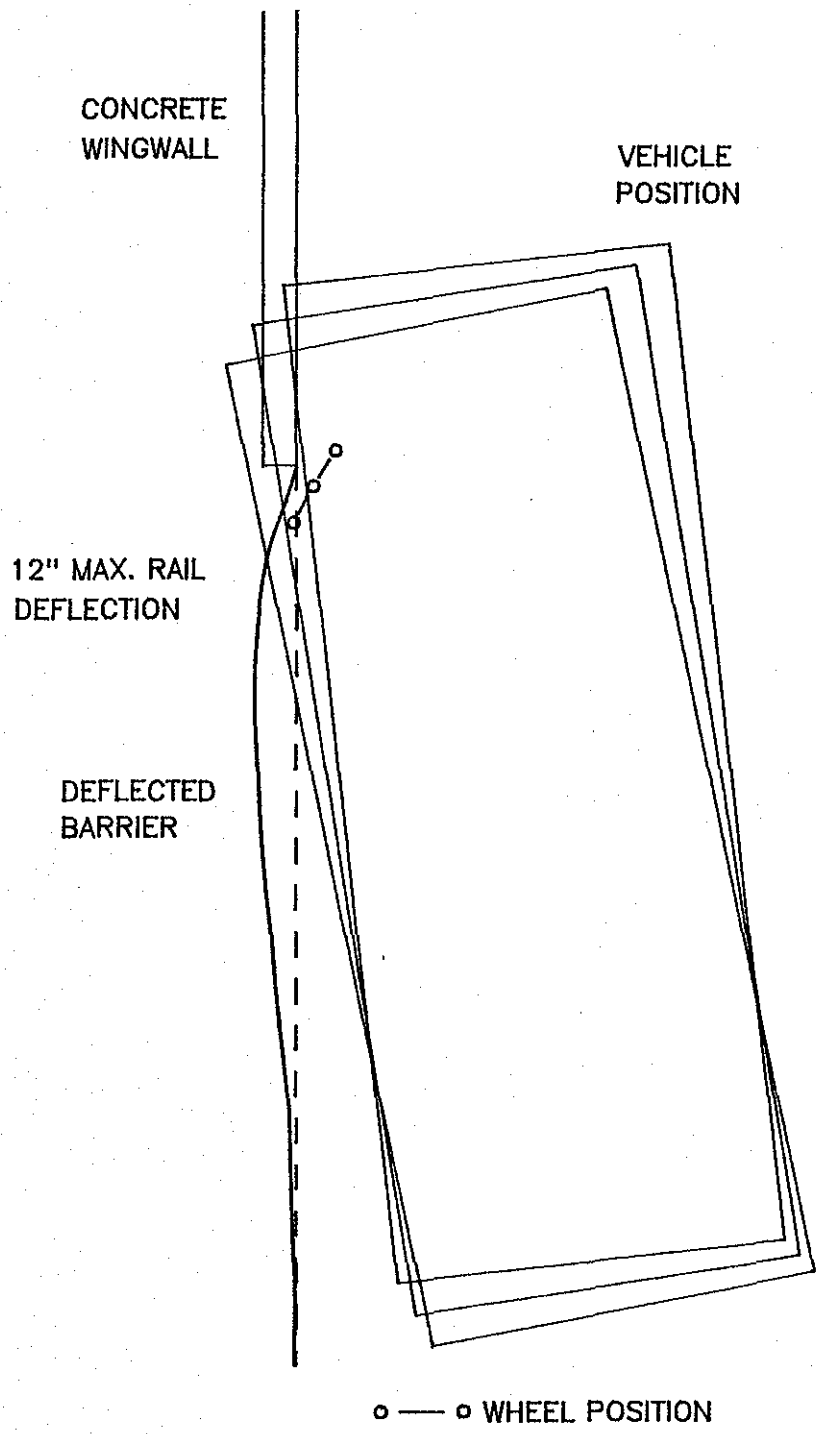

FIGURE 8. WHEEL TRAJECTORY, 12 IN. DEFLECTION

supported a deflection limit of 12 in. as the initial evaluation criteria in the transition design. Therefore, it was concluded that designs limiting maximum lateral deflections to less than 12 in. should provide acceptable performance. These configurations were considered candidate designs and were thus further evaluated against other selection guidelines in an effort to find an optimal design. All alternatives which had predicted deflections above the 12 in. deflection limit were discarded.

Selection of Transition System

As can be seen from Figures 4 and 5, numerous transition configurations were acceptable based on the 12 in. deflection limit criteria. Additional selection guidelines were therefore established to aid in the determination of a final design. It was desirable that the transition: (1) be able to retrofit existing bridge rails, (2) provide sufficient post spacing to allow for adequate bridge end drainage, (3) allow for ease of transition at both approach rail and bridge rail, and (4) use standard hardware items.

Consultations with officials from the Texas State Department of Highways and Public Transportation (SDHPT) were conducted to help ensure acceptance and implementation of the final design. SDHPT officials indicated that, due to inventory and maintenance problems associated with non-standard guardrail posts, the new transition should be constructed with standard 7 in. round wood guardrail posts. Further, SDHPT engineers expressed an interest in developing a transition that utilized a 12 gage tubular W-beam rail element (see Figure 9). This beam has an approximate moment capacity of 280 kip-in. As shown in Figure 4, Barrier VII predicts a maximum deflection of 13 in. for the tubular W-beam mounted on standard posts spaced at 3 ft.- 1 1/2 in. Although the predicted deflection for the design is slightly above the deflection limit criteria, it was believed that the added depth of the tubular W-beam (3 1/4 in. more than standard W-beam) would act as an effective blockout. Therefore, effective deflection of the beam would be reduced to 9.75 inches, well below the deflection criteria of 12 inches.

The tubular W-beam transition received high marks when evaluated against the selection guidelines. One of the primary objectives of this study was to develop a transition to retrofit existing bridge rail installations. The tubular W-beam transition makes use of the same post size and spacing currently being used in Texas for transitions to rigid walls. This permits easy retrofitting to both the vertical wall and safety-shaped bridge rails.

The post spacing adjacent to the bridge end was also an important consideration. Since the tubular W-beam transition uses the same post spacing at the bridge end that is presently provided by current transition installations, adequate space for proper end drainage is assured.

Another selection criteria satisfied by the tubular W-beam system was ease of transition. The tubular W-beam is essentially two standard W-beams welded back to back (see Figure 9). For this reason, the connections and splices are relatively easy to achieve at both the bridge end and the upstream end where the tubular rail transitions to the standard metal beam guardfence. The bridge end connection can be achieved using a standard terminal connector and, at the upstream end, the W-beam can be spliced directly to the tubular rail element. The tubular W-beam transition also makes use of many standard items of hardware. The tubular W-beam section is the standard beam element on the Texas T-6 bridge rail. Also, as stated above, the transition makes use of standard 7 in. diameter wood posts. The use of these standard pieces of hardware helps reduce the cost of the system, makes field installation easier, and helps insure acceptance and implementation of the design.

The proposed transition is practical from the standpoint of aesthetics as well. From the roadside, the tubular transition has the appearance of a standard W-beam guardrail. In fact, the change from the W-beam approach rail to the tubular W-beam transition would be hard to perceive.

Final Design Details

The final transition design consisted of a 25 ft. segment of 12 gage tubular W-beam mounted on 7 in. diameter round wood posts spaced 3 ft.- 1 1/2 in. with an embedment of 38 in. as shown in Figure 10. Barrier VII was then used to simulate impacts with the selected design at a number of locations in an effort to identify any other potential snagging problems and to determine the necessary connection design loadings. Barrier VII predicted that impacting the upstream transition from the single W-beam to a tubular W-beam would be less severe in terms of post snagging if the first post spacing on the tubular segment was maintained at 6 ft.- 3 in. (see Figure 11). Design loading conditions for the connection between the tubular W-beam and the concrete barrier end included a 140 kip tensile force, a 60 kip shear force, and a 280 kip-in bending moment. This connection was accomplished with six 7/8 in. diameter high strength bolts, (A325 or equivalent grade threaded rod), a steel end shoe and a tapered wood blockout as shown in Figure 12. The connection was designed to be used with either vertical parapets or concrete safety shaped barriers.

Note that the design shown in Figure 10 is a retrofit of the existing Texas standard transition and uses two small wood blockouts on the standard W-beam approach in order to move the rail to the outside of the tubular beam. No blockouts were used in the rest of the transition to maintain compatibility with the Texas standard guardrail. Further, due to retrofit considerations, the attachment between the single W-beam barrier and the tubular W-beam rail

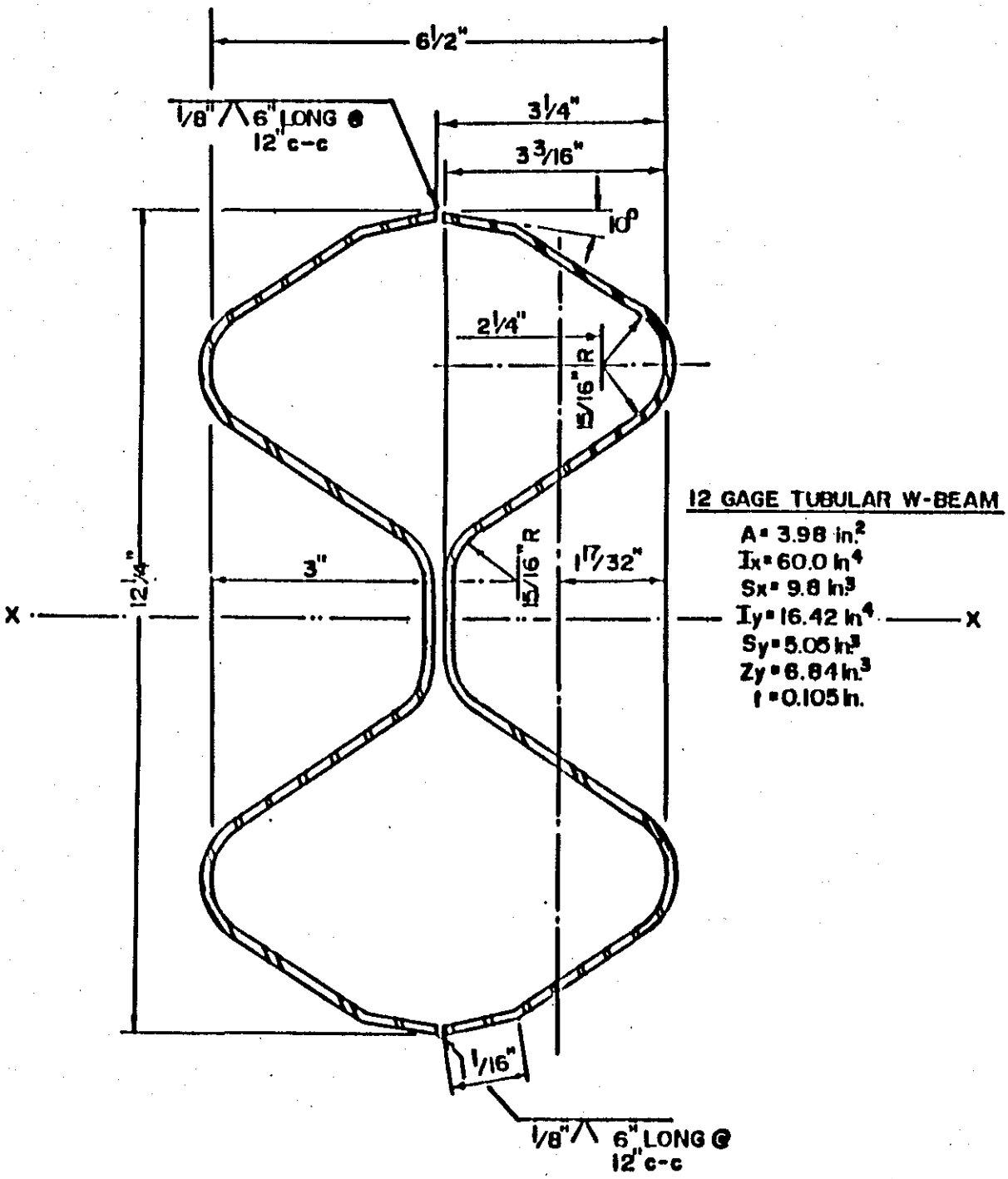

FIGURE 9. 12 GAGE TUBULAR W-BEAM

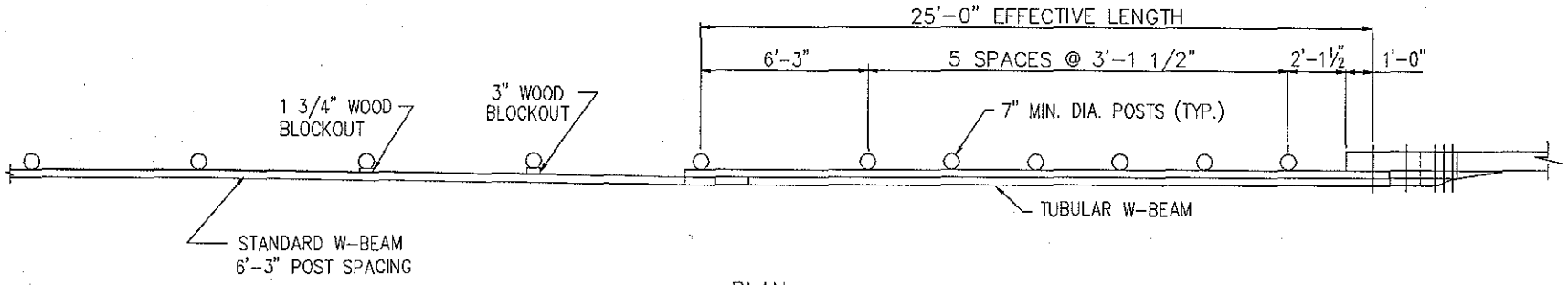

PLAN

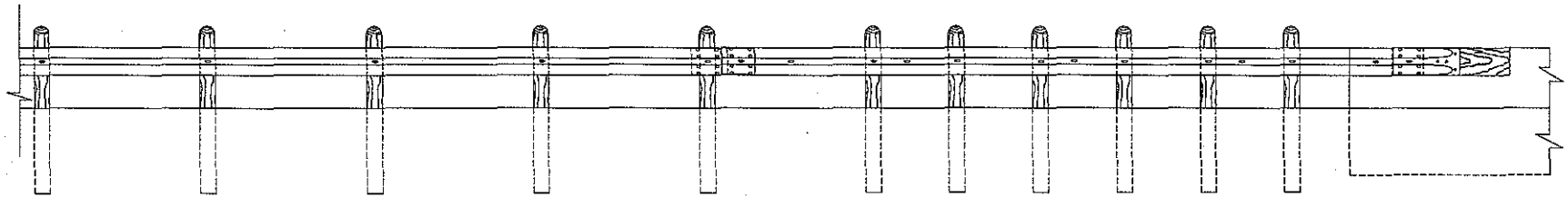

ELEVATION

FIGURE 10. SELECTED RETROFIT TRANSITION DESIGN

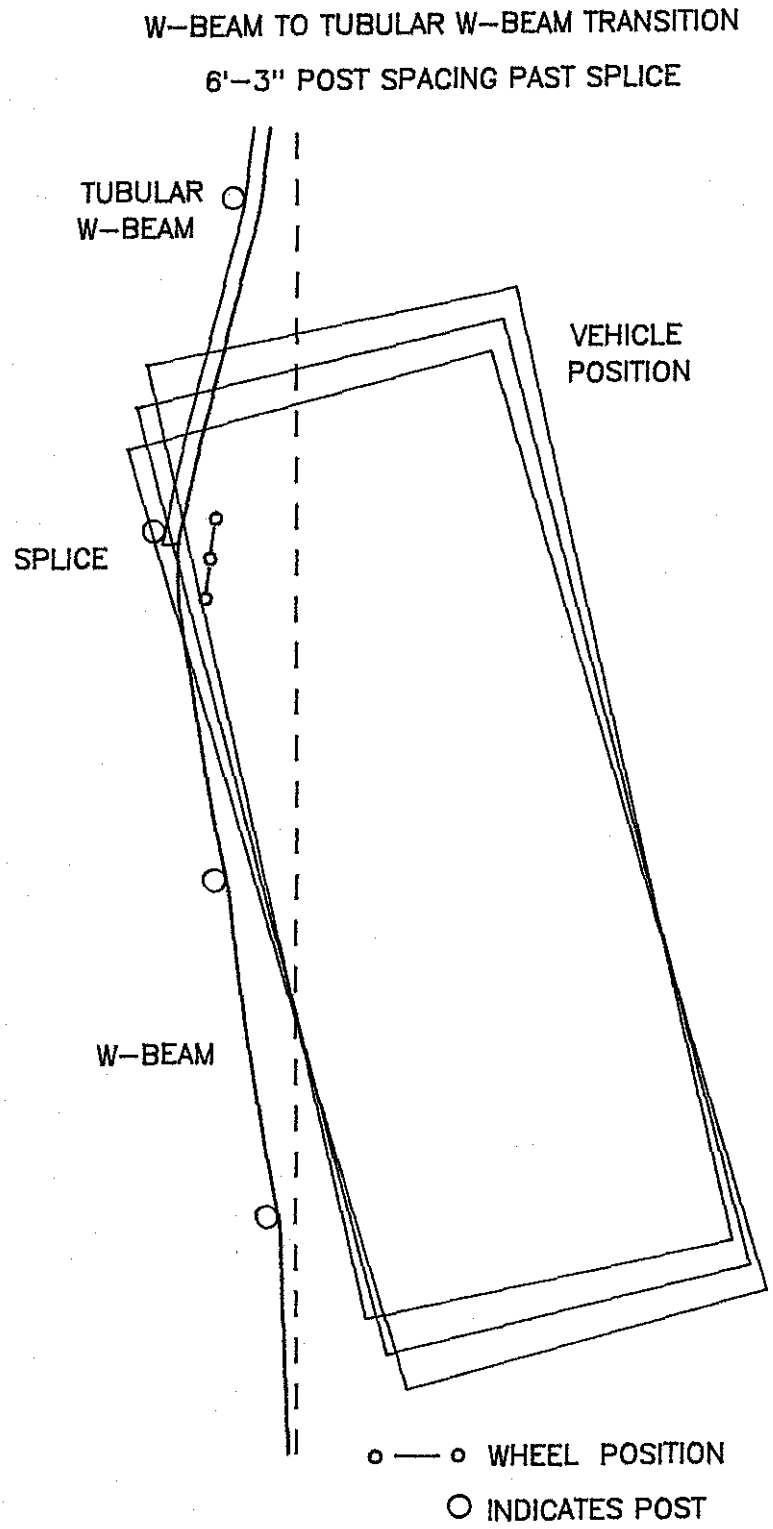

FIGURE 11. WHEEL TRAJECTORY, W–BEAM TO TUBULAR W–BEAM TRANSITION

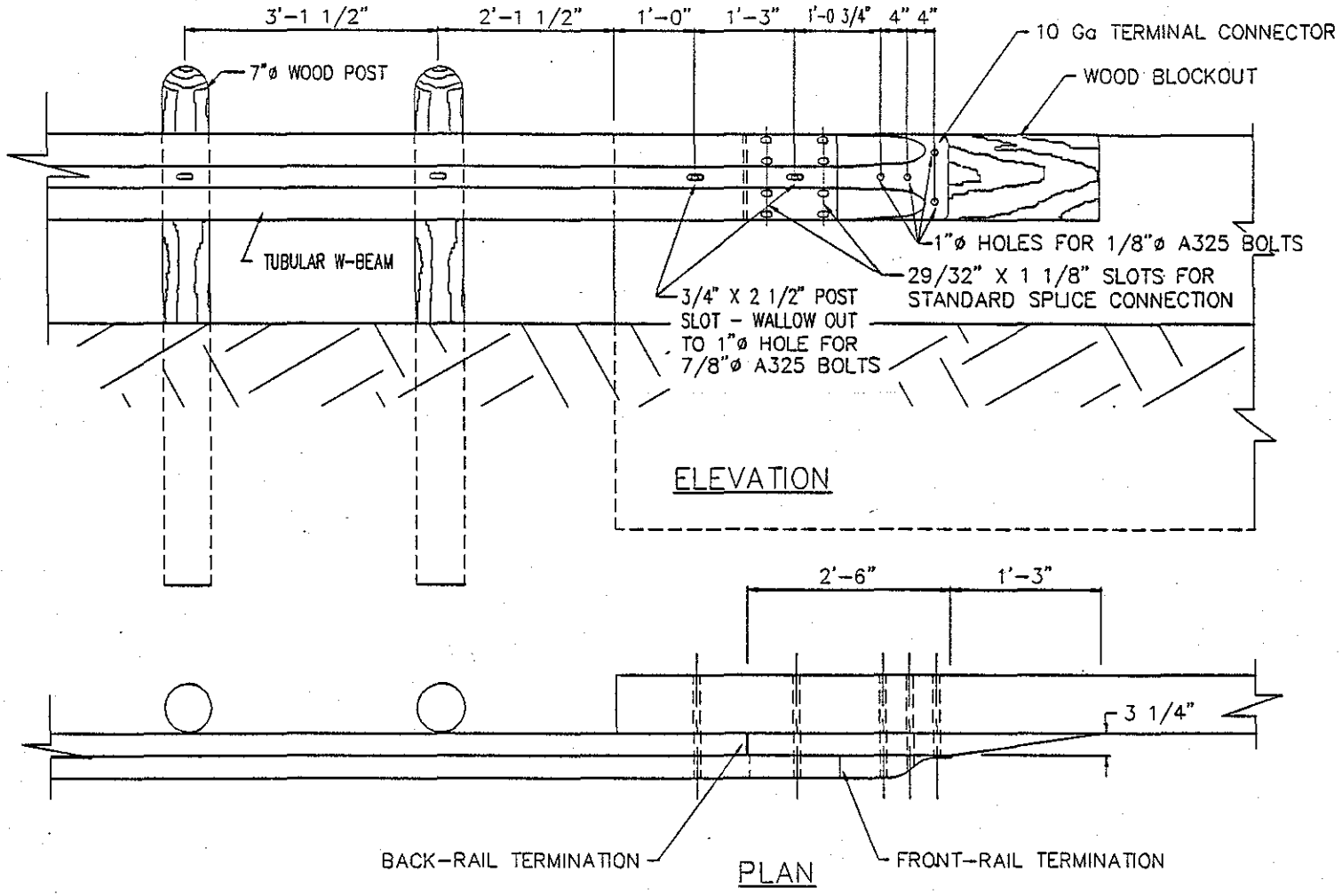

FIGURE 12. BRIDGE END CONNECTION DETAILS

required a small splice plate fabricated from a section of W-beam rail.

Retrofitting an existing installation thus involves replacing a 25 ft. length of W-beam railing with a section of tubular W-beam, drilling six holes in the concrete barrier for the terminal connection, placing two small blockouts in the approach rail, and removing the first post downstream of the W-beam to tubular W-beam splice. When retrofitting to a CSSB that does not have an existing 3ft. taper at its terminating end (i.e. Texas type T5 bridge rail), the standard taper should be created by breaking out the base of the concrete safety shape.

IV. FULL-SCALE TRANSITION CRASH TESTS

Standards for testing barrier transitions are presented in NCHRP Report 230 (2). This report requires that transitions be evaluated with a single test that involves a vehicle impacting the more flexible barrier upstream from its transition to the stiffer barrier. The tubular W-beam transition was evaluated for impact performance in accordance with test number 30 of NCHRP Report 230 . Test 30 involves a 4500 lb vehicle impacting the transition section at 60 mph at an angle of 25 degrees. This test condition examines the strength of the transition as well as the propensity for the more flexible barrier to deflect and allow the test vehicle to snag on the end of the stiffer barrier.

Note that in most practical guardrail-to-bridge rail transitions designs, the guardrail is first transitioned into an intermediate strength barrier which is then transitioned into the rigid bridge rail. Therefore, safety performance of the design must be evaluated at both transition points. The testing program for the tubular W-beam transition consisted of three full scale crash tests, each of which evaluated a different aspect of the transition design. The tests conducted were as follows:

1. Evaluation of tubular W-beam transitioning into a vertical concrete parapet.
2. Evaluation of tubular W-beam transitioning into a concrete safety shaped barrier.
3. Evaluation of the standard W-beam guardrail transitioning to the tubular W-beam.

Test 1

The purpose of this test was to evaluate the tubular W-beam transition to a vertical concrete wall. The transition was constructed as shown in Figure 10 above. Figure 13 shows the completed installation before Test 1.

A 4570 lb Cadillac impacted the transition at 55.0 mph and 26.4 degrees at a point 112 in. upstream from the bridge rail end. The vehicle was successfully redirected although significant wheel snagging on the bridge rail end was observed. Some sheet metal snagging occurred at the tops of the posts and minor wheel snagging at the base of the posts was also evident. While the top of the tubular rail was only partially flattened, the bottom half of the rail was completely collapsed. This collapse effectively increased

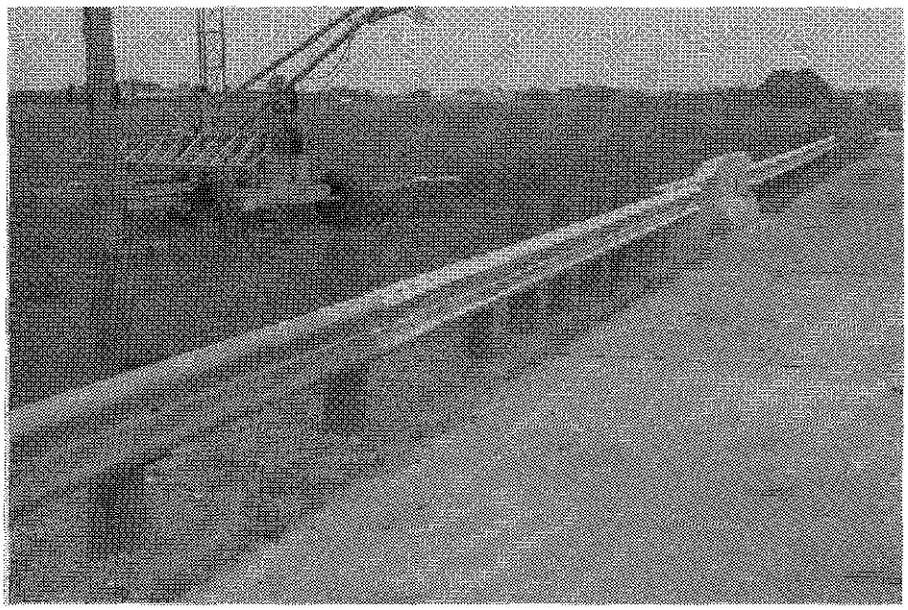

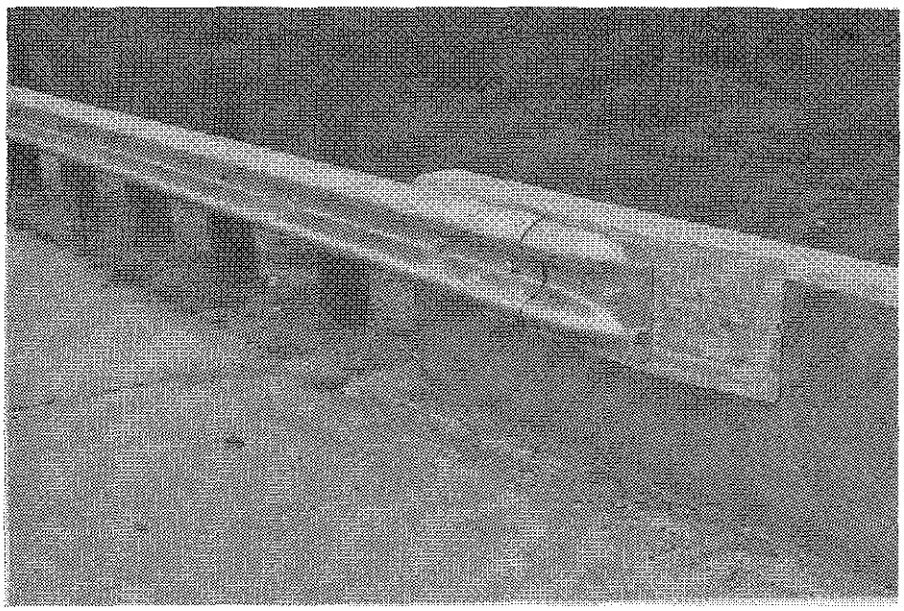

FIGURE 13. TUBULAR W-BEAM TRANSITION TO VERTICAL WALL, TEST 1 INSTALLATION.

the maximum deflection of the rail and thus the degree of snagging. The test vehicle was only moderately damaged for a test of this severity. Damage to both the vehicle and barrier after test 1 are shown in Figure 14.

NCHRP report 230 (2) does not require that a strength test, such as that used for evaluation of transition designs, meet occupant severity limits. However, the occupant severity measures from Test 1 were all within maximum acceptable limits. A summary of the test results is given in Figure 15.

Although the change in vehicular velocity was above the recommended value set forth in NCHRP 230 Evaluation Criteria I (2), this test was considered to be a success as presented in discussion of results.

Test 2

The purpose of this test was to evaluate the tubular W-beam transition to the concrete safety shaped barrier. The geometry of the safety shaped rail increases the potential for vehicle snagging. The lower curb face of the concrete projects beyond the face of the tubular W-beam and the 32 in. wall height extends above the approaching guardrail. In order to reduce the severity of snagging observed in Test 1, some modifications were made to improve the impact performance of the transition. Wood inserts were added in both the top and bottom of the tubular W-beam to prevent the rail from collapsing (see Figure 16). These wood inserts were secured in place with lag screws and washers through existing splice bolt holes. Further, the tops of the posts were cut with a 10 degree bevel at rail height in order to minimize sheet metal snagging. Figure 17 shows the modified transition before Test 2.

A 4637 lb Cadillac impacted the transition at 60.8 mph and 25.8 degrees at a point 112 in. upstream from the bridge rail end. The vehicle was smoothly redirected with greatly improved performance over Test 1. The wood inserts prevented the tubular rail from collapsing and greatly reduced the degree of snagging. Only minor wheel snagging was observed at the base of posts 1 and 2 and at the bridge rail end. Although some sheet metal snagging occurred on the top of the concrete rail and the tops of the guardrail posts, the forces involved did not appear to be significant. Evidence of the post and wingwall snagging is shown in Figure 18. Based on the results of tests 1 and 2, it was concluded that the use of full size, standard posts in the transition region did not adversely affect the performance of the barrier system. The hood snagging on top of the round wood posts and the concrete barrier was not considered to be a significant hazard since the hood rides up the post or barrier until it slips off the side or top. Further, there was no tendency for the hood to become detached from its hinges and penetrate the occupant compartment.

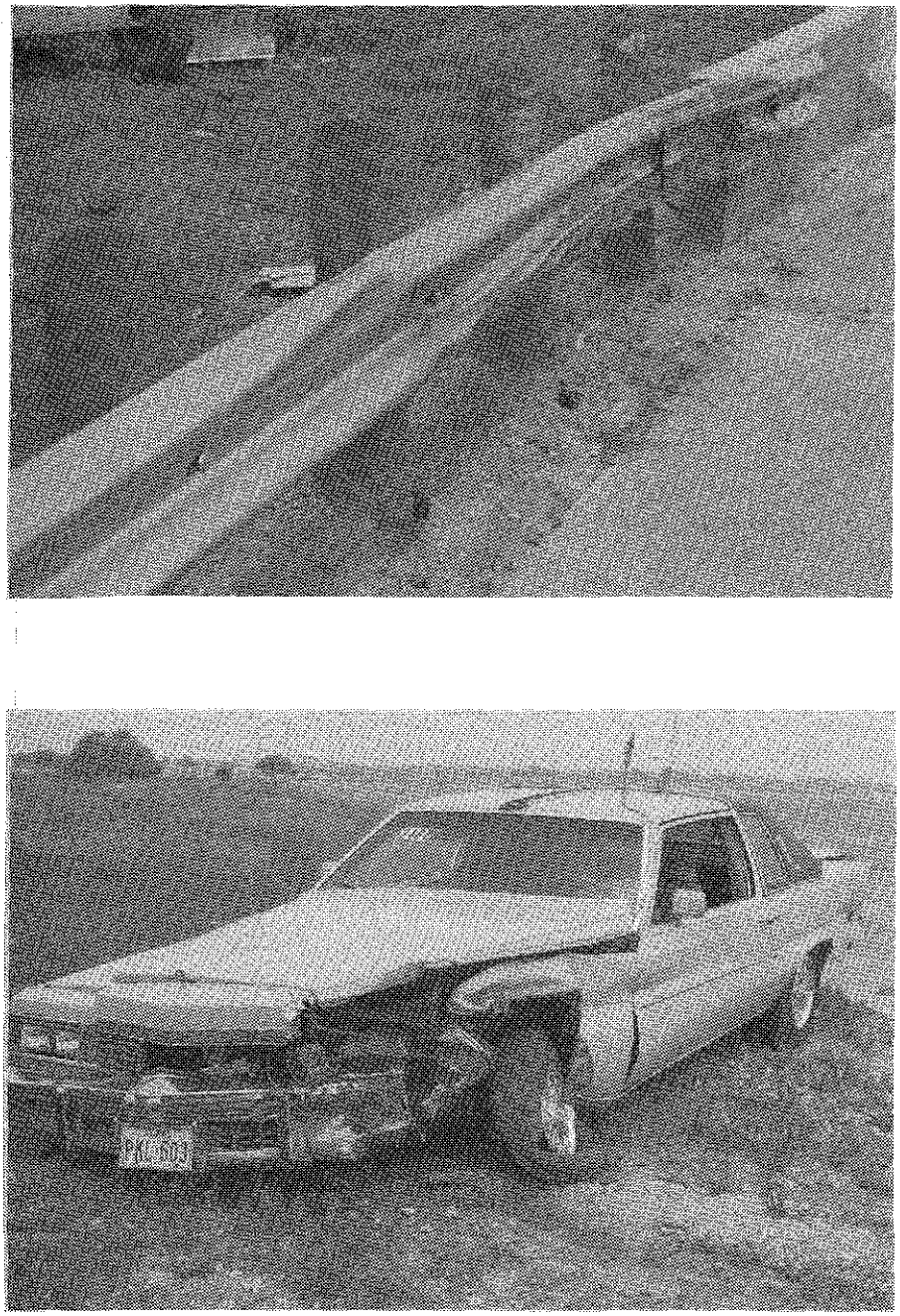

FIGURE 14. VEHICLE AND BARRIER DAMAGE AFTER TEST 1

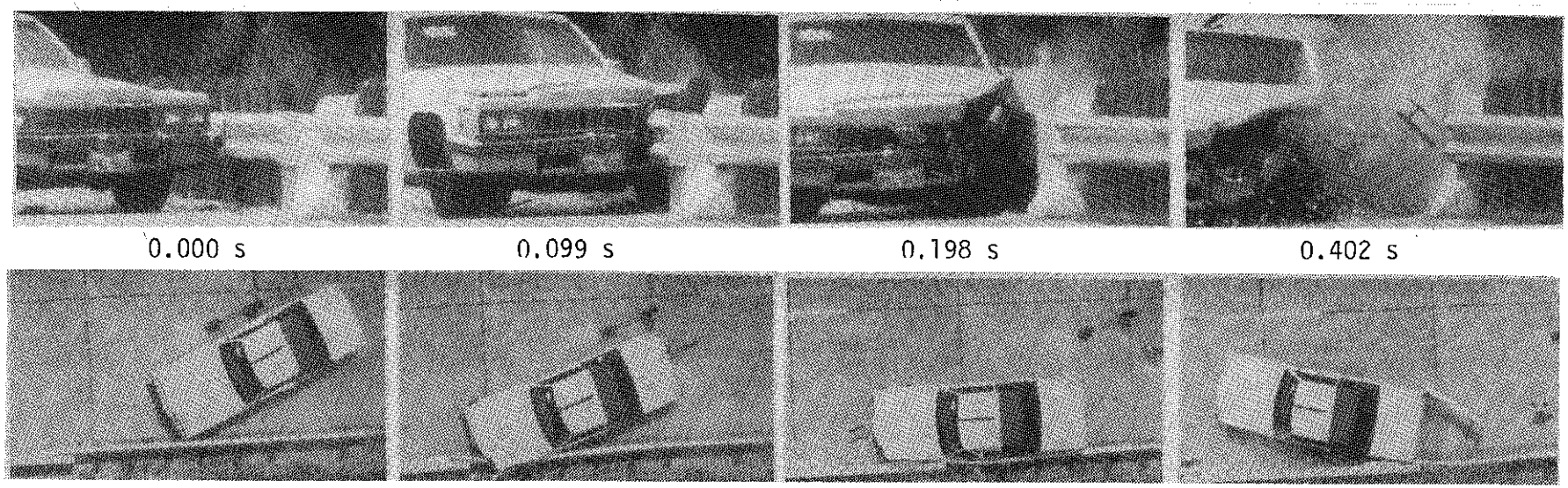

Test No	2461-1	Impact Speed	55.0 mi/h (88.5 km/h)
Date	5/14/87	Impact Angle	26.4 deg
Test Installation	Tubular W-Beam Transition to T201	Exit Speed	33.1 mi/h (53.3 km/h)
		Exit Angle	13.4 deg
Length of Transition	25 ft (7.6 m)	Vehicle Accelerations (Max. 0.050-sec Avg)	
Vehicle	1977 Cadillac	Longitudinal	-8.0 g
Vehicle Weight		Lateral	-9.4 g
Test Inertia	4400 lb (1998 kg)	Occupant Impact Velocity	
Gross Static	4570 lb (2075 kg)	Longitudinal	26.7 ft/s (8.1 m/s)
Vehicle Damage Classification		Lateral	22.0 ft/s (10.0 m/s)
TAD	11LFQ6	Occupant Ridedown Accelerations	
CDC	11LFES4	Longitudinal	-3.1 g
Maximum Vehicle Crush	13.0 in (33.0 cm)	Lateral	-11.5 g
Max. Dyn. Rail Deflection	9.6 in (24.4 cm)		
Max. Perm. Rail Deformation	4.8 in (12.2 cm)		

FIGURE 15. SUMMARY OF RESULTS FOR TEST 1

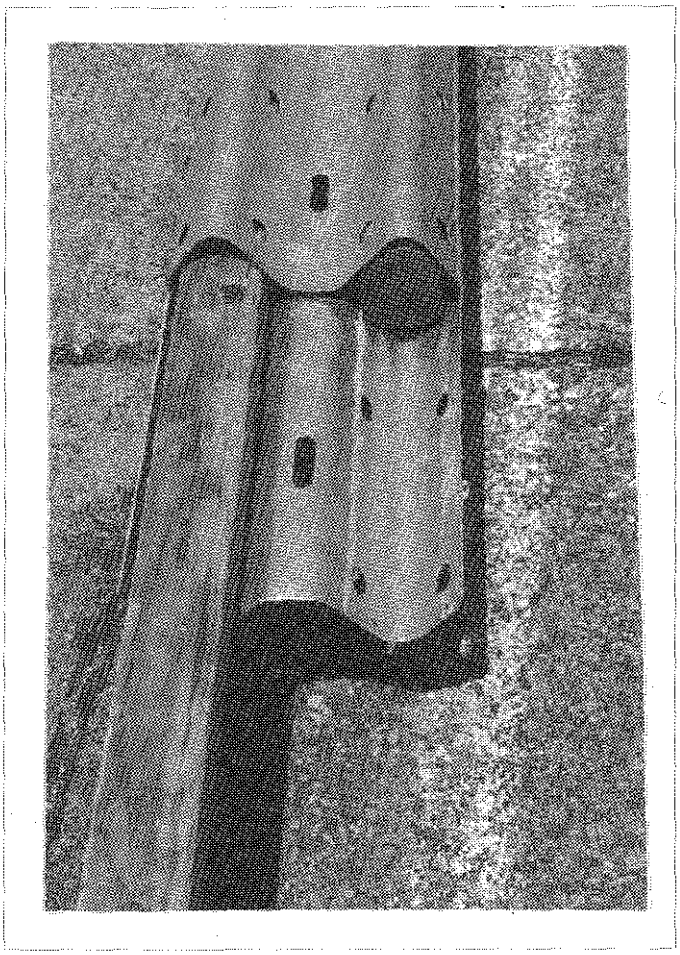

FIGURE 16. WOOD INSERTS FOR TUBULAR W-BEAM

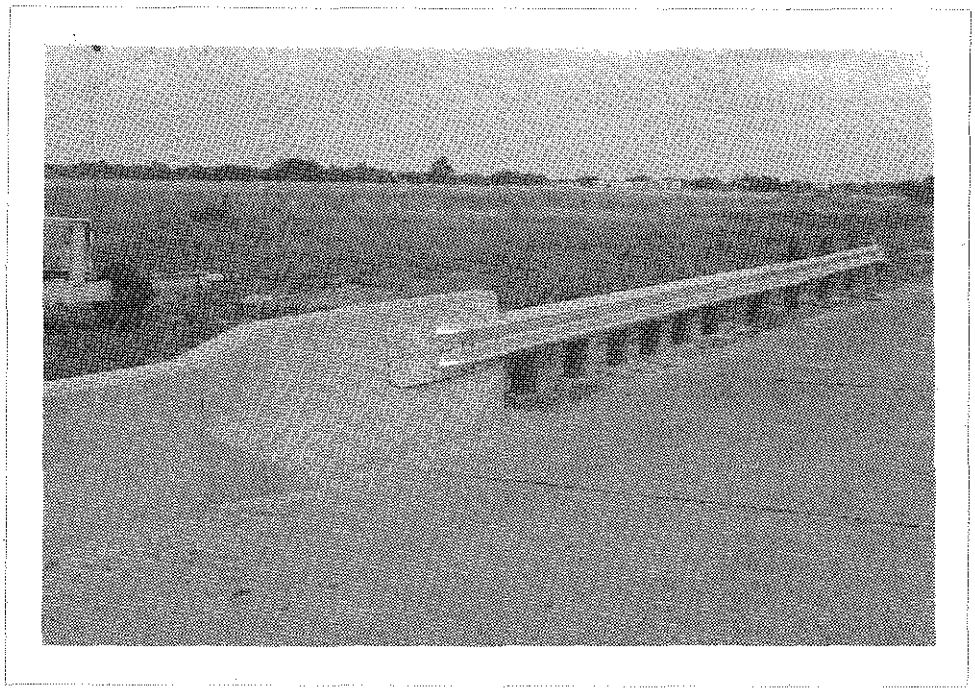

FIGURE 17. TUBULAR W-BEAM TRANSITION TO CSSB, TEST 2 INSTALLATION

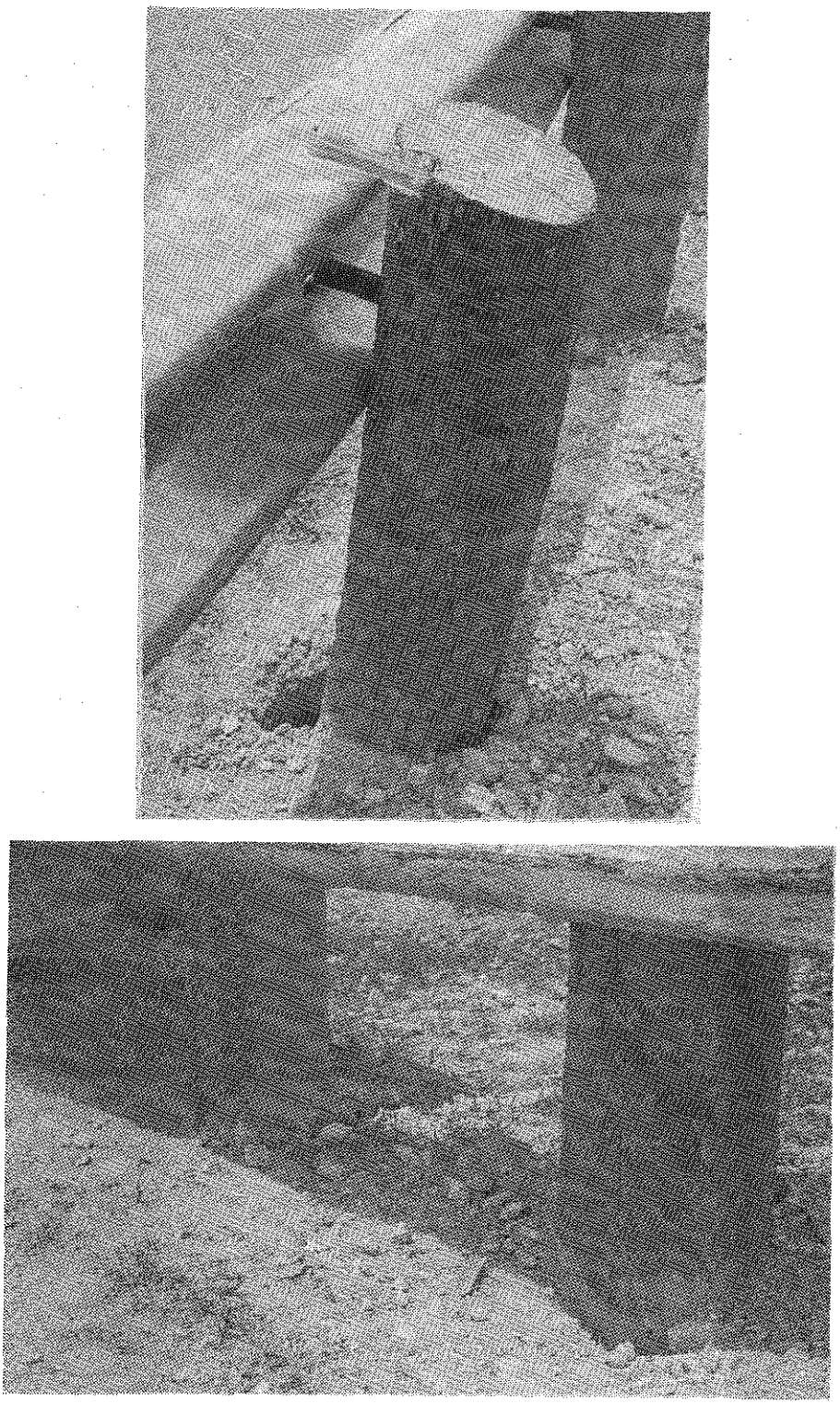

FIGURE 18. EVIDENCE OF SNAGGING ON POSTS AND CONCRETE WALL

The vehicle damage sustained in Test 2 was moderate for the severity of the impact. Damage to the vehicle and barrier after Test 2 is shown in Figure 19. Although not a requirement for the transition test, the occupant impact indices of NCHRP report 230 (2) were all within maximum acceptable limits. A summary of Test 2 results is given in Figure 20.

Test 3

The purpose of this test was to evaluate the performance of the W-beam transition to the tubular W-beam. The guardrail was not blocked out for this test except for the use of two small blockouts as spacers to back up the W-beam after the tubular W-beam terminated. Figure 21 shows the installation before Test 3.

A 4595 lb Cadillac impacted the rail at 61.8 mph and 24.2 degrees. The vehicle was safely redirected although significant wheel snagging was observed at several posts. The wheel snagging caused the post at the splice connection to separate from the rail and the next post downstream to splinter. This wheel snagging can be virtually eliminated by blocking out the railing in the transition region.

Vehicle damage was primarily concentrated in the area of the right front wheel which snagged on a number of posts. Figure 22 shows vehicle damage after Test 3. Barrier damage after Test 3 is shown in Figure 23.

The exit angle and change in velocity of the test vehicle were above the recommended values of NCHRP 230 Evaluation Criteria I (2). Blockouts throughout the length of the transition should greatly improve overall performance and correct the deficiencies mentioned above. Although not required for evaluation of a transition, all of the occupant severity measures from Test 3 were within recommended limits set forth in NCHRP report 230 (2). A summary of the test results is given in Figure 24.

Drawings of the tested transition installation are presented in Appendix D. Sequential photographs and angular displacements for each crash test are given in Appendix E.

Discussion of Results

The tubular W-beam transition was judged to have met the intent of the performance criteria set forth in NCHRP 230 (2). The transition test is, first and foremost, a strength test. In this regard, the tubular W-beam transition has been shown to be able to contain and redirect a 4500 lb vehicle impacting at a high speed and angle.

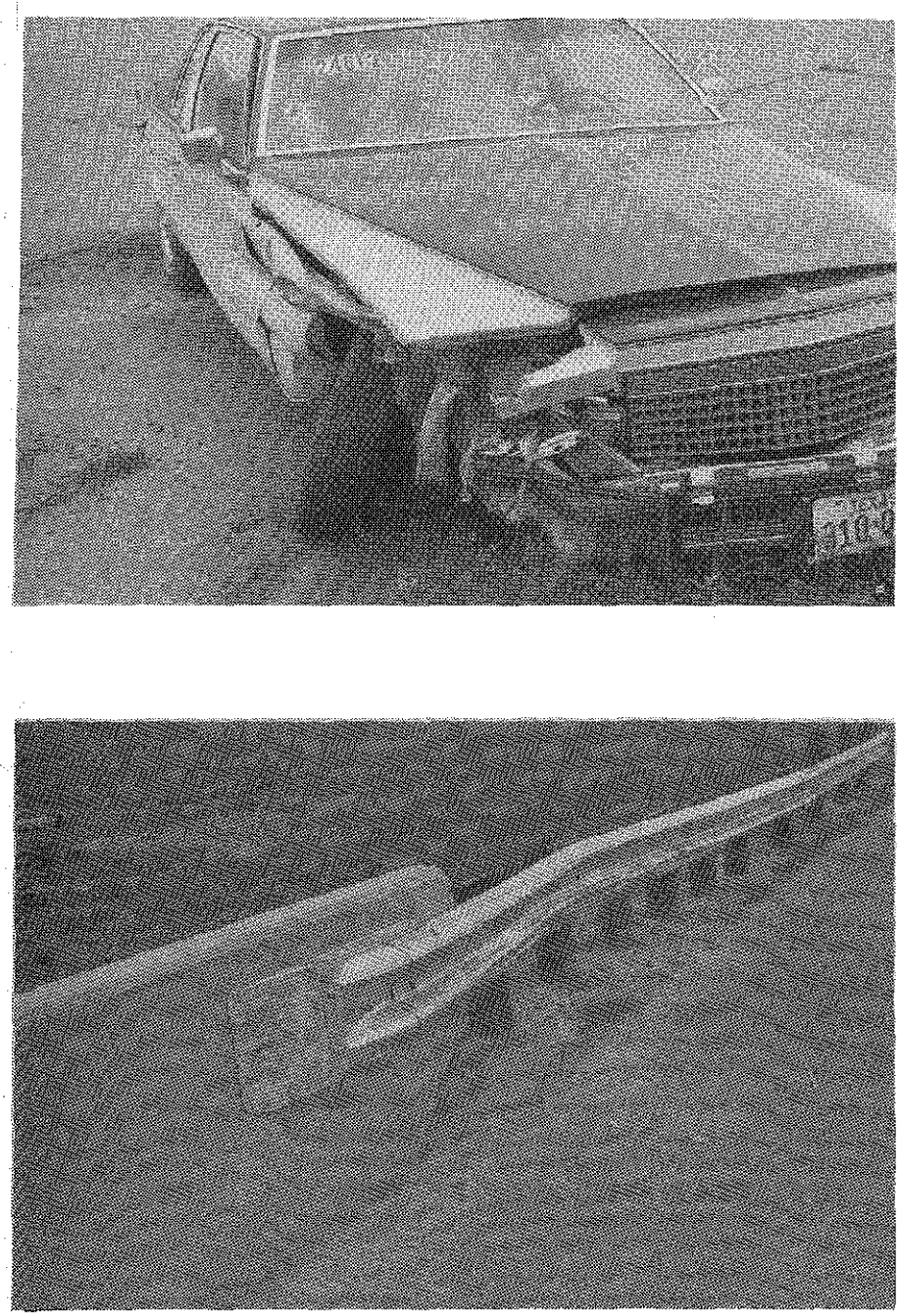

FIGURE 19. VEHICLE AND BARRIER DAMAGE AFTER TEST 2

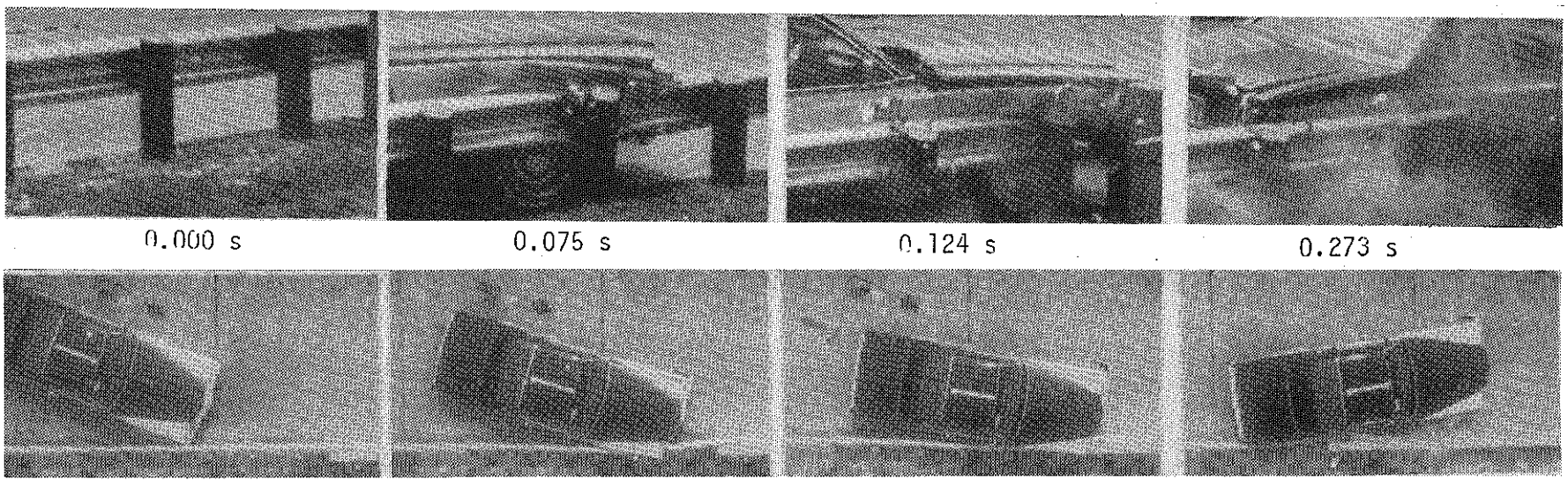

Test No	2461-2	Impact Speed	60.8 mi/h (97.8 km/h)
Date	5/28/87	Impact Angle	25.8 deg
Test Installation	Tubular W-Beam Transition to T501	Exit Speed	41.4 mi/h (66.6 km/h)
		Exit Angle	15.0 deg
Length of Transition	25 ft (7.6 m)	Vehicle Accelerations (Max. 0.050-sec Avg)	
Vehicle	1979 Cadillac	Longitudinal	-7.8 g
Vehicle Weight		Lateral	10.6 g
Test Inertia	4470 lb (2029 kg)	Occupant Impact Velocity	
Gross Static	4637 lb (2105 kg)	Longitudinal	24.6 ft/s (7.5 m/s)
Vehicle Damage Classification		Lateral	24.1 ft/s (7.3 m/s)
TAD	01RFQ5	Occupant Ridedown Accelerations	
CDC	01RYES3	Longitudinal	-2.9 g
Maximum Vehicle Crush	7.0 in (17.8 cm)	Lateral	13.8 g
Max. Dyn. Rail Deflection	9.6 in (24.4 cm)		
Max. Perm. Rail Deformation	6.0 in (15.2 cm)		

FIGURE 20. SUMMARY OF RESULTS FOR TEST 2

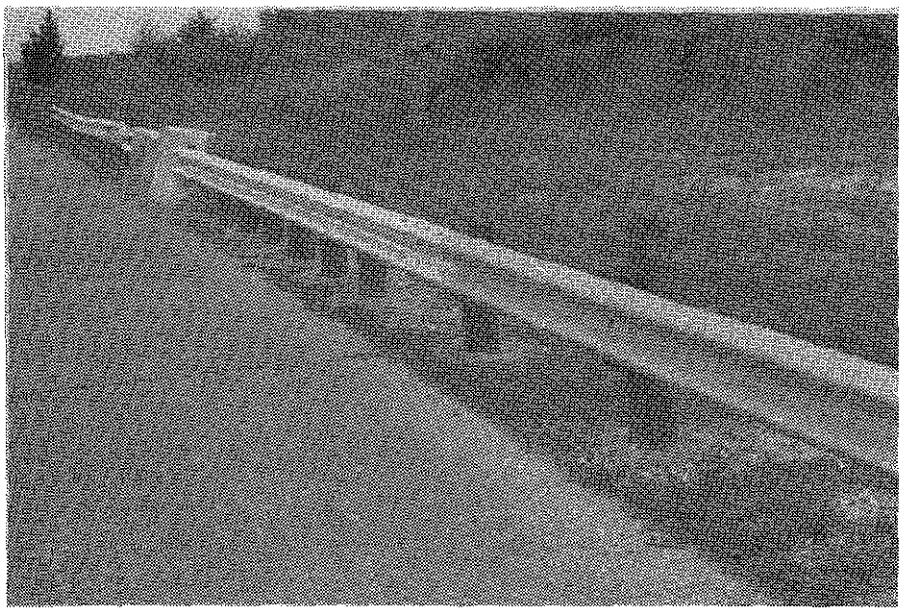

FIGURE 21. W-BEAM TO TUBULAR W-BEAM TRANSITION, TEST 3 INSTALLATION

FIGURE 22. VEHICLE DAMAGE AFTER TEST 3

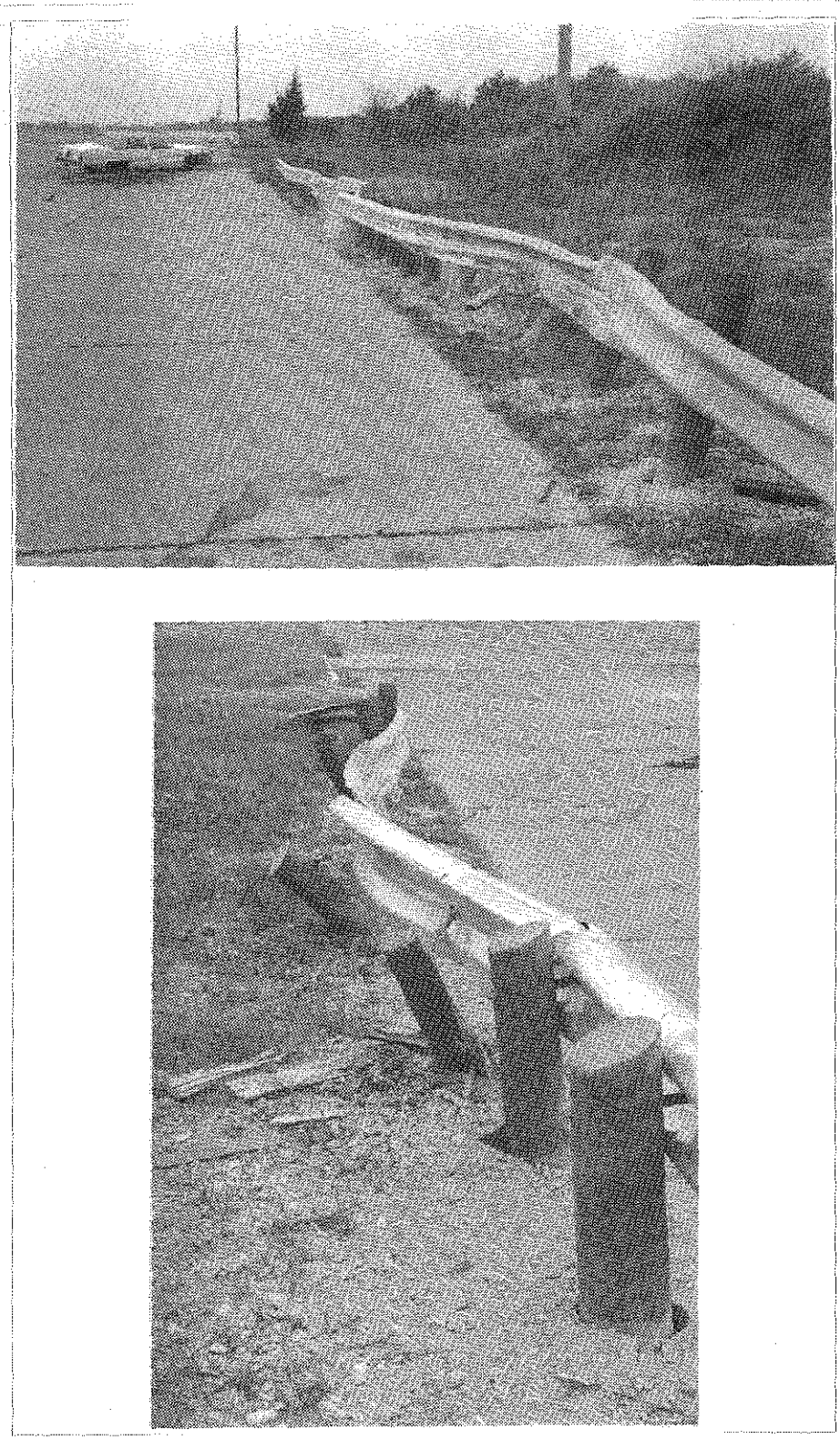

FIGURE 23. BARRIER DAMAGE AFTER TEST 3

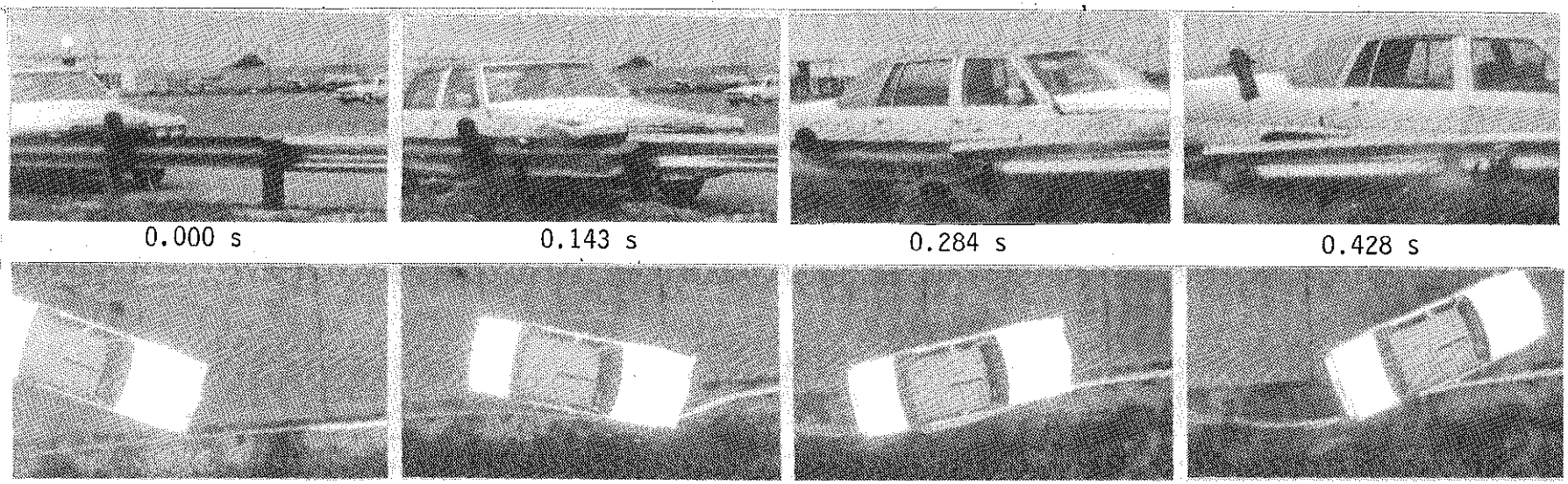

Test No	2461-3	Impact Speed	61.8 mi/h (99.4 km/h)
Date	6/08/87	Impact Angle	24.2 deg
Test Installation	W-Beam Transition to Tubular W-Beam	Exit Speed	33.6 mi/h (54.1 km/h)
		Exit Angle	18.1 deg
Length of Transition	25 ft (7.6 m)	Vehicle Accelerations (Max. 0.050-sec Avg)	
Vehicle	1979 Cadillac	Longitudinal	-6.2 g
Vehicle Weight		Lateral	7.9 g
Test Inertia	4430 lb (2011 kg)	Occupant Impact Velocity	
Gross Static	4595 lb (2086 kg)	Longitudinal	25.7 ft/s (7.8 m/s)
Vehicle Damage Classification		Lateral	17.5 ft/s (5.3 m/s)
TAD	01RFQ5	Occupant Ridedown Accelerations	
CDC	01RYES3	Longitudinal	-10.1 g
Maximum Vehicle Crush	12.0 in (30.5 cm)	Lateral	10.3 g
Max. Dyn. Rail Deflection	2.6 ft (0.8 m)		
Max. Perm. Rail Deformation	2.0 ft (0.6 m)		

FIGURE 24. SUMMARY OF RESULTS FOR TEST 3

It is noted that for all three tests, the change in vehicular velocity exceeded the 15 mph value recommended in NCHRP 230 Evaluation Criteria I (2). Although meeting this criteria is desirable, it is believed that strict compliance to this factor is not critical. This criteria is a subjective evaluation based on whether or not the vehicle is judged to have been redirected into or stopped while in adjacent traffic lanes. In all three crash tests described herein, the test vehicle returned to the side of the road after a short time interval and was not projected across traffic lanes. Depending on the existence and width of a shoulder, the test vehicles may or may not be judged to have briefly encroached on adjacent traffic lanes.

The primary intent of Evaluation Criteria I is to prevent the redirected vehicle from becoming a potential hazard to other traffic. It should be noted that, at this time, there is no definitive evidence that post impact trajectory is a serious problem. Furthermore, impacting the transition at such a severe speed and angle is a low probability event. Although, as stated above, the change in vehicular velocity exceeded the recommended value of 15 mph, the occupant impact velocities and ridedown accelerations were all within maximum acceptable limits (2) for all three tests. This fact suggests that the severity of impact was well within tolerance limits.

V. NEW CONSTRUCTION TRANSITION DESIGN

It should be emphasized that the design which was crash tested is a retrofit of the existing Texas standard transition. The basic tubular W-beam design can be adapted for new construction applications by simply moving the entire single W-beam approach barrier 15 in. closer to the end of the concrete barrier. This adjustment will eliminate the need for a splice plate and will allow the single W-beam to be spliced directly onto the front rail of the tubular W-beam. Furthermore, the posts upstream from the tubular W-beam (i.e. the posts to which the single W-beam approach rail is attached) can be offset 3 in. closer to the roadway. This will eliminate the need for the spacer blocks at the end of the single W-beam.

These two small blockouts upstream of the tubular W-beam are aesthetic in nature. Their purpose is to move the approach rail out to the transition in a gradual manner. The standard Texas guardfence which approaches the transition has passed exsiting test standards (7). Elimination of these blockouts for new construction applications should, therefore, not effect the performance of the W-beam to tubular W-beam transition.

The modifications described above are intended to reduce the number of details in the transition design and, thereby, aid in the ease of field installation. Further changes can be implemented to improve the impact performance of the design. For instance, the exposed end of the concrete bridge rail may be tapered or flared. In the case of a CSSB, the sloped barrier face can first be transitioned to a vertical wall before being tapered. These changes should further reduce the possibility of wheel snagging and would eliminate the need for the wood inserts used in Test 2. Second, block-outs can be provided in the transition region. This would effectively eliminate wheel snagging on guardrail posts and should improve the overall impact performance of the barrier.

A conceptual transition design which utilizes all of the above modifications is shown in Figure 25. Any or all of these variations may be employed to improve upon the retrofit transition. A complete set of construction drawings which detail these changes for new construction applications is given in Appendix F.

NEW CONSTRUCTION
GUARDRAIL / BRIDGE RAIL TRANSITION

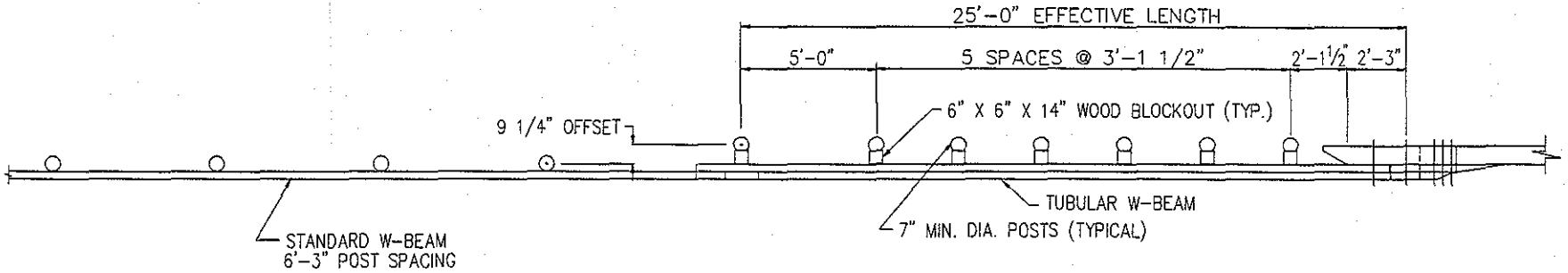

PLAN

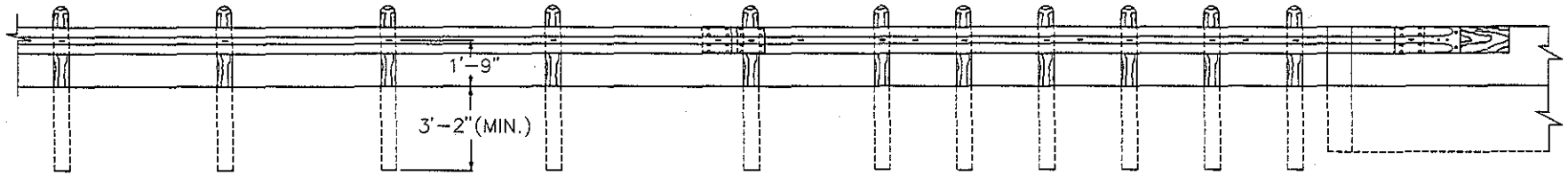

ELEVATION

FIGURE 25. NEW CONSTRUCTION TRANSITION

VI. SHORT-RADIUS GUARDRAIL TREATMENTS

A short-radius guardrail treatment is required whenever an approach condition exists such that the approach rail must be curved in a tight radius away from the main roadway and extended down a secondary roadway. This occurs when a side road or driveway intersects the main roadway in close proximity to a bridge end, thus preventing the approach rail from being extended past the length of need.

Although the need for short-radius guardrail treatments is quite common, there is a lack of acceptable designs from which to choose. An acceptable design can be characterized by two requirements. First, the system must be able to contain a large (4500 lb) vehicle within a reasonable distance. It is often necessary to strictly limit vehicle travel behind the barrier because of the presence of severe hazards. Second, the system must be able to decelerate a small vehicle (1900 lb) such that occupant severity criteria (2) are satisfied.

Consultations with officials from the SDHPT were conducted to help identify design conditions for a short-radius guardrail system. These SDHPT officials expressed interest in developing a short-radius treatment for low speed (40 mph or less), low traffic volume conditions which transitioned from a T6 bridge rail. The Texas type T6 bridge rail consists of a tubular W-beam rail mounted on W6x9 steel posts spaced at 6 ft.-3 in.

Research Approach

The Barrier VII computer program was used to analyze the short-radius guardrail problem. The simulations involved impacts with both 4500 lb and 1900 lb vehicles traveling at 40 mph and impacting the rail at angles up to and including 25 degrees. Four different impact locations were simulated in order to assure that the system was analyzed under the most critical condition. The basic design consisted of a T6 bridge rail transitioning to a curved guardrail with a 10 ft. radius (90 degree bend) and anchored along a secondary roadway with a standard W-beam turndown section. A typical set of Barrier VII input for these design runs is listed in Appendix C.

The major design parameters investigated include guardrail beam strength, post strength, and post spacing. It was evident from previous crash test results (1) that weakened posts should be used along the curved section of guardrail. The purpose of the weakened posts is to allow them to fracture or break away and thus prevent vehicle ramping during head on impacts. This break away mechanism is acheived by drilling two 3 1/2 in. diameter holes through a standard 7 in. diameter round wood post. One hole is located 16 in. below grade and the other is located at ground level. This type of weakened post is commonly referred to as a CRT post.

Since these CRT posts are designed to fracture upon impact, they possess little energy absorbing capability. The spacing of the posts along the curve was, therefore, not a critical variable and a standard post spacing of 6 ft.-3 in. was selected.

Beam strength and stiffness were varied by using the properties of various common guardrail types. Three different guardrails were analyzed for use in a short-radius system. They were: standard W-beam, nested W-beam, and tubular W-beam.

Simulation Results

The results of the Barrier VII simulation runs for the W-beam, nested W-beam, and tubular W-beam are presented in Tables 1, 2, and 3 respectively. These tables give predicted rail deflections, maximum average 50 msec accelerations, and occupant impact velocities for both large and small vehicle impacts.

W-beam - Some potential problems regarding the use of W-beam guardrail for the short-radius treatment became apparent after analysis of the Barrier VII computer output. Plots of the deflected barrier indicated a tendency for the rail to kink at several locations. This kinking could result in fracture of the rail or the formation of a "point" or "spear" which could cause deeper penetration into the vehicle.

Maximum vehicle travel for this system was predicted to be approximately 10 ft. and predicted occupant severity indices were all within maximum acceptable values (2).

Nested W-beam - Simulations of the short-radius guardrail treatment utilizing a nested W-beam had better overall performance than the single W-beam system. Although plots of the deflected shape showed some evidence of kinking, the degree of kinking was considerably less than that found in the previous runs. Furthermore, the possibility of this kinking causing rail fracture is not as acute since the strength of the nested W-beam is twice that of the single W-beam.

Although the predicted occupant severity criteria were higherfor the nested W-beam installation, they were still within maximum acceptable limits. The predicted vehicle travel was approximately 8 ft. for a large sized vehicle.

Tubular W-beam - Plots of the tubular W-beam installation indicated a smooth deflected shape with little evidence of kinking. The increased strength and stiffness of the tubular rail eliminated the problems of kinking, fracture, and vehicle penetration. However, this increased stiffness resulted in higher occupant impact velocities for small car impacts. Predicted occupant severity

W-BEAM

RUN	IMPACT CONDITIONS			MAX. RAIL DEFL.		MAX. 50 MSEC. AVG. ACCEL.		OCCUPANT IMPACT VELOCITY	
#	Vehicle Wt. (lb.)	Speed (mph)	Angle (deg)	X (in.)	Y (in.)	Long. (g)	Lat. (g)	Long. (ft./sec.)	Lat. (ft./sec.)
1	4,500	40	0	80.3	63.7	7.8	2.4	26.3	0.2
2	4,500	40	15	94.6	96.8	5.7	2.5	26.6	3.3
3	4,500	40	25	101.4	119.5	5.3	2.2	24.0	4.0
4	4,500	40	15	88.7	82.2	6.9	1.8	19.8	---
1	1,900	40	0	55.0	36.5	9.7	2.6	32.8	1.9
2	1,900	40	15	53.5	40.5	10.7	1.9	34.2	3.5
3	1,900	40	25	67.0	57.2	11.6	1.4	32.7	3.6
4	1,900	40	15	15.2	50.2	8.7	4.2	28.1	10.0

TABLE 1. BARRIER VII SIMULATION, SHORT-RADIUS GUARDRAIL - W-BEAM

NESTED W-BEAM

RUN	IMPACT CONDITIONS			MAX. RAIL DEFL.		MAX. 50 MSEC. AVG. ACCEL.		OCCUPANT IMPACT VELOCITY	
#	Vehicle Wt. (lb.)	Speed (mph)	Angle (deg)	X (in.)	Y (in.)	Long. (g)	Lat. (g)	Long. (ft./sec.)	Lat. (ft./sec.)
1	4,500	40	0	77.1	60.2	8.7	2.4	28.0	.3
2	4,500	40	15	80.5	80.1	6.5	2.8	27.75	3.4
3	4,500	40	25	91.0	105.4	6.4	2.2	26.6	4.7
4	4,500	40	15	57.3	94.0	9.7	2.3	20.2	6.9
1	1,900	40	0	44.8	26.0	11.6	3.6	35.1	4.1
2	1,900	40	15	44.7	30.5	12.3	2.1	36.7	1.3
3	1,900	40	25	49.1	34.7	13.7	1.8	36.8	.8
*4	1,900	40	15	-12.3	29.1	10.7	5.4	29.3	13.0

* INDICATES VEHICLE REDIRECTED

TABLE 2. BARRIER VII SIMULATION, SHORT RADIUS GUARDRAIL - NESTED W-BEAM

TUBULAR W-BEAM

RUN	IMPACT CONDITIONS			MAX. RAIL DEFL.		MAX. 50 MSEC. AVG. ACCEL.		OCCUPANT IMPACT VELOCITY	
#	Vehicle Wt. (lb.)	Speed (mph)	Angle (deg)	X (in.)	Y (in.)	Long. (g)	Lat. (g)	Long. (ft./sec.)	Lat. (ft./sec.)
1	4,500	40	0	70.5	43.5	9.8	2.1	29.6	1.2
2	4,500	40	15	67.6	52.2	10.1	2.7	30.7	3.9
3	4,500	40	25	76.9	67.6	7.8	2.7	29.7	5.5
*4	4,500	40	15	16.2	53.2	6.1	3.1	20.3	8.0
1	1,900	40	0	32.6	15.2	14.2	4.8	39.0	8.7
2	1,900	40	15	33.0	20.4	15.9	2.3	40.8	2.2
3	1,900	40	25	34.1	20.7	17.0	2.0	42.0	---
*4	1,900	40	15	-12.5	17.1	12.9	7.0	32.3	16.8

* INDICATES VEHICLE REDIRECTED

TABLE 3. BARRIER VII SIMULATION, SHORT RADIUS GUARDRAIL - TUBULAR W-BEAM

measures are very close to the maximum acceptable values (2).

The predicted maximum vehicle travel for the tubular W-beam system was approximately 6 1/2 ft. This distance is significantly less than the travel distance predicted for the W-beam installation. This could be important at constricted sites where the barrier is constructed immediately in front of a severe hazard. It should also be noted that the tubular W-beam was able to redirect both the large and small vehicles when impacting a point higher on the curved section of rail. This corresponds to impact condition 4 on Table 3.

It should be noted that these short-radius treatments are designed for sites where a main roadway intersects a secondary roadway. In these instances, there is sufficient right-of-way beyond the bridge rail to install 20 ft. of guardrail and a standard turndown anchor. This runout distance is an important variable in the short-radius guardrail design. It is essential to provide adequate run out distance along the secondary roadway to prevent vehicle penetration during impacts on the curved guardrail section. Sites at which right-of-way is restricted, such as where a private driveway intersects a road, require a shorter runout distance than provided in the above mentioned designs. It is therefore recommended that further analysis be conducted to develop short-radius guardrail installations with shorter anchorage lengths for use at such sites.

Detailed drawings of both the nested and tubular W-beam short-radius guardrail treatments are given in Appendix G.

VII. CONCLUSIONS AND RECOMMENDATIONS

A guardrail/bridge rail transition from a W-beam to a rigid concrete barrier has been successfully designed and crash tested. A number of favorable characteristics have been incorporated into the design to help insure its acceptance and implementation in both retrofit and new construction applications. The tubular W-beam transition (1) can easily retrofit existing installations, (2) provides sufficient post spacing to allow implementation where bridge end drains are required, and (3) is designed for use with either a vertical concrete parapet or concrete safety shaped barrier.

Although the change in vehicular velocity for the transition tests exceeded the recommended value of Evaluation Criteria I (2), it should be noted that the system which was tested is a retrofit design. In order to maintain compatibility with the standard Texas system, no blockouts were used. It is believed that implementation of the changes recommended for new construction would reduce these numbers to recommended levels.

Because of its improved impact performance, it is recommended that the modified transition with wood inserts be used in conjunction with both the vertical parapet and safety shaped barriers in retrofit situations. The wood inserts are necessary to eliminate the propensity for the tubular beam to collapse. Detailed drawings of the recommended retrofit transition are given in Appendix F.

For new construction applications it is recommended that the end of the concrete bridge rail be tapered or flared thereby reducing the potential for wheel snag. It is further recommended that blockouts be used in the transition region to eliminate post snagging. Use of these modifications should improve the overall impact performance of the transition and may eliminate the need for wood reinforcement of the tubular W-beam. Details of these changes for new construction applications are shown in Appendix G.

Although this system was developed for a 7 in. diameter round wood post, it is believed that it will perform equally well with 6 in. X 8 in. wood or W 6X9 steel posts since they have equivalent lateral strength characteristics.

The transition developed in this study greatly simplifies retrofit operations and offers designers another alternative for new construction projects. Based on the results of the full-scale testing, the tubular W-beam transition is suitable for immediate implementation for field evaluation.

Improved short radius guardrail systems have been developed for low speed and low volume applications where severe hazards near intersections require construction of a protective barrier. Three designs utilizing W-beam, nested W-beam, and tubular W-beam,

respectively, were analyzed and found to provide an acceptable safety performance for use at such sites. The nested W-beam design appears to provide the best overall performance where a minimum 8 ft. of clear recovery area behind the railing is available. At constricted sites where a clear recovery area is not available, the tubular W-beam design is recommended. Although these designs have been carefully analyzed with sophisticated simulation techniques, no crash testing has been conducted to verify the safety performance of any of the designs. Therefore, implementation of any of the designs should be limited to those sites where low speeds and low traffic volumes preclude more costly safety treatments such as moving the intersection. Details of the short radius guardrail designs are shown in Appendix H.

REFERENCES

1. Bronstad, M. E., Calcote, L. R., Ray, M. H., Mayer, J. B., "Guardrail-Bridge Rail Transition Designs," Report No. FHWA/RD-86/178, June 1986.

2. Michie, Jarvis. D., "Recommended Procedures for the Safety Performance Evaluation of Highway Appurtenances," NCHRP REPORT 230, Transportation Research Board, March 1981.

3. Post, Ed, University of Nebraska, Informal Presentation, TRB Committee A2A04 Meeting, January 1987.

4. Powell, G. H., "A Computer Program for Evaluation of Automobile Barrier Systems," Report No. FHWA-RD-73-51. April 1973.

5. Bruce, R. W., Hahn, E. E., Iwankiw, N. R., "Guardrail Vehicle Dynamic Interaction," Report No. FHWA-RD-&&-29, December 1976. (Guard Program)

6. Segal, D. J., "Highway - Vehicle - Object - Simulation - Model--1976," 4 volumes, Report Numbers FHWA-RD-75-162 through 165, February 1976.

7. Sicking, D. L., et al., "Development of New Guardrail End Treatments," Reasearch Report 404-1F, Texas Transportation Institute, Texas A&M University, January 1988.

8. Ross Jr., H. E., "Analysis and Design of Safety Appurtenances by Computer Simulation," Proceedings ASCE Specialty Conference on the Role of the Civil Engineer in Highway Safety, New Orleans, Louisiana, September 1983.

9. Beason, W. Lynn, et al., "A Low-Maintenance, Energy-Absorbing Bridge Rail," Transportation Research Record 1065, Transportation Research Board, Washington, D. C., 1986.

10. Buth, C. E., et. al, "Safer Bridge Railings," 4volumes, Report Numbers FHWA-RD-82-072, 073, 074.1, 074.2, June 1984.

11. Calcote, L. R., "Development of a Cost-Effectiveness Model for Guardrail Selection," Southwest Research Institute Report 03-4309, FHWA contract DOT-FH-11-8827, Nov. 1977.

12. Dewey, Jr. James, F., et.al., "A Study of the Soil Structure Interaction Behavior of Highway Guardrail Posts,"Report No. FHWA/TX-84/12+343-1, July 1983.

APPENDIX A

EVALUATION OF CANDIDATE SIMULATION PROGRAMS

Barrier VII

Barrier VII is a two-dimensional simulation program that models vehicular impacts with deformable barriers (4). The program employs a sophisticated barrier model that is idealized as an assemblage of discrete structural members possessing geometric and material nonlinearities. The available structural members include: beams, cables, posts, columns, springs, links, and damping devices. The vehicle is idealized as a plain rigid body surrounded by a series of discrete inelastic springs. Because of its two-dimensional nature, the program is limited in its ability to predict rollover or vaulting-type behavior of the vehicle. It also suffers from an inability to predict such problems as vehicle underride and sheet metal snagging on barrier components. These limitations notwithstanding, Barrier VII has been used successfully as a design tool in the development and analysis of various longitudinal barrier systems (8,9). During the course of its application, the program has been validated against a wide range of test data and good correlation was observed, especially for tests that exhibited two-dimensional response.

As mentioned previously, a guardrail-to-bridge rail transition must be designed to prevent impacting vehicles from deflecting the guardrail sufficiently to allow vehicle snagging on the end of the rigid barrier. A 4500 lb. automobile impacting at a high speed and angle is the critical test of a transition design (2). The Barrier VII simulation model has been shown to be capable of accurately predicting barrier response for these types of impact.

GUARD

GUARD is a three-dimensional vehicle-barrier program (5). A primary objective in its original development was an evaluation of the effects of the energy absorbing automobile bumper on the performance of widely used longitudinal barrier systems. It employs a finite element idealization of the barrier. The vehicle model permits interaction between the "sheet metal" and the barrier, the tires and rigid barriers, and the bumper and the barrier. GUARD's idealization of the vehicle's tire/suspension system is a simple bilinear spring. This model can only detect tire deflection immediately below the center of the wheel hub and, therefore, cannot accurately predict radial or circumferential tire forces. Although wheel snag can be indirectly determined from a GUARD simulation, the program is unable to allow the tires to interact with guardrail posts.

Use of GUARD to date has been somewhat limited. This has been attributed to problems encountered with coding errors and numerical stability of the solution scheme. These errors make use of the program very costly in terms of professional and computer time required to obtain a successful simulation. The majority of the

validation work that has been performed on GUARD has been limited to small vehicles and small impact angles. Very little validation work has been done for the more severe impact conditions required to evaluate the strength of a barrier system.

HVOSM

The Highway-Vehicle-Object-Simulation-Model (HVOSM) (6) was developed to simulate the three-dimensional behavior of a vehicle as it interacts with roadway and/or roadside features. The program employs a more sophisticated vehicle model than any other simulation program available today. A complex vehicle suspension model is capable of simulating all combinations of independent and solid axle suspension arrangements. The tire model in HVOSM is comprised of a thin disk containing a group of springs radiating from the center of the wheel. Although this tire model does a good job of predicting forces generated on the face of the tire, the program does not have the capability to allow the tire to interact with guardrail posts or other barrier components. Due to the sophistication of the vehicle model, a relatively large number of vehicle parameters are required as input and are sometimes difficult to acquire.

HVOSM is best suited for nonimpact type events. The program's worst problems arise from its poor flexible barrier model and impact routine. The barrier is modeled by an equivalent stiffness function. This equivalent stiffness function (force vs. deflection curve) must somehow be determined or estimated and then input into the program. This aspect of HVOSM is very difficult to work with and has not been sufficiently validated to use with any confidence.

Program Selection

An effective transition is one which limits dynamic deflections and minimizes vehicle snagging in the transition zone. Consequently, a major criterion in the selection of a simulation program was the ability to accurately predict maximum dynamic deflection of the rail. In some instances, barriers which may be idealized identically by a program for simulation purposes, may in fact perform quite differently in actual full scale tests due to differences in structural details. It was therefore essential for the program to have a sophisticated barrier model.

Evaluation of the impact performance of a transition is based on the results of a strength test with a 4500 lb vehicle impacting the rail at 60 mph and at an angle of 25 degrees (2). It has been observed that large vehicle impacts of this nature generally exhibit two-dimensional behavior. Therefore, for such impacts into barriers placed on flat terrain, vehicle vaulting, override, and underride are of little concern. It was thus determined that a 3-D model was not necessary for the accurate simulation of the barrier systems

evaluated in this study.

The problem of vehicle snagging is also an important consideration in transition design. The analysis of such vehicle/barrier interaction is very complex. While all of the aforementioned programs can indirectly predict wheel snagging on guardrail posts and on the bridge rail end by tracking wheel trajectory, none of these programs are capable of accurately simulating this interaction. Subsequently, a sophisticated tire/suspension model was not regarded as a criterion for the program selection.

Based on these considerations, Barrier VII was chosen as the simulation program for use in developing the new transition design. The Barrier VII simulation model employs a sophisticated flexible barrier model which was ideal for use in simulating impacts into transition and approach barriers. It has been shown to be capable of accurately predicting barrier deflections under severe impact conditions. Further, for impacts into barriers placed on flat terrain, such as that found on the approach to a bridge, vehicle vaulting, override, and underride are of little concern. Thus the 2-D nature of the Barrier VII program was not considered to be a severe limitation in its ability to evaluate the strength and performance of a transition system. In addition, the program has been shown to have a very stable solution scheme.

APPENDIX B

BARRIER VII VALIDATION

Although Barrier VII has been successfully used to simulate impacts with a variety of flexible barriers, its use in studying impacts near the transition from a flexible to a rigid barrier has been somewhat limited. Therefore, one of the first steps taken in the development of a new transition was to conduct a validation of Barrier VII for analysis of impacts in these regions. Before the validation runs could begin, however, it was necessary to determine Barrier VII's input parameters, including rail, post, and vehicle properties.

Vehicle Parameters

When preliminary runs were made, it was evident from vehicle/barrier plots that the vehicle input parameters being used resulted in excessive vehicle crush. Comparison of the program output with crash test photographs indicated that the vehicle deformations obtained from Barrier VII were unrealistic and that new vehicle input parameters were required.

The vehicle model in Barrier VII is idealized as a plane body of arbitrary shape surrounded by discrete, inelastic springs. These springs define possible contact points at which the automobile may interact with the barrier. The unit stiffnesses assigned to these contact points act over a specified tributary width and are user defined. New vehicle stiffnesses were calibrated for this study by simulating the impact of the vehicle into a rigid wall. A comparison was then made between the vehicle deformations obtained from Barrier VII output and actual vehicle crush measurements obtained from the results of full-scale crash tests. Use of the rigid wall tests eliminated the beam and post parameters as variables in the solution scheme and allowed a more direct analysis of vehicle deformation versus contact stiffness.

The crash tests used for recalibrating the vehicle parameters were tests 33 and 36 of reference 9. These tests involved impacts with large vehicles (4500 lb.) traveling 60 mph and impacting a rigid concrete wall at 25 degrees. Barrier VII output was compared to crush measurements averaged from these two full scale tests. As shown in Figure B-1, the new vehicle stiffnesses were found to give very good predictions of vehicle crush. Other values, such as exit velocity and time for the vehicle to become parallel, also showed good correlation, further indicating that the new vehicle parameters were reasonable. Vehicle parameters for the small car (1900 lb.) were similarly obtained using results from tests 29 and 37 (10).

Barrier Members

Along with the vehicle parameters, both beam and posts properties had to be determined for input into Barrier VII. Simulated guardrail beam elements were assumed to be of uniform cross section and to have bilinear elastic/perfectly plastic properties

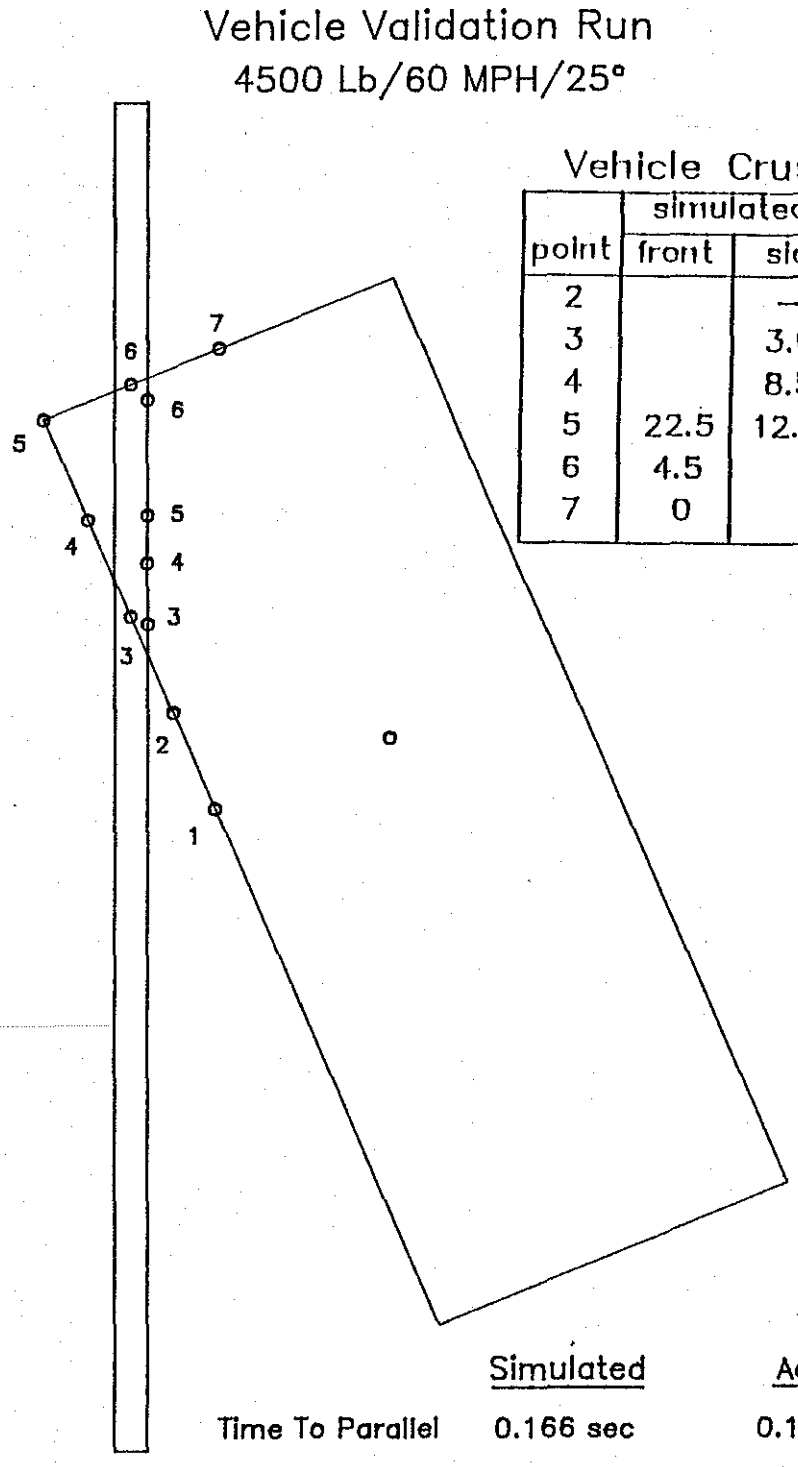

Vehicle Crush (inches)

point	simulated		actual	
	front	side	front	side
2		–		2.1
3		3.0		2.5
4		8.5		–
5	22.5	12.5	19.25	10.6
6	4.5		9.25	
7	0		0	

	Simulated	Actual
Time To Parallel	0.166 sec	0.185 sec
Exit Speed	44.5 mph	44.1 mph

FIGURE B–1. VEHICLE STIFFNESS VALIDATION

both flexurally and extensionally. Simulated beam stiffness characteristics were estimated to be approximately 1.5 times calculated static values.

Specifying post properties was a much more complex problem. Stiffness for elastic horizontal deflections, base yield moments, shear forces to failure, and deflections to failure all had to be specified as input to the program for both the longitudinal and lateral directions. A deflection failure represents separation of the rail from the post or withdrawal of the post from the ground. A shear failure represents fracture of a weakened post or separation of the post from a break-away base. All of these parameters are difficult to define by analytical means because of the wide variance in the material properties and behavior of both the wood posts and surrounding soil. The analysis is further complicated by the dynamic impact loading and its effects on soil-post interaction.

Because of these complexities, the guardrail posts were characterized using experimental data obtained from a series of pendulum and dynamic load tests found in references 1, 11, and 12. These tests were conducted with various sized wood and steel posts embedded in various types of soil. Table B-1 shows the simulated post properties obtained from these tests.

Validation Runs

Having determined the program input parameters, the validation study was conducted. Two full scale crash tests of guardrail-to-bridge rail transitions from reference 1 were selected for the validation effort. Since barrier deflection is the primary indicator of the propensity for a vehicle to snag on the end of a concrete barrier, this parameter was selected as the primary measure of correlation between simulation and crash testing. As shown in Table B-2, Barrier VII was found to give very close predictions of maximum barrier deflections for the tests that were simulated. Other measures of simulation validity, including vehicle trajectory and crush, also showed excellent correlation between Barrier VII and the two crash tests.

TABLE B–1. POST PARAMETERS FOR BARRIER VII INPUT

(Effective Rail Height = 21")

MATERIAL	WOOD	WOOD	STEEL
SIZE	6" X 8" (1)	7" DIAM. (7)	W6 X 8.5 (1)
k_A (k/in.)	1.95	2.9	1.15
k_B (k/in.)	1.56	2.9	2.46
M_A (in–k)	191.1	256.	256.2
M_B (in–k)	214.2	256.	107.1
F_A (k)	10.2	12.2	5.1
F_B (k)	9.1	12.2	12.2
Δ_A (in.)	4.7	18.	13.6
Δ_B (in.)	15.5	18.	13.2

A – Denotes Longitudinal or Major Axis

B – Denotes Transverse or Minor Axis

k – Stiffness of Post For Elastic Horizontal Deflections

M – Base Moment At Which Post Yields

F – Shear Force Causing Failure of Post

Δ – Deflection Causing Failure of Post

TABLE B-2. BARRIER VII CRASH TEST SIMULATIONS

TEST NO.	DESCRIPTION	CONCRETE WINGWALL	IMPACT DATA LB/MPH/DEG	IMPACT POINT FROM WINGWALL	MAXIMUM LATERAL DEFLECTION ACTUAL	SIMULATED	% DIFF
T-1 (1)	THRIE BEAM BRIDGE TRANSITION	STRAIGHT	4658/61.5/25.2	96.5"	9.4"	9.92"	5.5
T-2 (1)	THRIE BEAM BRIDGE TRANSITION	TAPERED w/ WOOD BLOCK OUT	4650/64.0/25.6	112.5"	14.4"	14.74"	2.4

APPENDIX C

BARRIER VII INPUT

```
1BARRIER VII  -  ANALYSIS OF AUTOMOBILE BARRIERS  -  U.C. BERKELEY,  1972

 ************************************************************************

OCONTROL INFORMATION

 NUMBER OF BARRIER NODES              =    39
 NUMBER OF CONTROL NODES              =     5
 NUMBER OF NODE GENERATIONS           =     4

 NUMBER OF INTERFACES                 =     1

 NUMBER OF MEMBERS                    =    57
 NUMBER OF MEMBER GENERATIONS         =     9
 NUMBER OF DIFFERENT MEMBER SERIES    =     2

 NUMBER  OF ADDITIONAL WEIGHT SETS    =     0

OBASIC TIME STEP (SEC)                =    .00100
 LARGEST ALLOWABLE TIME STEP (SEC)    =    .00100
 MAXIMUM TIME SPECIFIED (SEC)         =    .20000
 MAX. NO. OF STEPS WITH NO CONTACT    =   100

 OVERSHOOT INDEX                      =     0
 ROTATIONAL DAMPING MULTIPLIER        =  1.00

 STEP-BY-STEP INTEGRATION TYPE        =     1


 OUTPUT FREQUENCIES

 AUTOMOBILE DATA      =  1
 BARRIER DEFLECTIONS  = 10
 BARRIER FORCES       = 10

 ENERGY BALANCE       = 10

 CONTACT INFORMATION  = 10

 PUNCHED JOINT DATA   =  0
 PUNCHED TRAJECTORY   =  0
1CONTROL NODE COORDINATES (IN)

 NODE         X-ORD         Y-ORD

    1           .00           .00
    7        450.00           .00
   19        600.00           .00
   35        750.00           .00
   39       1230.00           .00
```

FIGURE C-1. TYPICAL BARRIER VII INPUT FOR TRANSITION RUNS

COORDINATE GENERATION COMMANDS

FIRST NODE	LAST NODE	NO. OF NODES	NODE DIFF	DISTANCE
1	7	5	1	75.00
7	19	11	1	12.50
19	35	15	1	9.38
35	39	3	1	120.00

1NODE COORDINATES (IN)

NODE	X-ORD	Y-ORD
1	.00	.00
2	75.00	.00
3	150.00	.00
4	225.00	.00
5	300.00	.00
6	375.00	.00
7	450.00	.00
8	462.50	.00
9	475.00	.00
10	487.50	.00
11	500.00	.00
12	512.50	.00
13	525.00	.00
14	537.50	.00
15	550.00	.00
16	562.50	.00
17	575.00	.00
18	587.50	.00
19	600.00	.00
20	609.38	.00
21	618.75	.00
22	628.13	.00
23	637.50	.00
24	646.88	.00
25	656.25	.00
26	665.63	.00
27	675.00	.00
28	684.38	.00
29	693.75	.00
30	703.13	.00
31	712.50	.00
32	721.88	.00
33	731.25	.00
34	740.63	.00
35	750.00	.00
36	870.00	.00
37	990.00	.00
38	1110.00	.00
39	1230.00	.00

1CONTACT INTERFACES

FIGURE C-1. CONTINUED

INTERFACE 1

NO. OF NODES = 33, FRICTION COEFF. = .300

LIST OF NODES

39	38	37	36	35	34	33	32	31	30
29	28	27	26	25	24	23	22	21	20
19	18	17	16	15	14	13	12	11	10
9	8	7							

1BEAM ELEMENTS, 100 SERIES

TYPE NUMBER	=	1	2	3	4
M. OF I. (IN4)	=	2.330E+00	1.642E+01	1.642E+01	1.000E+04
AREA (IN2)	=	1.990E+00	3.980E+00	3.980E+00	1.000E+02
LENGTH (IN)	=	7.500E+01	1.250E+01	9.375E+00	1.200E+02
YOUNGS MODULUS (KSI)	=	3.000E+04	3.000E+04	3.000E+04	3.000E+06
WEIGHT (LB/FT)	=	6.770E+00	1.353E+01	1.353E+01	5.000E+02
YIELD FORCE (K)	=	1.075E+02	2.149E+02	2.149E+02	1.000E+04
YIELD MOMENT (K.IN)	=	7.400E+01	2.727E+02	2.727E+02	1.000E+04
YIELD ACCURACY LIMIT	=	1.000E-01	1.000E-01	1.000E-01	1.000E-01

1POSTS, 300 SERIES

TYPE NUMBER	=	1	2	3
HEIGHT OF NODE I (IN)	=	2.100E+01	2.100E+01	2.100E+01
HEIGHT OF NODE J (IN)	=	.000E+00	.000E+00	.000E+00
A AXIS STIFFNESS (K/IN)	=	1.500E+01	2.900E+00	1.000E+02
B AXIS STIFFNESS (K/IN)	=	2.900E+00	2.900E+00	1.000E+03
EFFECTIVE WEIGHT (LB)	=	5.100E+01	5.100E+01	3.000E+02
B AXIS YIELD MOMENT (K.IN)	=	1.000E+04	2.560E+02	1.000E+04
A AXIS YIELD MOMENT (K.IN)	=	1.000E+04	2.560E+02	1.000E+04
YIELD ACCURACY LIMIT	=	1.000E-01	1.000E-01	1.000E-01
A SHEAR AT FAILURE (K)	=	1.000E+04	2.000E+01	1.000E+04
B SHEAR AT FAILURE (K)	=	1.000E+04	2.000E+01	1.000E+04
A DEFLN AT FAILURE (IN)	=	1.000E+04	2.000E+01	1.000E+04
B DEFLN AT FAILURE (IN)	=	1.000E+04	2.000E+01	1.000E+04

1MEMBER GENERATION COMMANDS

FIRST MEMBER	NODE I	NODE J	LAST MEMBER	NODE DIFF	TYPE NO.	PRESTRESS DATA 1	2	3	4	5
1	1	2	6	1	101	.000	.000	.000	.000	.000
7	7	8	18	1	102	.000	.000	.000	.000	.000
19	19	20	34	1	103	.000	.000	.000	.000	.000
35	35	36	38	1	104	.000	.000	.000	.000	.000
39	1	0	0	0	301	.000	.000	.000	.000	.000
40	2	0	45	1	302	.000	.000	.000	.000	.000
46	10	0	49	3	302	.000	.000	.000	.000	.000
50	23	0	52	4	302	.000	.000	.000	.000	.000
53	35	0	57	1	303	.000	.000	.000	.000	.000

1COMPLETE MEMBER DATA

FIGURE C-1. CONTINUED

BEAMS, 100 SERIES

MEMBER	NODE I	NODE J	TYPE	FORCE	I-MOMENT	J-MOMENT
1	1	2	101	.00	.00	.00
2	2	3	101	.00	.00	.00
3	3	4	101	.00	.00	.00
4	4	5	101	.00	.00	.00
5	5	6	101	.00	.00	.00
6	6	7	101	.00	.00	.00
7	7	8	102	.00	.00	.00
8	8	9	102	.00	.00	.00
9	9	10	102	.00	.00	.00
10	10	11	102	.00	.00	.00
11	11	12	102	.00	.00	.00
12	12	13	102	.00	.00	.00
13	13	14	102	.00	.00	.00
14	14	15	102	.00	.00	.00
15	15	16	102	.00	.00	.00
16	16	17	102	.00	.00	.00
17	17	18	102	.00	.00	.00
18	18	19	102	.00	.00	.00
19	19	20	103	.00	.00	.00
20	20	21	103	.00	.00	.00
21	21	22	103	.00	.00	.00
22	22	23	103	.00	.00	.00
23	23	24	103	.00	.00	.00
24	24	25	103	.00	.00	.00
25	25	26	103	.00	.00	.00
26	26	27	103	.00	.00	.00
27	27	28	103	.00	.00	.00
28	28	29	103	.00	.00	.00
29	29	30	103	.00	.00	.00
30	30	31	103	.00	.00	.00
31	31	32	103	.00	.00	.00
32	32	33	103	.00	.00	.00
33	33	34	103	.00	.00	.00
34	34	35	103	.00	.00	.00
35	35	36	104	.00	.00	.00
36	36	37	104	.00	.00	.00
37	37	38	104	.00	.00	.00
38	38	39	104	.00	.00	.00

POSTS, 300 SERIES

MEMBER	NODE I	NODE J	TYPE	A-SHEAR	B-SHEAR	B-MOMENT	A-MOMENT	ANGLE
39	1	0	301	.00	.00	.00	.00	.00
40	2	0	302	.00	.00	.00	.00	.00
41	3	0	302	.00	.00	.00	.00	.00
42	4	0	302	.00	.00	.00	.00	.00

FIGURE C-1. CONTINUED

43	5	0	302	.00	.00	.00	.00	.00
44	6	0	302	.00	.00	.00	.00	.00
45	7	0	302	.00	.00	.00	.00	.00
46	10	0	302	.00	.00	.00	.00	.00
47	13	0	302	.00	.00	.00	.00	.00
48	16	0	302	.00	.00	.00	.00	.00
49	19	0	302	.00	.00	.00	.00	.00
50	23	0	302	.00	.00	.00	.00	.00
51	27	0	302	.00	.00	.00	.00	.00
52	31	0	302	.00	.00	.00	.00	.00
53	35	0	303	.00	.00	.00	.00	.00
54	36	0	303	.00	.00	.00	.00	.00
55	37	0	303	.00	.00	.00	.00	.00
56	38	0	303	.00	.00	.00	.00	.00
57	39	0	303	.00	.00	.00	.00	.00

STIFFNESS MATRIX STORAGE

REQUIRED = 702
ALLOCATED = 6000
1AUTOMOBILE PROPERTIES

WEIGHT (LB)	=	4500.0
MOMENT OF INERTIA (LB.IN.SEC2)	=	47000.0
NO. OF CONTACT POINTS	=	15
NO. OF UNIT STIFFNESSES	=	1
NO. OF WHEELS	=	4
BRAKE CODE (1=ON, 0=OFF)	=	0
NO. OF OUTPUT POINTS	=	2

UNIT STIFFNESSES (K/IN/IN)

NO.	BEFORE BOTTOMING	AFTER BOTTOMING	UNLOADING	BOTTOMING DISTANCE
1	.040	.250	.330	12.00

CONTACT POINT DATA

POINT	R COORD	S COORD	STIFFNESS NO.	TRIBUTARY LENGTH	INTERFACE CONTACTS			
1	-122.00	40.00	1	31.00	1	0	0	0
2	-91.00	40.00	1	31.00	1	0	0	0

FIGURE C-1. CONTINUED

3	-60.00	40.00	1	31.00	1	0	0	0
4	-30.00	40.00	1	30.00	1	0	0	0
5	.00	40.00	1	27.00	1	0	0	0
6	-67.00	31.00	1	1.00	0	0	0	0
7	23.00	40.00	1	23.00	1	0	0	0
8	46.00	40.00	1	23.00	1	0	0	0
9	69.00	40.00	1	23.00	1	0	0	0
10	93.00	40.00	1	22.00	1	0	0	0
11	93.00	20.00	1	20.00	1	0	0	0
12	93.00	.00	1	20.00	1	0	0	0
13	57.00	31.00	1	1.00	0	0	0	0
14	93.00	-40.00	1	1.00	0	0	0	0
15	-122.00	-40.00	1	1.00	0	0	0	0

OWHEEL COORDINATES (IN), STEER ANGLES (DEG), AND DRAG FORCES (LB)

POINT	R-ORD	S-ORD	STEER ANGLE	DRAG FORCE
1	57.00	31.00	.00	608.00
2	57.00	-31.00	.00	608.00
3	-67.00	31.00	.00	517.00
4	-67.00	-31.00	.00	517.00

OOUTPUT POINT COORDINATES (IN)

POINT	R-ORD	S-ORD
1	.00	.00
2	93.00	.00

1INITIAL POSITION AND VELOCITIES OF AUTO

SPECIFIED BOUNDARY POINT	=	10
X ORDINATE OF POINT	=	637.50
Y ORDINATE OF POINT	=	.00
ANGLE FROM X AXIS TO R AXIS (DEG)	=	25.00
VELOCITY IN R DIRECTION (M.P.H)	=	60.00
VELOCITY IN S DIRECTION (M.P.H)	=	.00
ANGULAR VELOCITY (RAD/SEC)	=	.000
MINIMUM RESULTANT VELOCITY (M.P.H)	=	5.00
TRANSLATIONAL KINETIC ENERGY (K.IN)	=	6500.15
ROTATIONAL KINETIC ENERGY (K.IN)	=	.00
TOTAL INITIAL KINETIC ENERGY (K.IN)	=	6500.15

FIGURE C-1. CONTINUED

```
1BARRIER VII  -  ANALYSIS OF AUTOMOBILE BARRIERS  -  U.C. BERKELEY,  1972

 ************************************************************************


0CONTROL INFORMATION


 NUMBER OF BARRIER NODES              =    63
 NUMBER OF CONTROL NODES              =    25
 NUMBER OF NODE GENERATIONS           =     3

 NUMBER OF INTERFACES                 =     1

 NUMBER OF MEMBERS                    =    76
 NUMBER OF MEMBER GENERATIONS         =    10
 NUMBER OF DIFFERENT MEMBER SERIES    =     2

 NUMBER  OF ADDITIONAL WEIGHT SETS    =     0

0BASIC TIME STEP (SEC)                =    .00100
 LARGEST ALLOWABLE TIME STEP (SEC)    =    .00100
 MAXIMUM TIME SPECIFIED (SEC)         =    .40000
 MAX. NO. OF STEPS WITH NO CONTACT    =   100

 OVERSHOOT INDEX                      =     0
 ROTATIONAL DAMPING MULTIPLIER        =  1.00

 STEP-BY-STEP INTEGRATION TYPE        =     1



 OUTPUT FREQUENCIES

 AUTOMOBILE DATA      =  1
 BARRIER DEFLECTIONS  =  10
 BARRIER FORCES       =  0

 ENERGY BALANCE       =  0

 CONTACT INFORMATION  =  0

 PUNCHED JOINT DATA   =  0
 PUNCHED TRAJECTORY   =  0
1CONTROL NODE COORDINATES (IN)

 NODE         X-ORD         Y-ORD

    1           .00        412.50
    2           .00        112.50
```

FIGURE C-2. TYPICAL BARRIER VII INPUT FOR SHORT-RADIUS GUARDRAIL RUNS

14	.00	.00
15	.37	-9.42
16	1.48	-18.77
17	3.32	-28.01
18	5.87	-37.08
19	9.13	-45.92
20	13.08	-54.48
21	17.68	-62.70
22	22.92	-70.53
23	28.75	-77.93
24	35.15	-84.85
25	42.07	-91.25
26	49.47	-97.08
27	57.30	-102.32
28	65.52	-106.92
29	74.08	-110.87
30	82.92	-114.13
31	91.99	-116.68
32	101.23	-118.52
33	110.59	-119.63
34	120.00	-120.00
58	345.00	-120.00
63	720.00	-120.00

COORDINATE GENERATION COMMANDS

FIRST NODE	LAST NODE	NO. OF NODES	NODE DIFF	DISTANCE
2	14	11	1	.00
34	58	23	1	.00
58	63	4	1	.00

1NODE COORDINATES (IN)

NODE	X-ORD	Y-ORD
1	.00	412.50
2	.00	112.50
3	.00	103.13
4	.00	93.75
5	.00	84.38
6	.00	75.00
7	.00	65.63
8	.00	56.25
9	.00	46.88
10	.00	37.50
11	.00	28.13
12	.00	18.75
13	.00	9.38
14	.00	.00

FIGURE C-2. CONTINUED

```
 15          .37        -9.42
 16         1.48       -18.77
 17         3.32       -28.01
 18         5.87       -37.08
 19         9.13       -45.92
 20        13.08       -54.48
 21        17.68       -62.70
 22        22.92       -70.53
 23        28.75       -77.93
 24        35.15       -84.85
 25        42.07       -91.25
 26        49.47       -97.08
 27        57.30      -102.32
 28        65.52      -106.92
 29        74.08      -110.87
 30        82.92      -114.13
 31        91.99      -116.68
 32       101.23      -118.52
 33       110.59      -119.63
 34       120.00      -120.00
 35       129.38      -120.00
 36       138.75      -120.00
 37       148.13      -120.00
 38       157.50      -120.00
 39       166.88      -120.00
 40       176.25      -120.00
 41       185.63      -120.00
 42       195.00      -120.00
 43       204.38      -120.00
 44       213.75      -120.00
 45       223.13      -120.00
 46       232.50      -120.00
 47       241.88      -120.00
 48       251.25      -120.00
 49       260.63      -120.00
 50       270.00      -120.00
 51       279.38      -120.00
 52       288.75      -120.00
 53       298.13      -120.00
 54       307.50      -120.00
 55       316.88      -120.00
 56       326.25      -120.00
 57       335.63      -120.00
 58       345.00      -120.00
 59       420.00      -120.00
 60       495.00      -120.00
 61       570.00      -120.00
 62       645.00      -120.00
 63       720.00      -120.00
1CONTACT INTERFACES
```

FIGURE C-2. CONTINUED

INTERFACE 1

NO. OF NODES = 40, FRICTION COEFF. = .300

LIST OF NODES

50	49	48	47	46	45	44	43	42	41
40	39	38	37	36	35	34	33	32	31
30	29	28	27	26	25	24	23	22	21
20	19	18	17	16	15	14	13	12	11

1BEAM ELEMENTS, 100 SERIES

TYPE NUMBER	=	1	2	3	4
M. OF I. (IN4)	=	5.390E+00	5.390E+00	1.642E+01	1.642E+01
AREA (IN2)	=	3.980E+00	3.980E+00	3.980E+00	3.980E+00
LENGTH (IN)	=	3.000E+02	9.400E+00	9.400E+00	7.500E+01
YOUNGS MODULUS (KSI)	=	3.000E+04	3.000E+04	3.000E+04	3.000E+04
WEIGHT (LB/FT)	=	1.353E+01	1.353E+01	1.353E+01	1.353E+01
YIELD FORCE (K)	=	1.990E+02	1.990E+02	1.990E+02	1.990E+02
YIELD MOMENT (K.IN)	=	1.375E+02	1.375E+02	2.525E+02	2.525E+02
YIELD ACCURACY LIMIT	=	1.000E-01	1.000E-01	1.000E-01	1.000E-01

1POSTS, 300 SERIES

TYPE NUMBER	=	1	2	3	4
HEIGHT OF NODE I (IN)	=	2.100E+01	2.100E+01	2.100E+01	2.100E+01
HEIGHT OF NODE J (IN)	=	.000E+00	.000E+00	.000E+00	.000E+00
A AXIS STIFFNESS (K/IN)	=	1.500E+01	2.900E+00	3.560E+00	1.150E+00
B AXIS STIFFNESS (K/IN)	=	2.900E+00	2.900E+00	4.550E+00	3.950E+00
EFFECTIVE WEIGHT (LB)	=	5.100E+01	5.100E+01	5.100E+01	2.000E+01
B AXIS YIELD MOMENT (K.IN)	=	1.000E+04	2.560E+02	1.000E+03	1.000E+03
A AXIS YIELD MOMENT (K.IN)	=	1.000E+04	2.560E+02	1.000E+03	1.000E+03
YIELD ACCURACY LIMIT	=	1.000E-01	1.000E-01	1.000E-01	1.000E-01
A SHEAR AT FAILURE (K)	=	1.000E+04	2.000E+01	5.100E+00	1.600E+01
B SHEAR AT FAILURE (K)	=	1.000E+04	2.000E+01	1.120E+01	1.600E+01
A DEFLN AT FAILURE (IN)	=	1.000E+04	2.000E+01	2.000E+01	1.000E+01
B DEFLN AT FAILURE (IN)	=	1.000E+04	2.000E+01	2.000E+01	1.000E+01

1MEMBER GENERATION COMMANDS

FIRST MEMBER	NODE I	NODE J	LAST MEMBER	NODE DIFF	TYPE NO.	PRESTRESS DATA 1	2	3	4	5
1	1	2	0	0	101	.000	.000	.000	.000	.000
2	2	3	41	1	102	.000	.000	.000	.000	.000
42	42	43	57	1	103	.000	.000	.000	.000	.000
58	58	59	62	1	104	.000	.000	.000	.000	.000
63	1	0	0	0	301	.000	.000	.000	.000	.000
64	2	0	65	8	302	.000	.000	.000	.000	.000
66	18	0	67	8	303	.000	.000	.000	.000	.000
68	34	0	0	0	303	.000	.000	.000	.000	.000
69	42	0	71	8	304	.000	.000	.000	.000	.000
72	59	0	76	1	304	.000	.000	.000	.000	.000

FIGURE C-2. CONTINUED

1COMPLETE MEMBER DATA

BEAMS, 100 SERIES

MEMBER	NODE I	NODE J	TYPE	FORCE	I-MOMENT	J-MOMENT
1	1	2	101	.00	.00	.00
2	2	3	102	.00	.00	.00
3	3	4	102	.00	.00	.00
4	4	5	102	.00	.00	.00
5	5	6	102	.00	.00	.00
6	6	7	102	.00	.00	.00
7	7	8	102	.00	.00	.00
8	8	9	102	.00	.00	.00
9	9	10	102	.00	.00	.00
10	10	11	102	.00	.00	.00
11	11	12	102	.00	.00	.00
12	12	13	102	.00	.00	.00
13	13	14	102	.00	.00	.00
14	14	15	102	.00	.00	.00
15	15	16	102	.00	.00	.00
16	16	17	102	.00	.00	.00
17	17	18	102	.00	.00	.00
18	18	19	102	.00	.00	.00
19	19	20	102	.00	.00	.00
20	20	21	102	.00	.00	.00
21	21	22	102	.00	.00	.00
22	22	23	102	.00	.00	.00
23	23	24	102	.00	.00	.00
24	24	25	102	.00	.00	.00
25	25	26	102	.00	.00	.00
26	26	27	102	.00	.00	.00
27	27	28	102	.00	.00	.00
28	28	29	102	.00	.00	.00
29	29	30	102	.00	.00	.00
30	30	31	102	.00	.00	.00
31	31	32	102	.00	.00	.00
32	32	33	102	.00	.00	.00
33	33	34	102	.00	.00	.00
34	34	35	102	.00	.00	.00
35	35	36	102	.00	.00	.00
36	36	37	102	.00	.00	.00
37	37	38	102	.00	.00	.00
38	38	39	102	.00	.00	.00
39	39	40	102	.00	.00	.00
40	40	41	102	.00	.00	.00
41	41	42	102	.00	.00	.00
42	42	43	103	.00	.00	.00
43	43	44	103	.00	.00	.00
44	44	45	103	.00	.00	.00
45	45	46	103	.00	.00	.00

FIGURE C-2. CONTINUED

46	46	47	103	.00	.00	.00
47	47	48	103	.00	.00	.00
48	48	49	103	.00	.00	.00
49	49	50	103	.00	.00	.00
50	50	51	103	.00	.00	.00
51	51	52	103	.00	.00	.00
52	52	53	103	.00	.00	.00
53	53	54	103	.00	.00	.00
54	54	55	103	.00	.00	.00
55	55	56	103	.00	.00	.00
56	56	57	103	.00	.00	.00
57	57	58	103	.00	.00	.00
58	58	59	104	.00	.00	.00
59	59	60	104	.00	.00	.00
60	60	61	104	.00	.00	.00
61	61	62	104	.00	.00	.00
62	62	63	104	.00	.00	.00

POSTS, 300 SERIES

MEMBER	NODE I	NODE J	TYPE	A-SHEAR	B-SHEAR	B-MOMENT	A-MOMENT	ANGLE
63	1	0	301	.00	.00	.00	.00	.00
64	2	0	302	.00	.00	.00	.00	.00
65	10	0	302	.00	.00	.00	.00	.00
66	18	0	303	.00	.00	.00	.00	.00
67	26	0	303	.00	.00	.00	.00	.00
68	34	0	303	.00	.00	.00	.00	.00
69	42	0	304	.00	.00	.00	.00	.00
70	50	0	304	.00	.00	.00	.00	.00
71	58	0	304	.00	.00	.00	.00	.00
72	59	0	304	.00	.00	.00	.00	.00
73	60	0	304	.00	.00	.00	.00	.00
74	61	0	304	.00	.00	.00	.00	.00
75	62	0	304	.00	.00	.00	.00	.00
76	63	0	304	.00	.00	.00	.00	.00

STIFFNESS MATRIX STORAGE

REQUIRED = 1134
ALLOCATED = 6000
1AUTOMOBILE PROPERTIES

WEIGHT (LB) = 4500.0
MOMENT OF INERTIA (LB.IN.SEC2) = 47000.0
NO. OF CONTACT POINTS = 19
NO. OF UNIT STIFFNESSES = 2

FIGURE C-2. CONTINUED

NO. OF WHEELS = 4
BRAKE CODE (1=ON, 0=OFF) = 0
NO. OF OUTPUT POINTS = 2

UNIT STIFFNESSES (K/IN/IN)

NO.	BEFORE BOTTOMING	AFTER BOTTOMING	UNLOADING	BOTTOMING DISTANCE
1	.040	.250	.330	12.00
2	1.440	9.000	11.880	1.00

CONTACT POINT DATA

POINT	R COORD	S COORD	STIFFNESS NO.	TRIBUTARY LENGTH	INTERFACE CONTACTS			
1	57.00	31.00	2	1.00	1	0	0	0
2	57.00	-31.00	2	1.00	1	0	0	0
3	-122.00	40.00	1	31.00	1	0	0	0
4	-30.00	40.00	1	30.00	1	0	0	0
5	.00	40.00	1	27.00	1	0	0	0
6	23.00	40.00	1	23.00	1	0	0	0
7	46.00	40.00	1	23.00	1	0	0	0
8	69.00	40.00	1	23.00	1	0	0	0
9	93.00	40.00	1	22.00	1	0	0	0
10	93.00	20.00	1	20.00	1	0	0	0
11	93.00	.00	1	20.00	1	0	0	0
12	93.00	-20.00	1	20.00	1	0	0	0
13	93.00	-40.00	1	22.00	1	0	0	0
14	69.00	-40.00	1	23.00	1	0	0	0
15	46.00	-40.00	1	23.00	1	0	0	0
16	23.00	-40.00	1	23.00	1	0	0	0
17	.00	-40.00	1	27.00	1	0	0	0
18	-30.00	-40.00	1	30.00	1	0	0	0
19	-122.00	-40.00	1	31.00	1	0	0	0

OWHEEL COORDINATES (IN), STEER ANGLES (DEG), AND DRAG FORCES (LB)

POINT	R-ORD	S-ORD	STEER ANGLE	DRAG FORCE
1	57.00	31.00	.00	608.00
2	57.00	-31.00	.00	608.00
3	-67.00	31.00	.00	517.00
4	-67.00	-31.00	.00	517.00

FIGURE C-2. CONTINUED

```
0OUTPUT POINT COORDINATES (IN)

 POINT        R-ORD         S-ORD

    1          .00           .00
    2        93.00           .00
1INITIAL POSITION AND VELOCITIES OF AUTO


 SPECIFIED BOUNDARY POINT              =          9
 X ORDINATE OF POINT                   =      21.50
 Y ORDINATE OF POINT                   =     -65.50

 ANGLE FROM X AXIS TO R AXIS (DEG)     =        .00
 VELOCITY IN R DIRECTION (M.P.H)       =      40.00
 VELOCITY IN S DIRECTION (M.P.H)       =        .00
 ANGULAR VELOCITY (RAD/SEC)            =        .000

 MINIMUM RESULTANT VELOCITY (M.P.H)    =        .00


 TRANSLATIONAL KINETIC ENERGY (K.IN)   =    2888.95
 ROTATIONAL KINETIC ENERGY (K.IN)      =        .00

 TOTAL INITIAL KINETIC ENERGY (K.IN)   =    2888.95
```

FIGURE C-2. CONTINUED

APPENDIX D

DRAWINGS FOR TESTED TRANSITION INSTALLATION

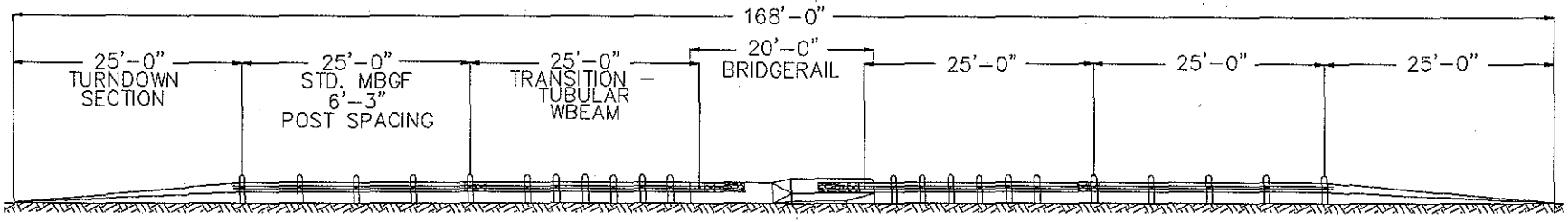

TEST LAYOUT

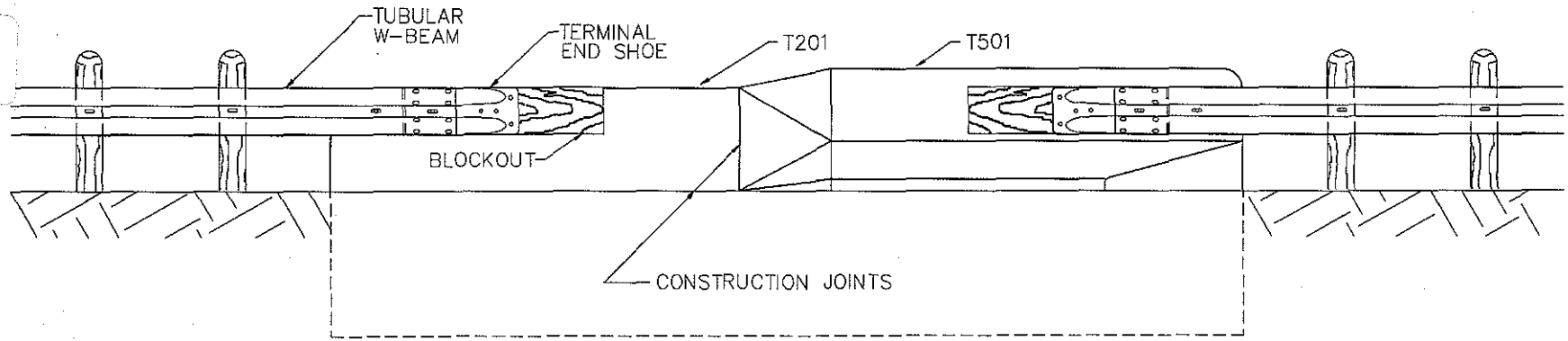

FOUNDATION AND TRAFFIC RAILING - ELEVATION

FIGURE D-1. TEST INSTALLATION LAYOUT

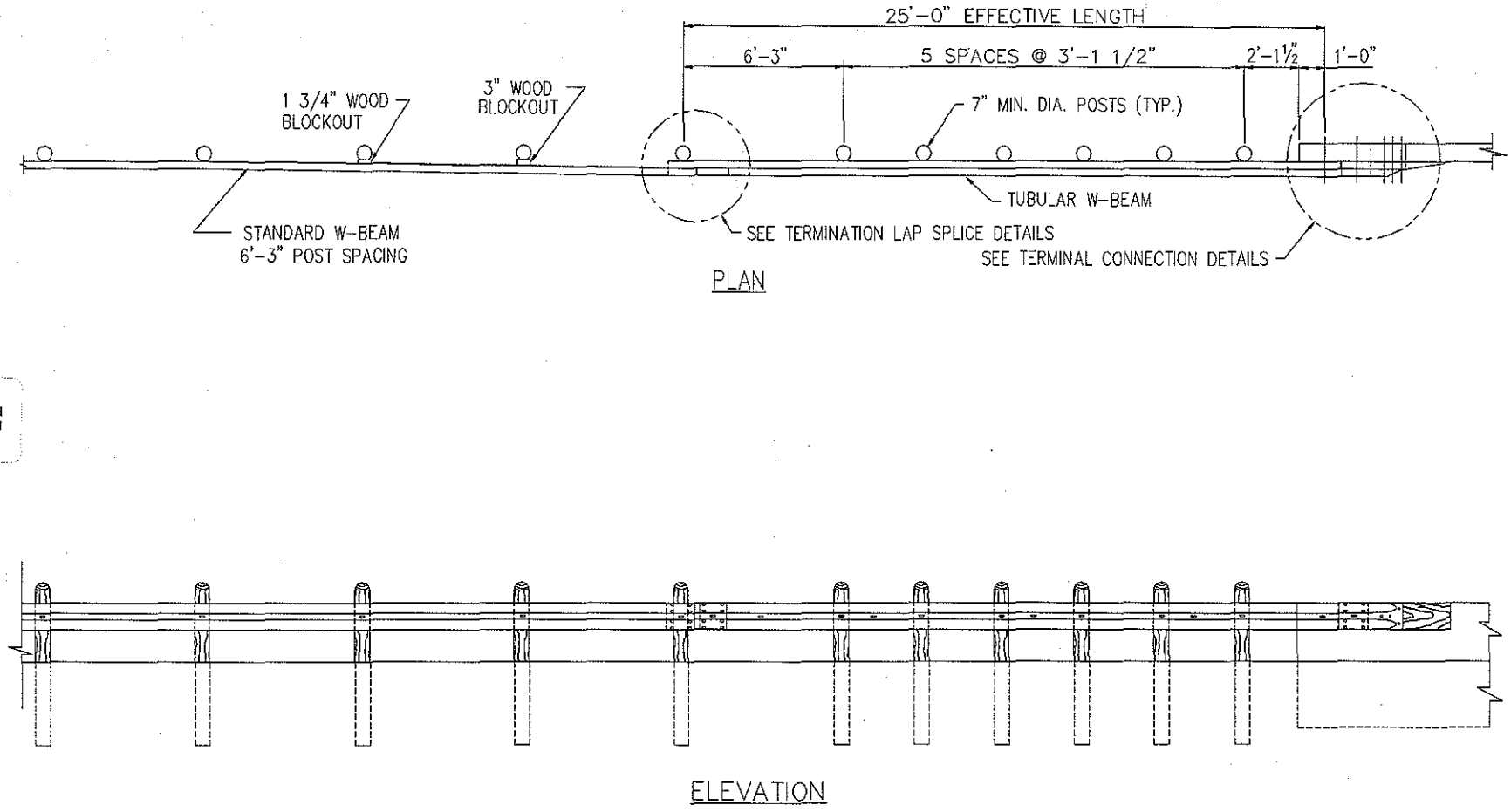

FIGURE D-2. GUARDRAIL TO BRIDGERAIL TRANSITION USED IN TEST PROGRAM

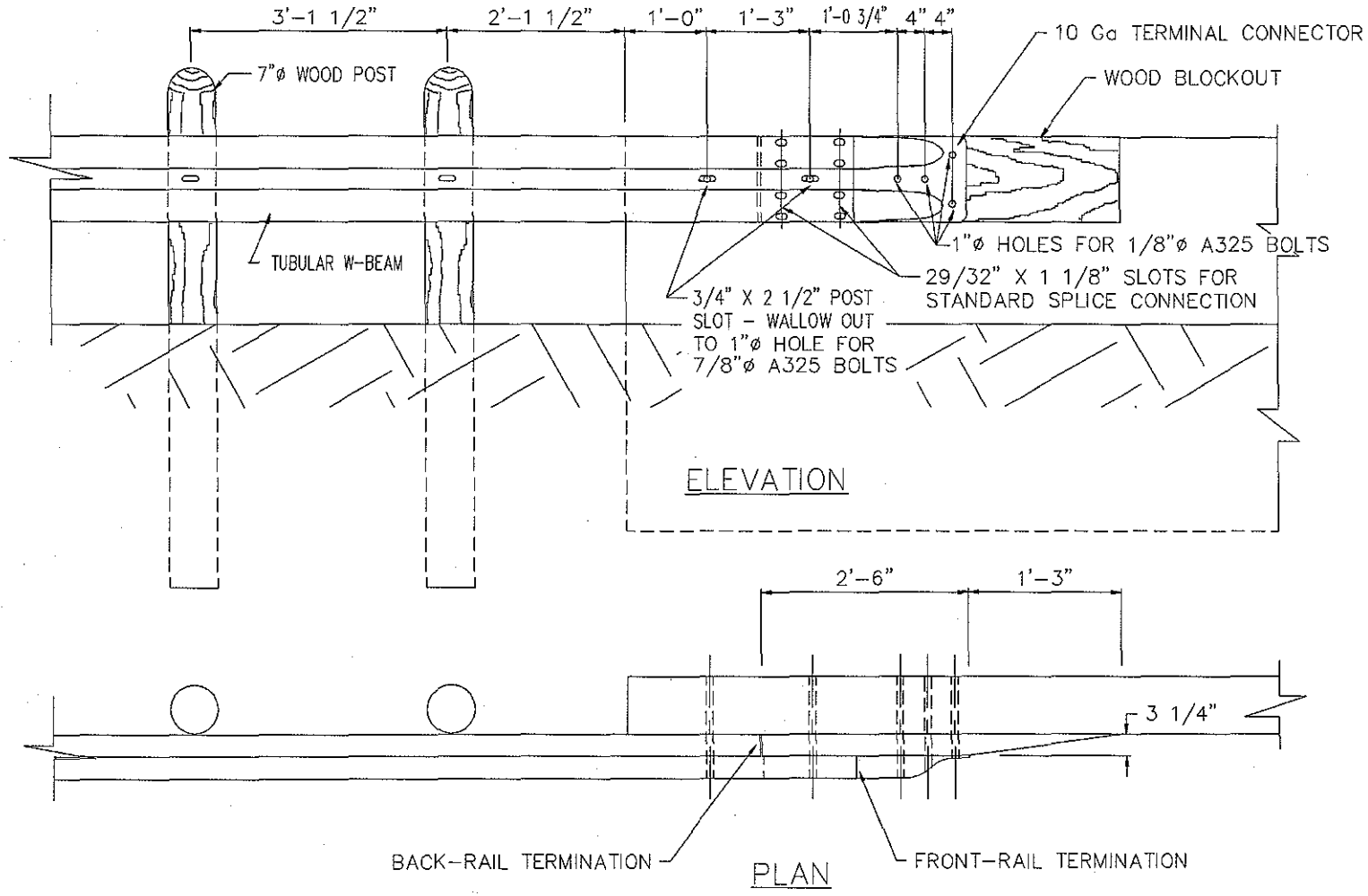

FIGURE D-3. TERMINAL CONNECTION TO VERTICAL WALL AS USED IN TESTED INSTALLATION

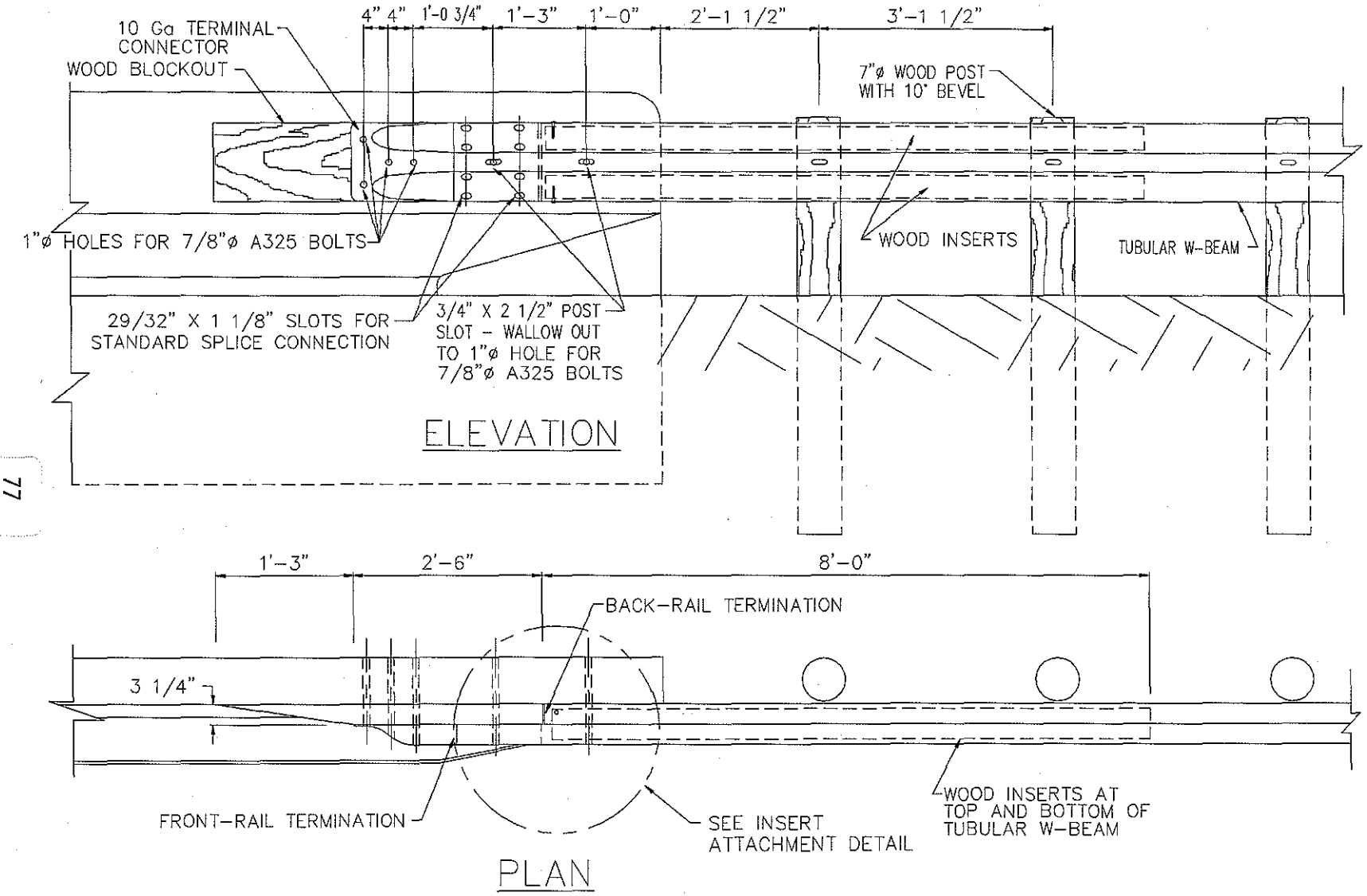

FIGURE D-4. TERMINAL CONNECTION TO SAFETY SHAPE AS USED IN TESTED INSTALLATION

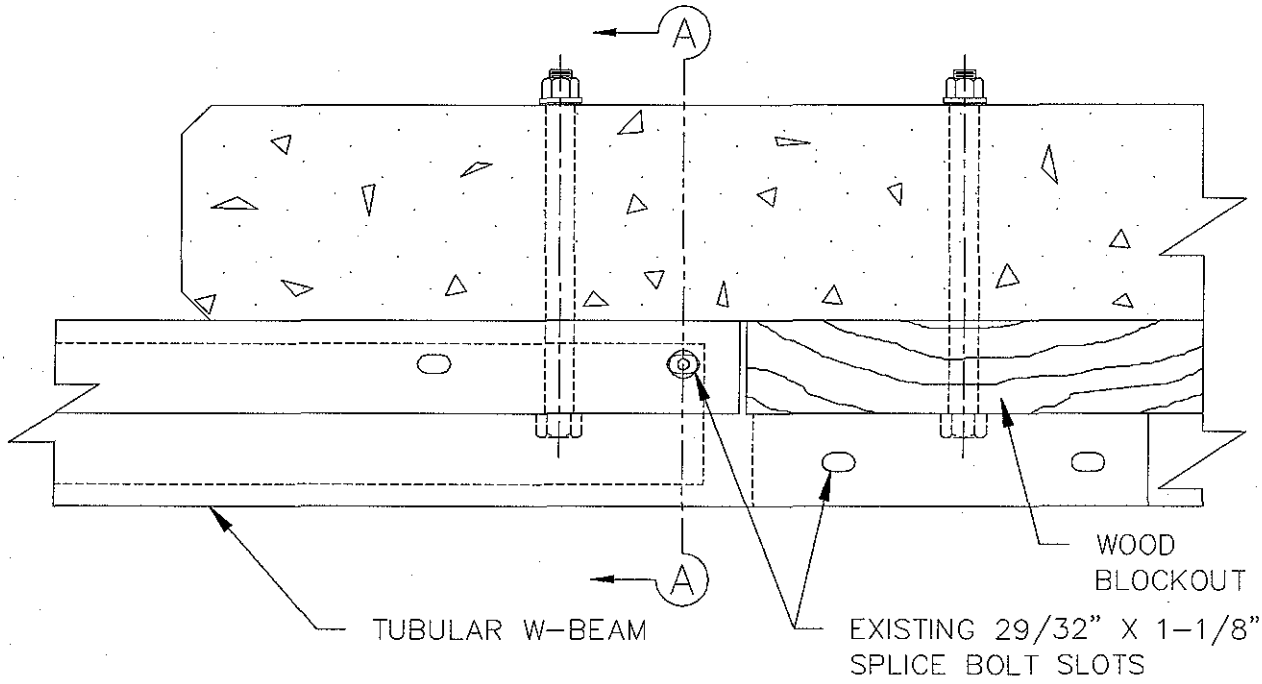

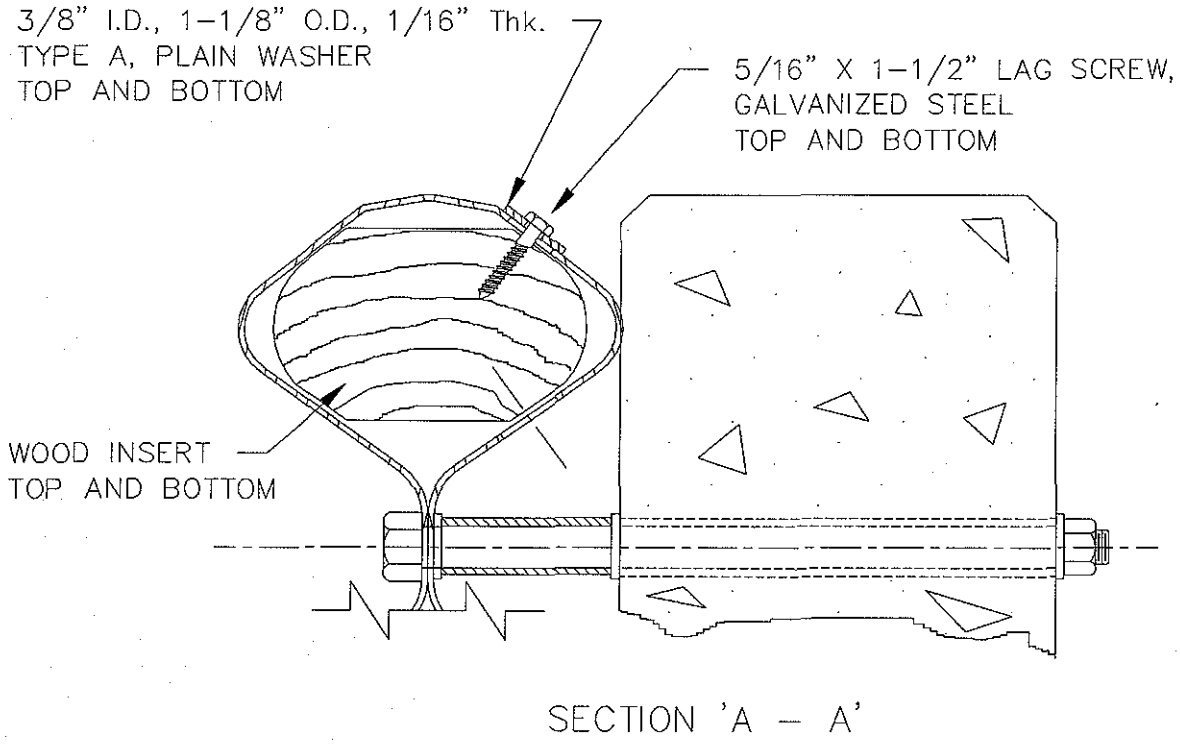

SECTION 'A – A'

FIGURE D-5. WOOD INSERT ATTACHMENT DETAILS

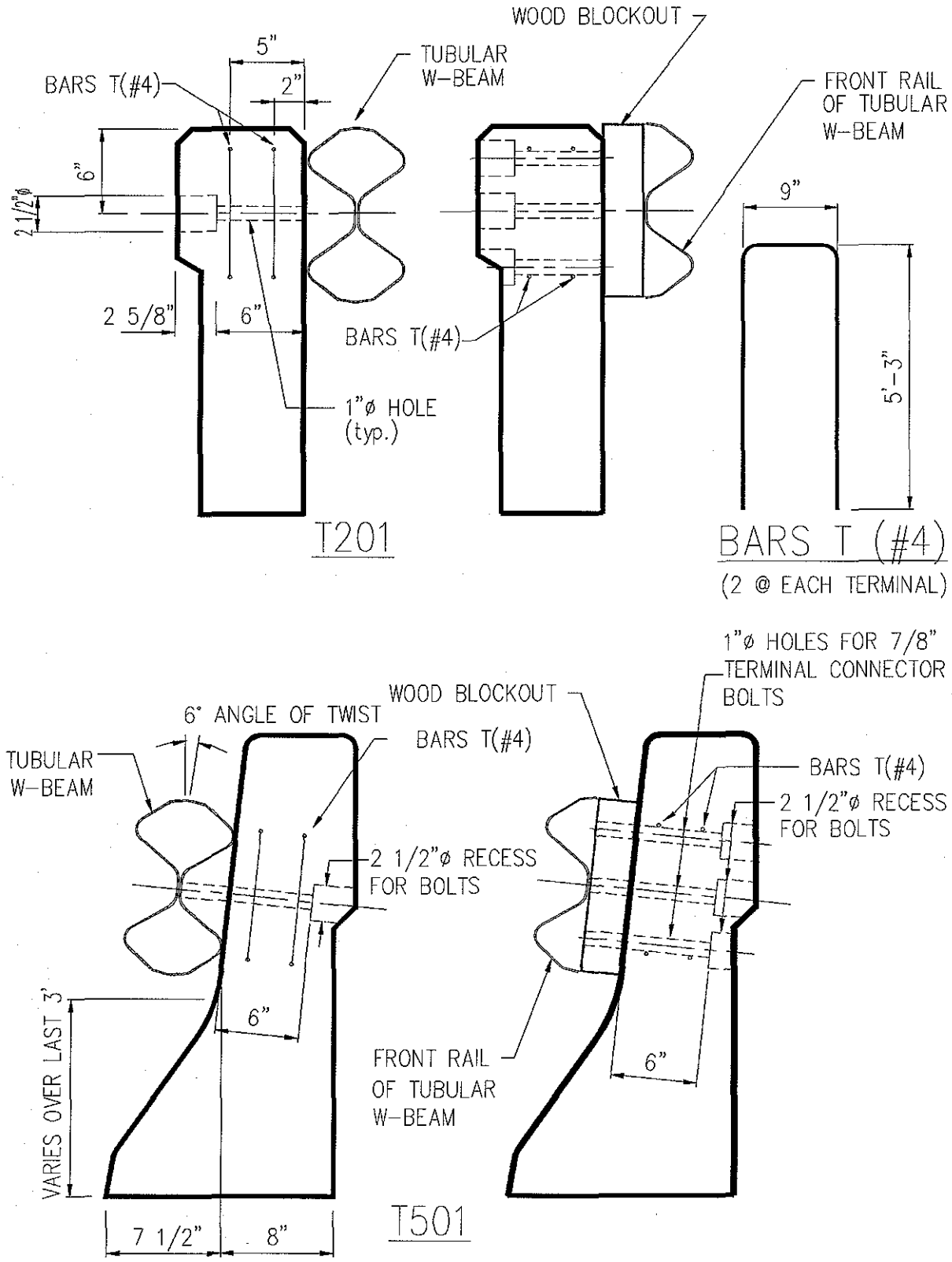

FIGURE D-6. TERMINAL CONNECTION DETAILS USED IN TESTED INSTALLATION

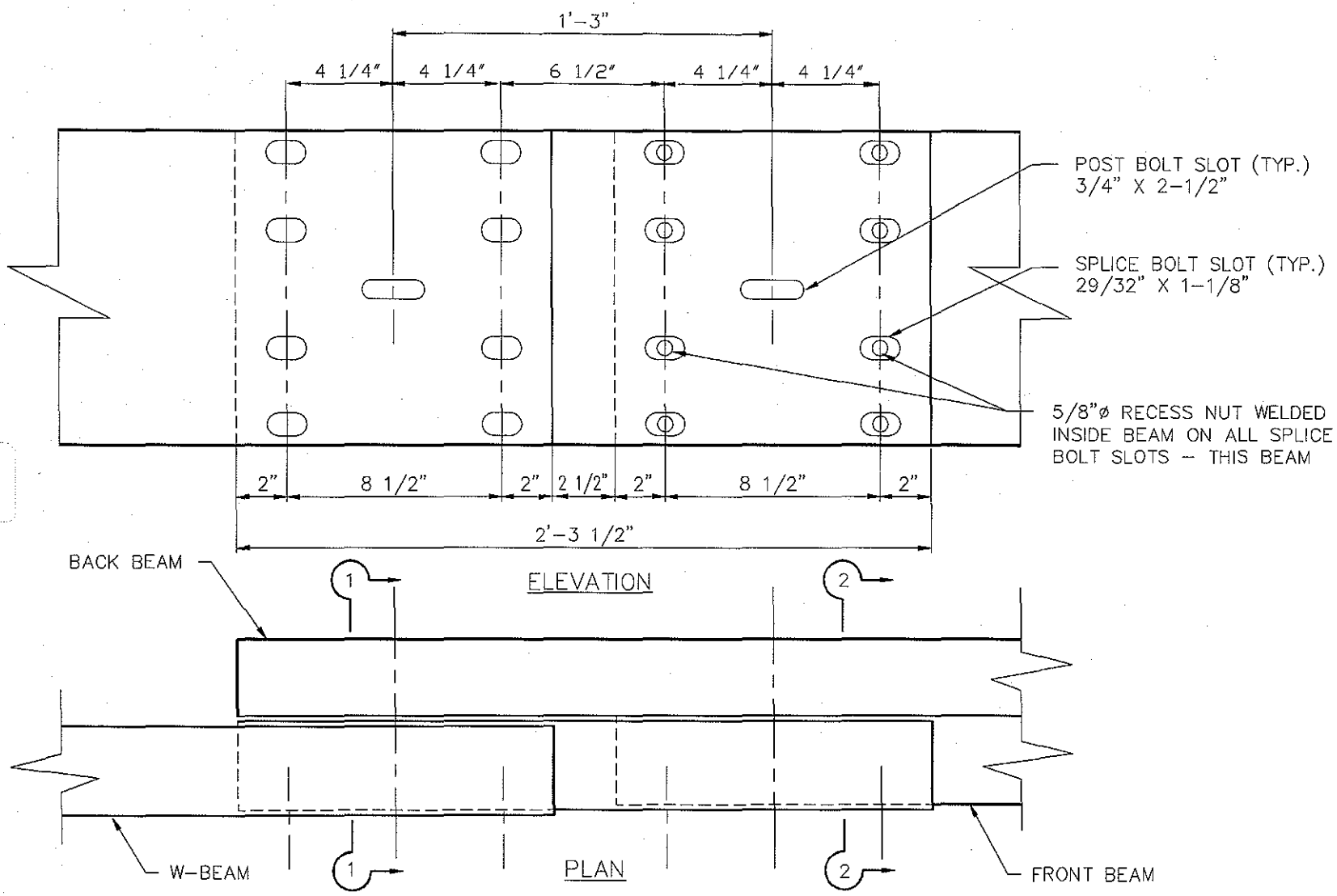

FIGURE D-7. TERMINATION LAP SPLICE DETAILS USED IN TESTED INSTALLATION

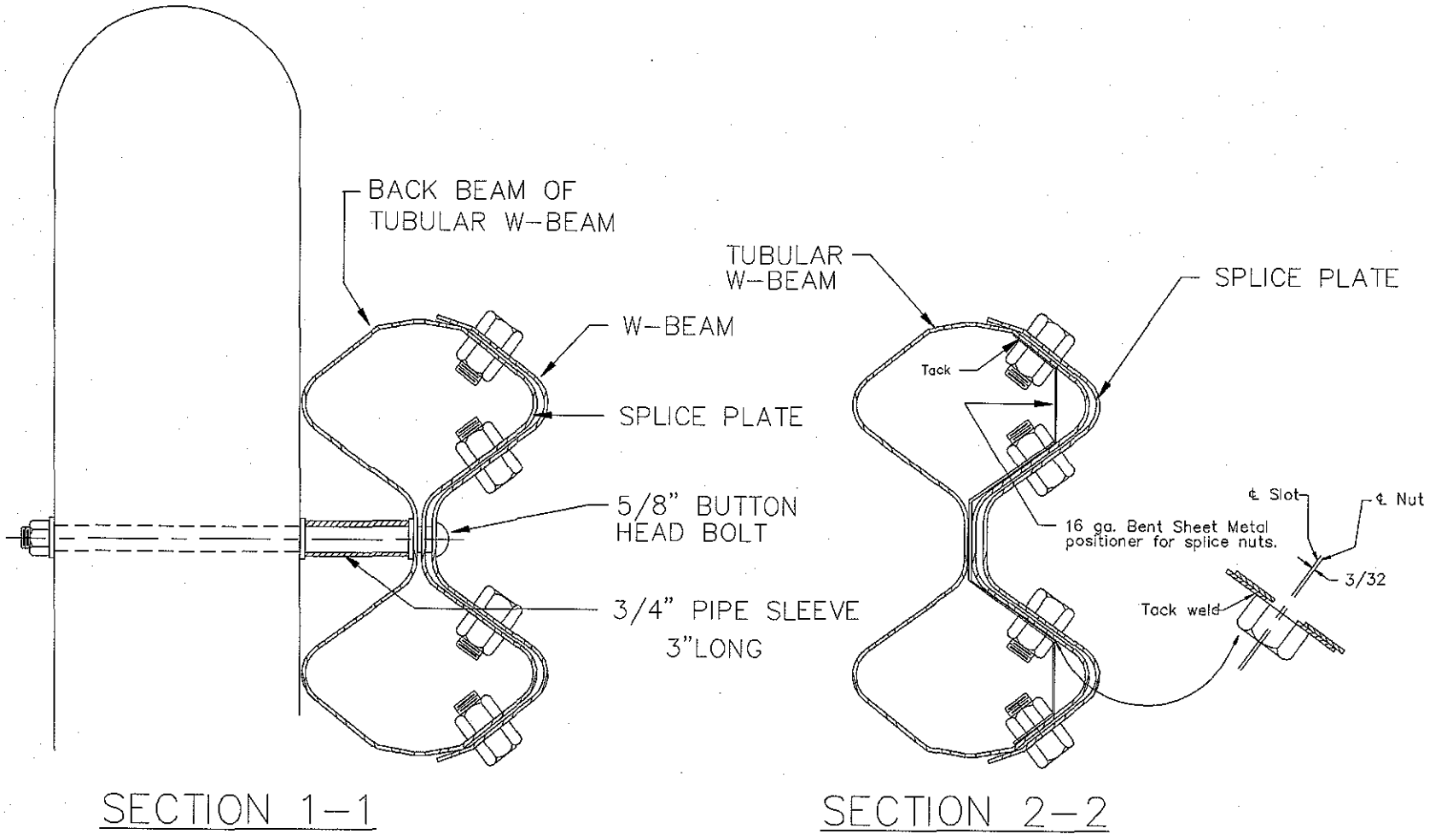

FIGURE D-7. CONTINUED

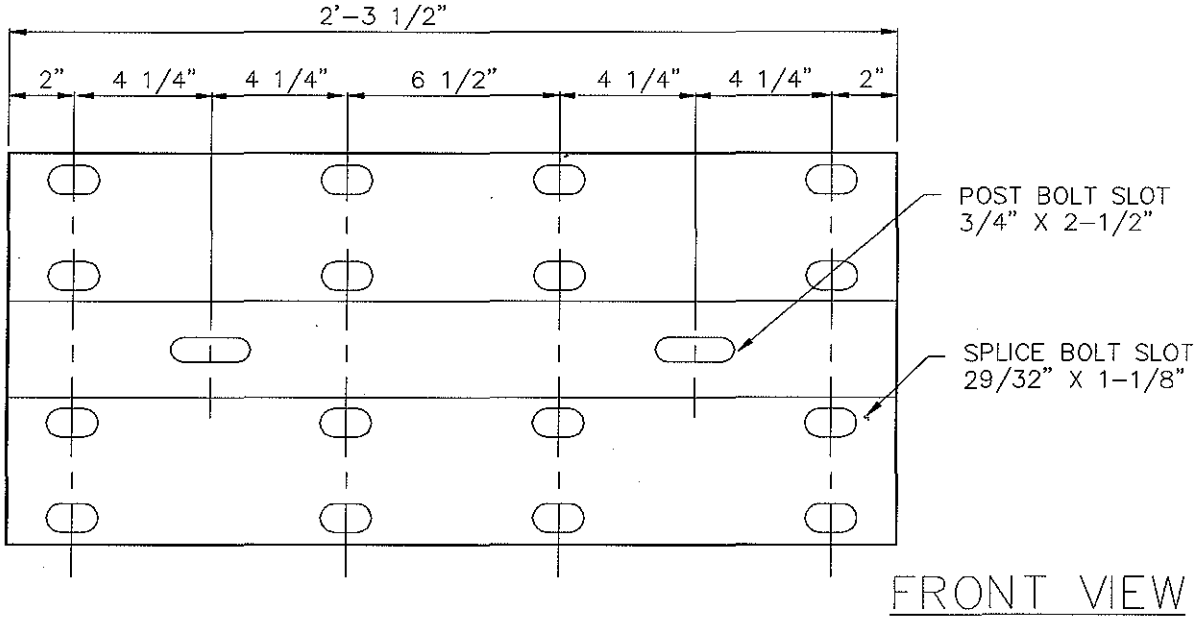

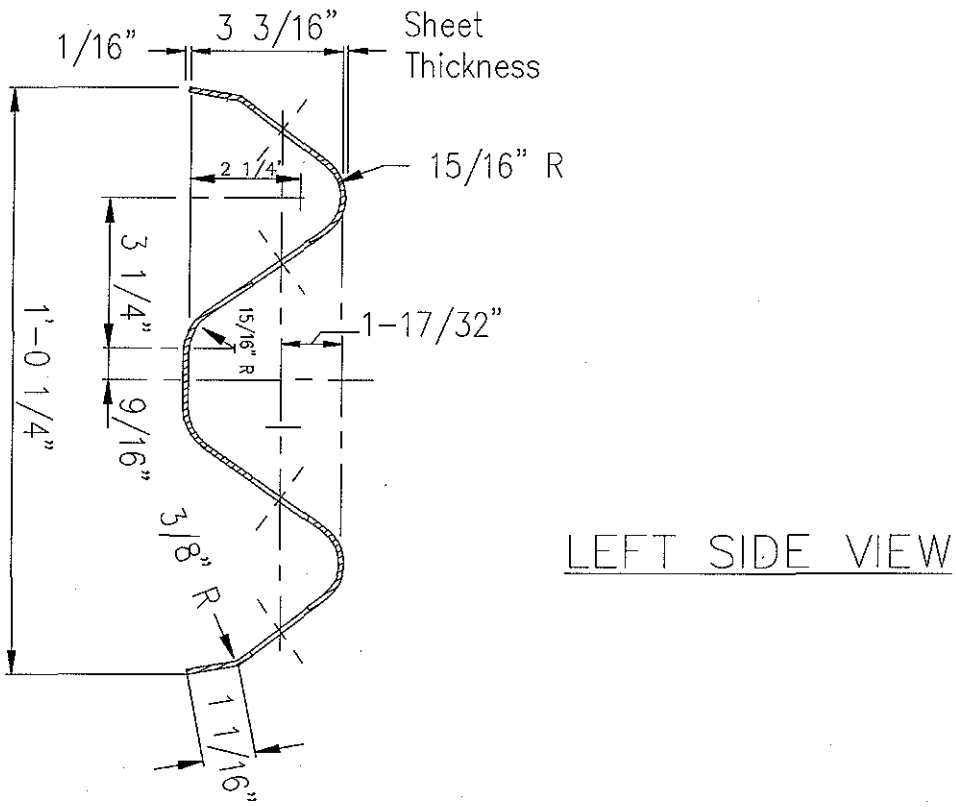

FIGURE D-7. CONTINUED

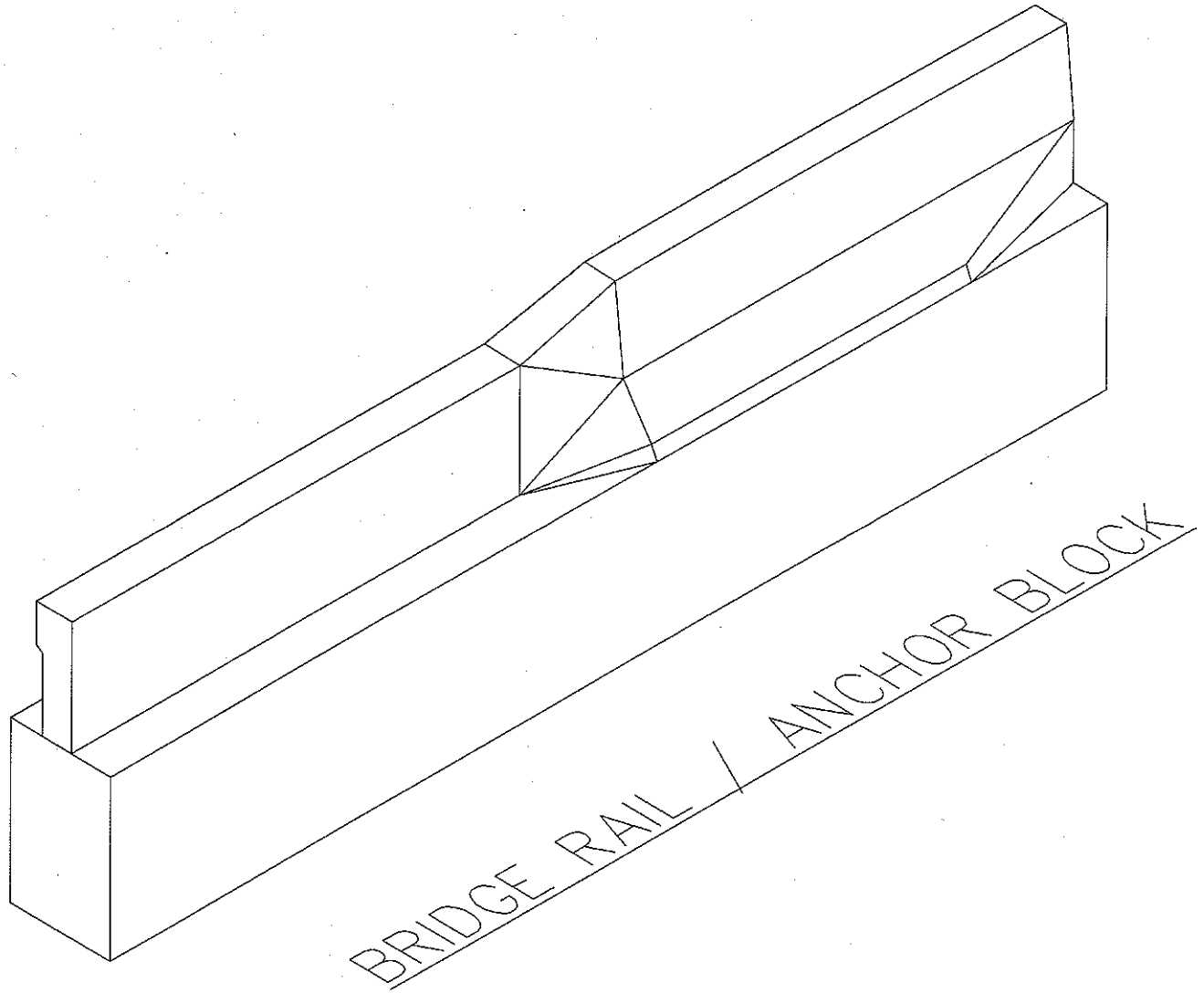

FIGURE D-8. BRIDGE RAIL / ANCHOR BLACK INSTALLATION

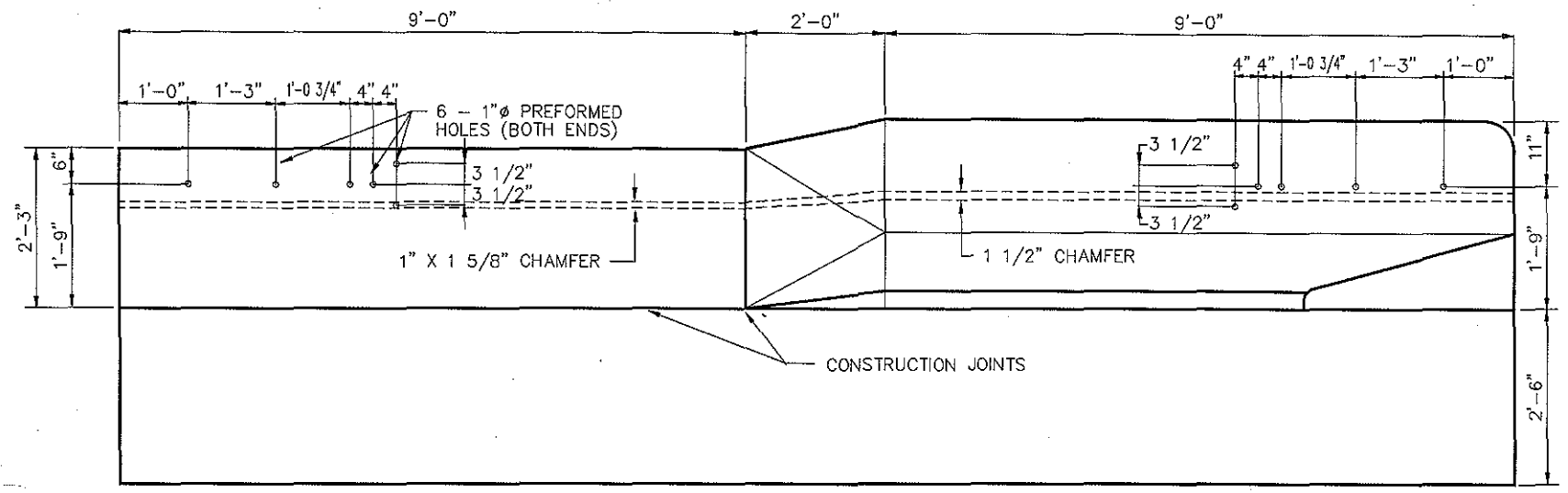

ELEVATION

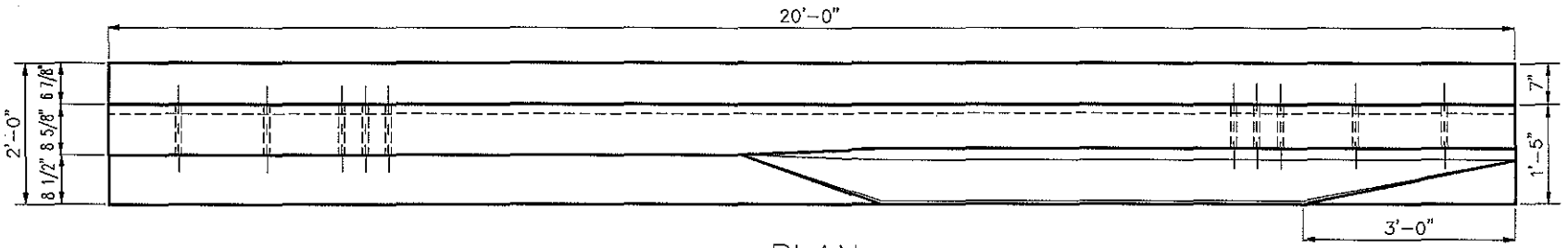

PLAN

FIGURE D-9. BRIDGE RAIL / ANCHOR BLOCK DETAILS

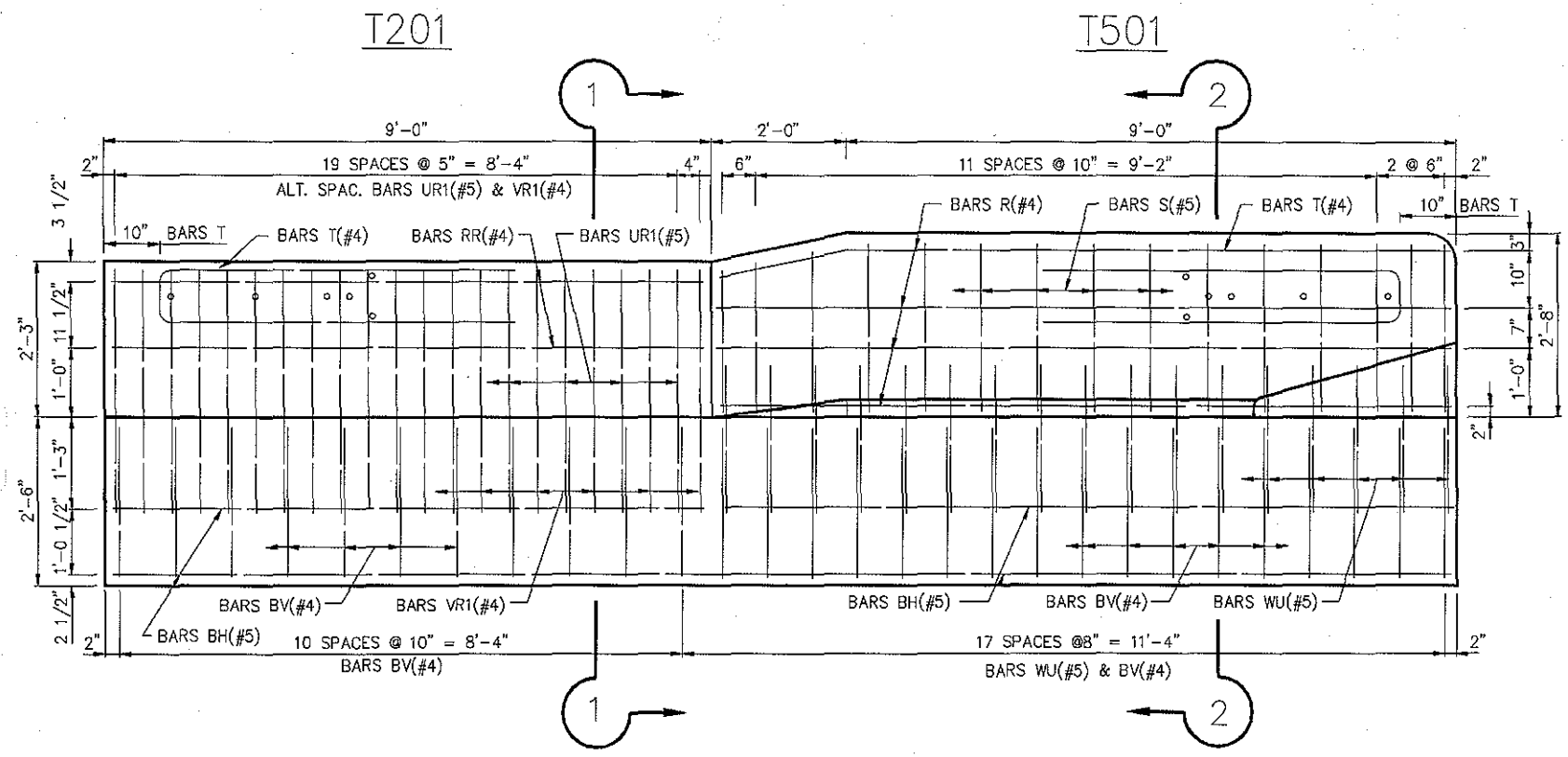

NOTE : FIELD BEND REINF. AS NECESSARY AT TAPERS

FIGURE D-10. BRIDGE RAIL / ANCHOR BLOCK REINFORCEMENT

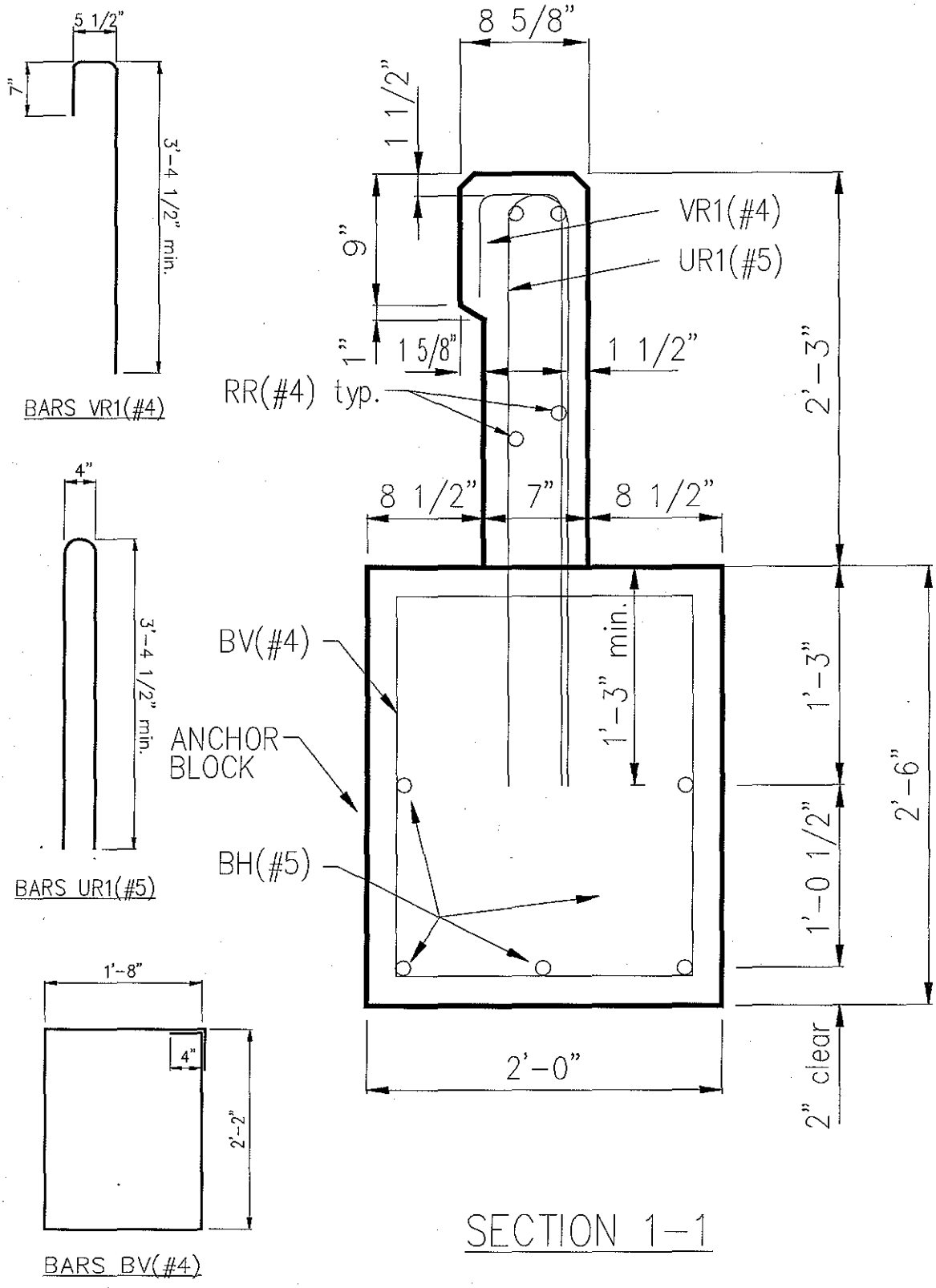

FIGURE D-11. T201 TRAFFIC RAIL (VERTICAL WALL)

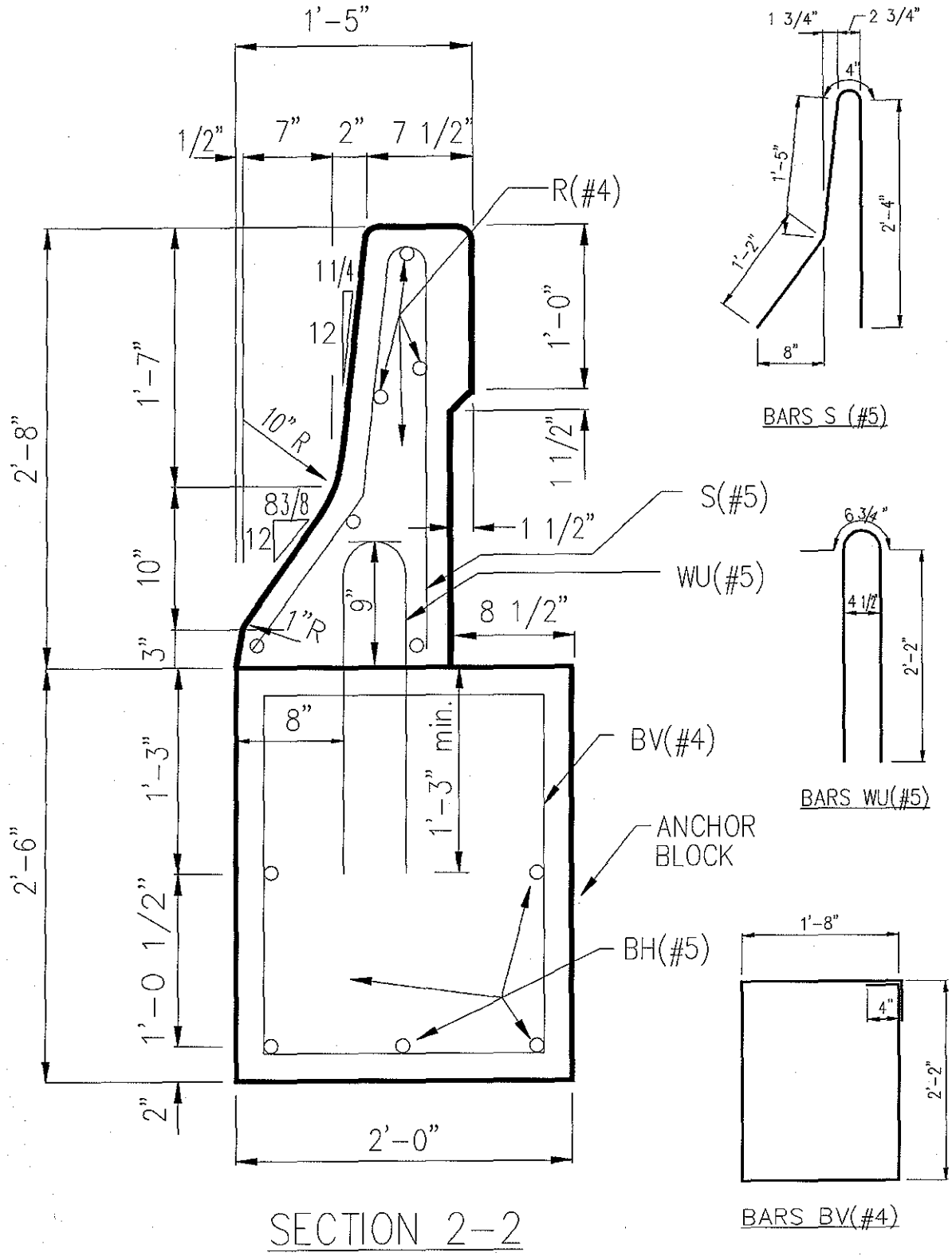

FIGURE D-12. T501 TRAFFIC RAIL (SAFETY SHAPE)

APPENDIX E

SEQUENTIAL PHOTOGRAPHS AND ANGULAR DISPLACEMENTS FOR TRANSITION CRASH TESTS

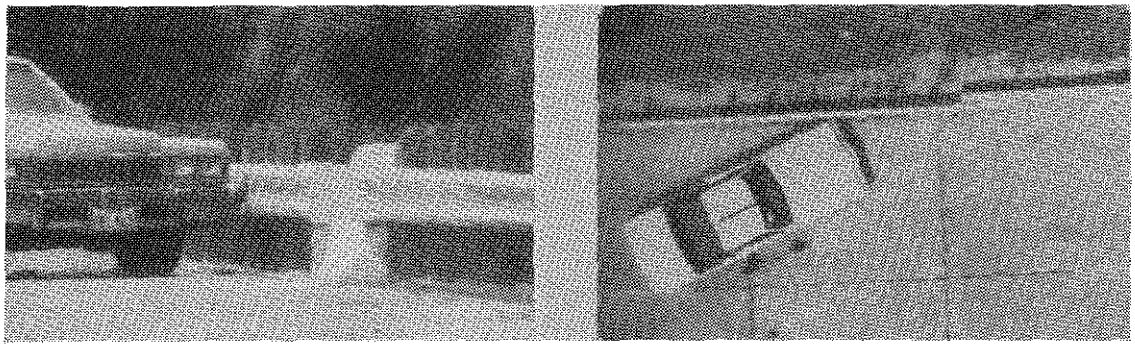

0.000 s

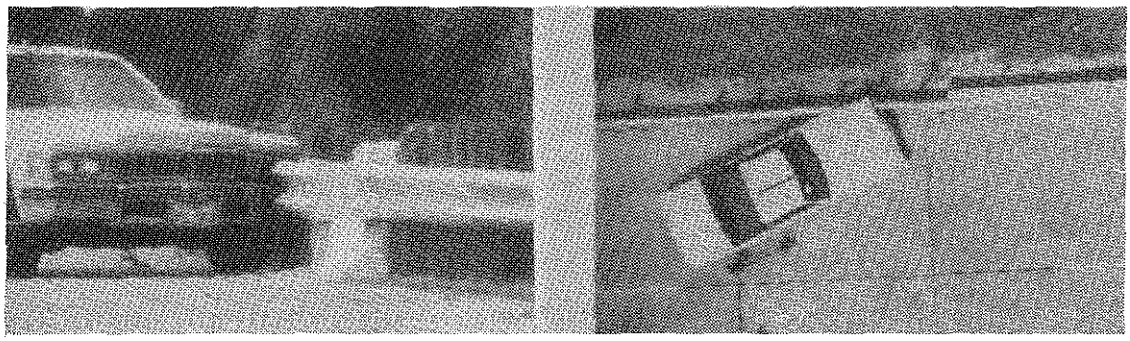

0.050 s

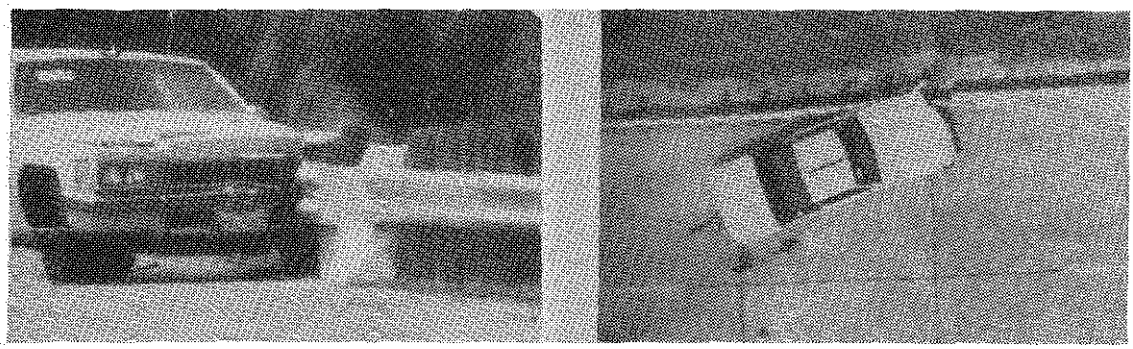

0.099 s

0.149 s

FIGURE E-1. SEQUENTIAL PHOTOGRAPHS FOR TEST 1

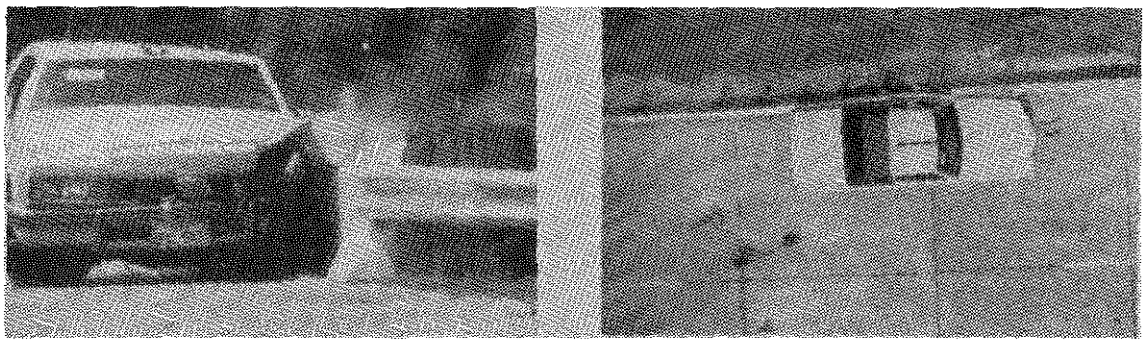

0.198 s

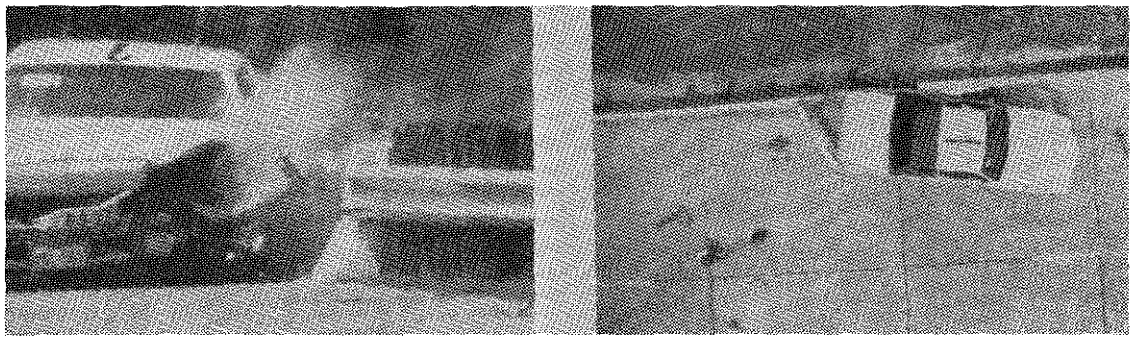

0.300 s

0.402 s

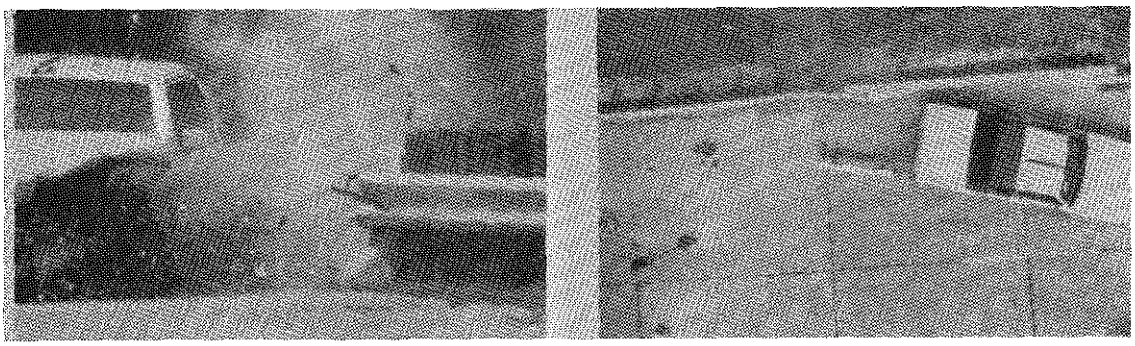

0.501 s

FIGURE E-1. CONTINUED

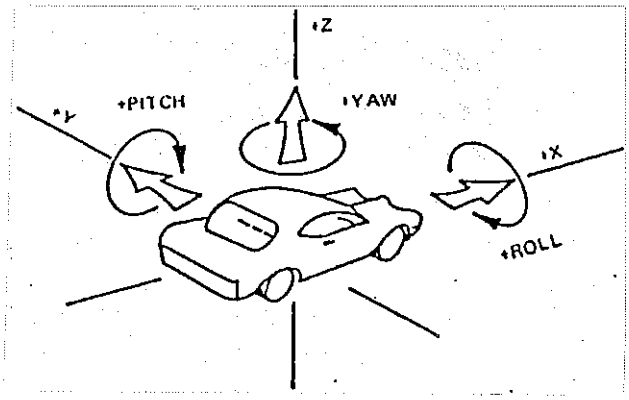

Axes are vehicle fixed.
Sequence for determining orientation is:

1. Yaw
2. Pitch
3. Roll

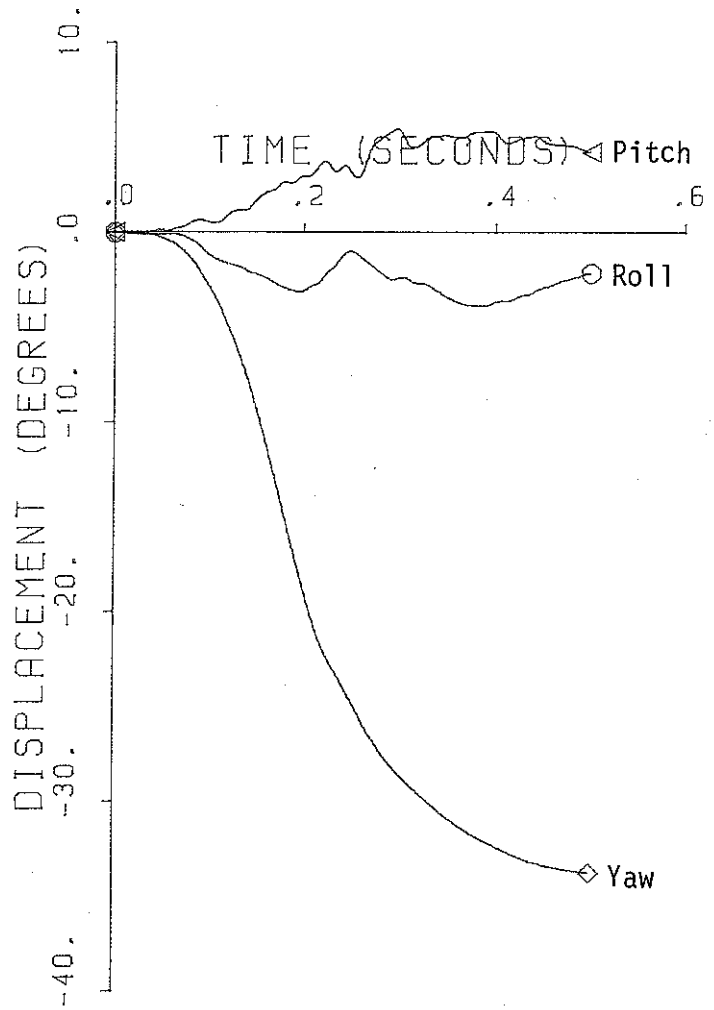

FIGURE E-2. VEHICLE ANGULAR DISPLACEMENT FOR TEST 1

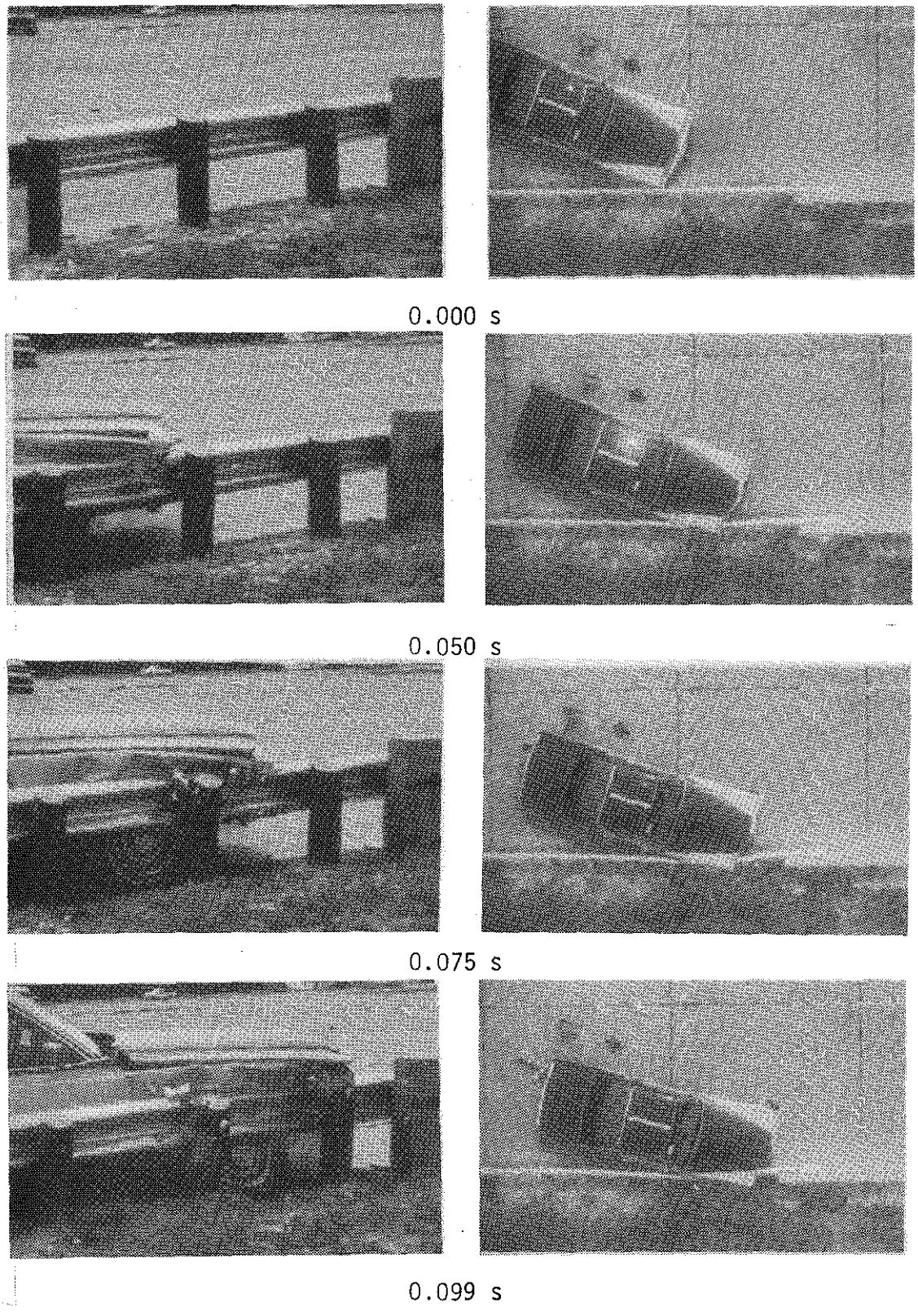

FIGURE E-3. SEQUENTIAL PHOTOGRAPHS FOR TEST 2

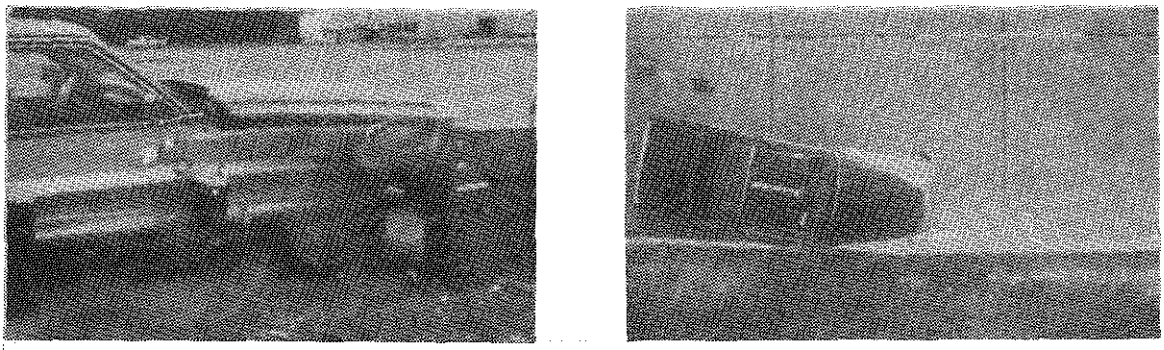

0.124 s

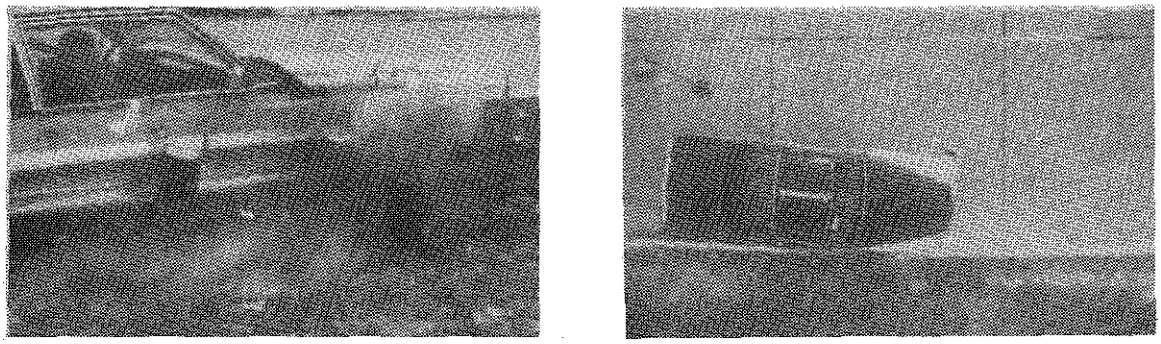

0.149 s

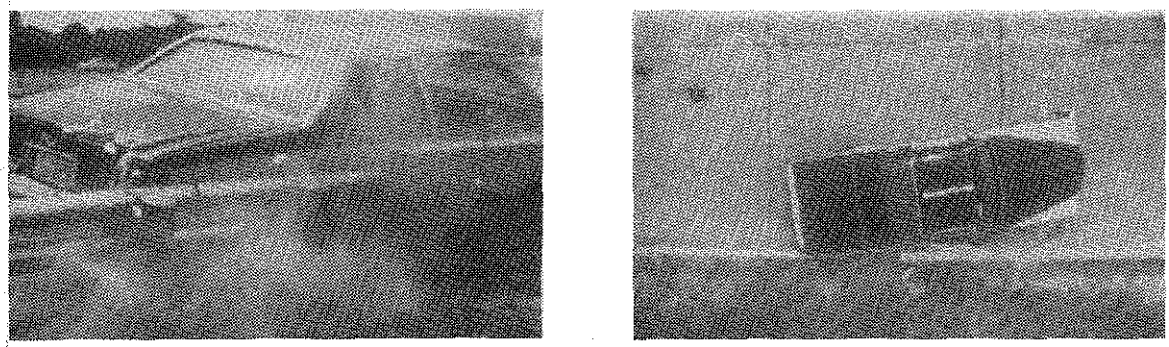

0.273 s

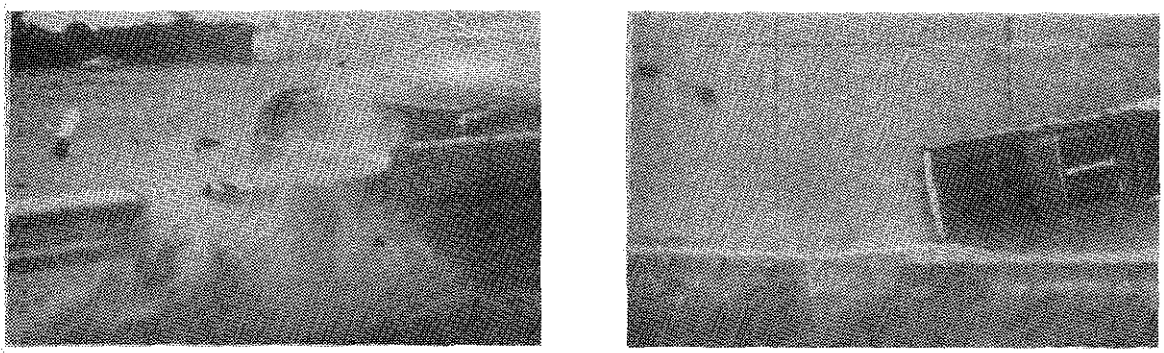

0.398 s

FIGURE E-3. CONTINUED

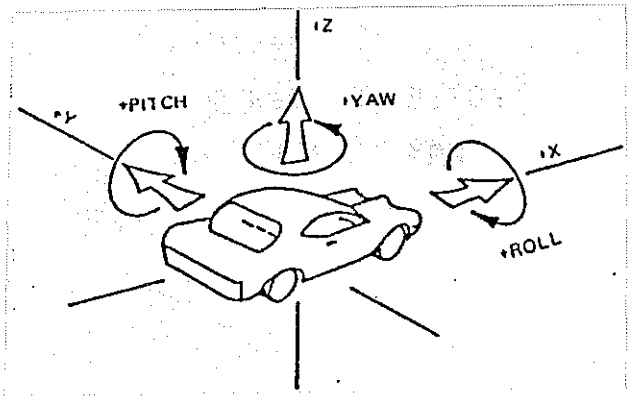

Axes are vehicle fixed.
Sequence for determining orientation is:

1. Yaw
2. Pitch
3. Roll

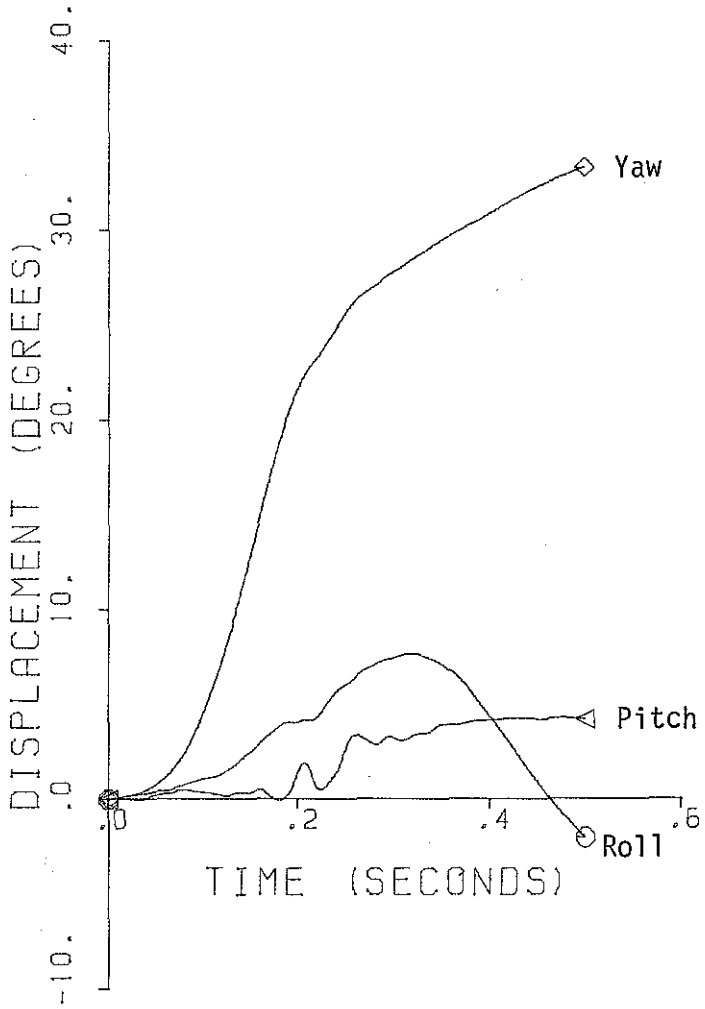

FIGURE E-4. VEHICLE ANGULAR DISPLACEMENTS FOR TEST 2

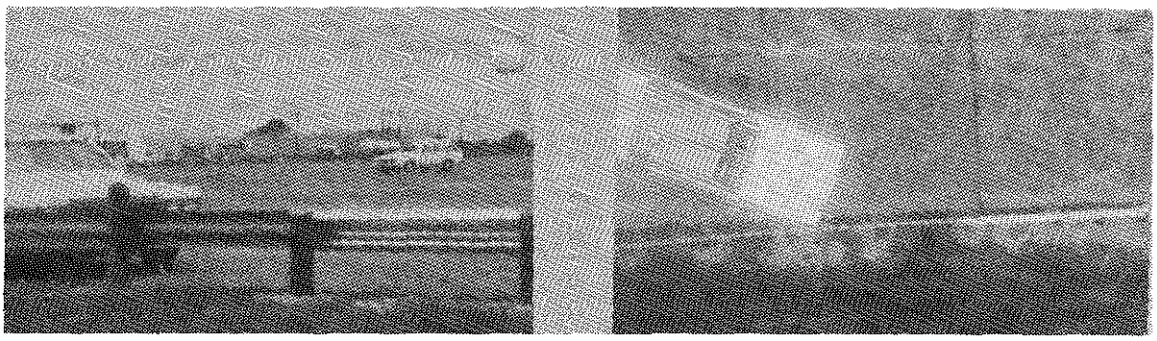

0.000 s

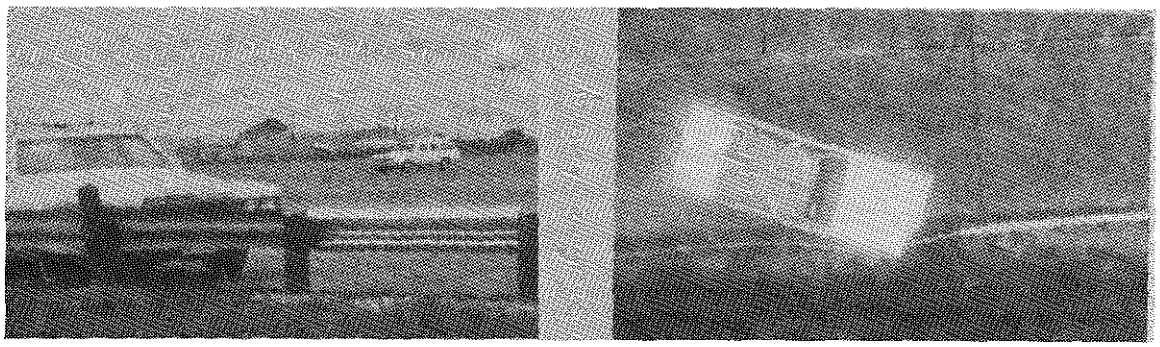

0.071 s

0.106 s

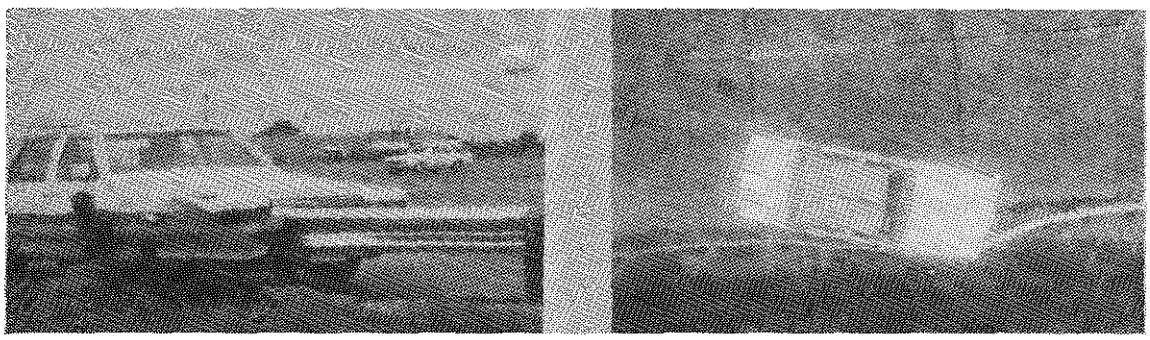

0.143 s

FIGURE E-5. SEQUENTIAL PHOTOGRAPHS FOR TEST 3

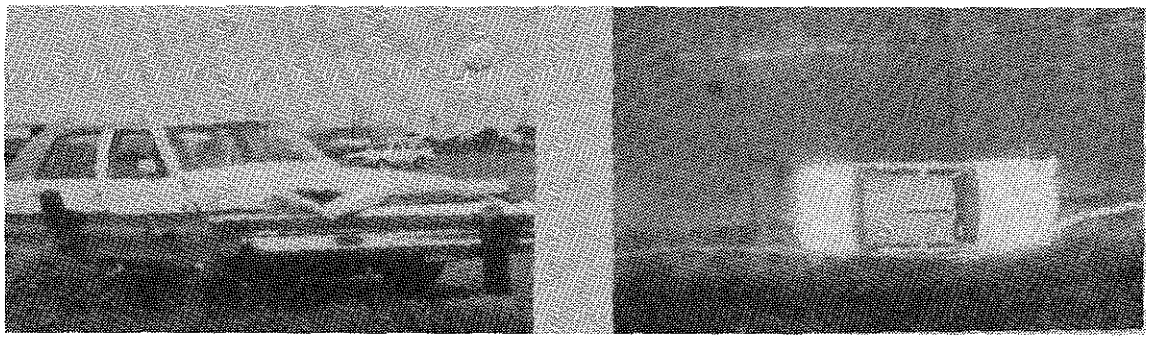

0.213 s

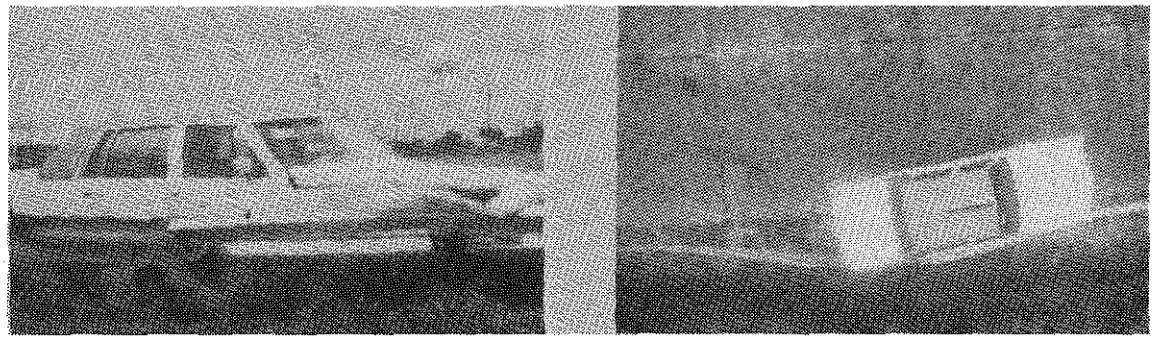

0.284 s

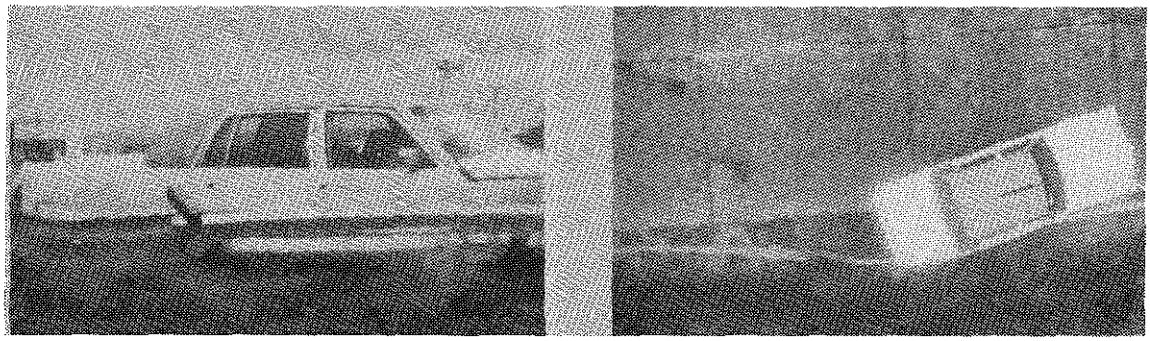

0.356 s

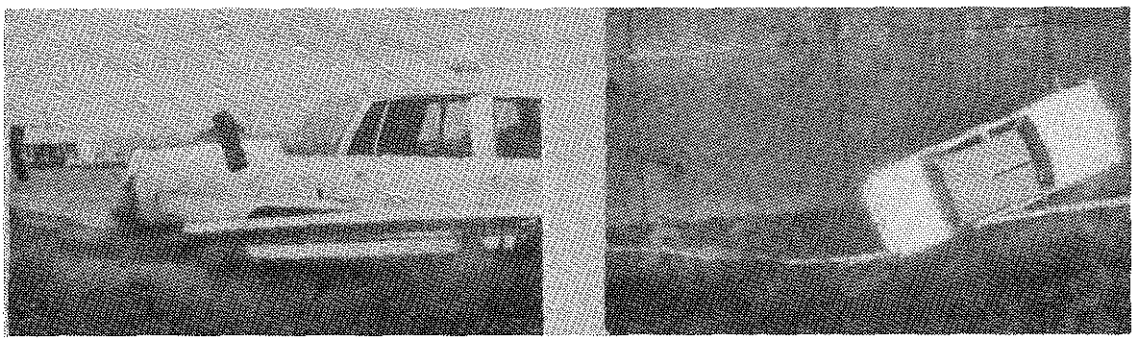

0.428 s

FIGURE E-5. CONTINUED

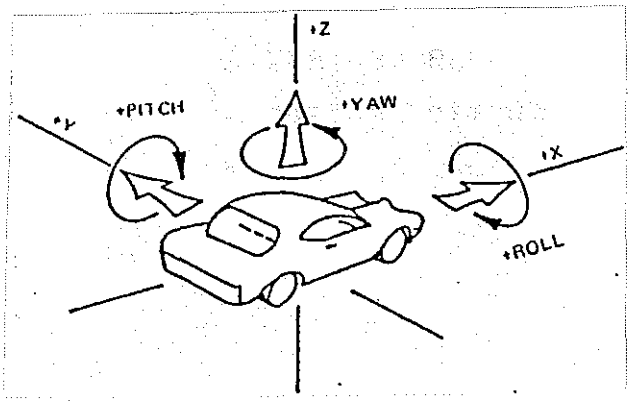

Axes are vehicle fixed.
Sequence for determining orientation is:

1. Yaw
2. Pitch
3. Roll

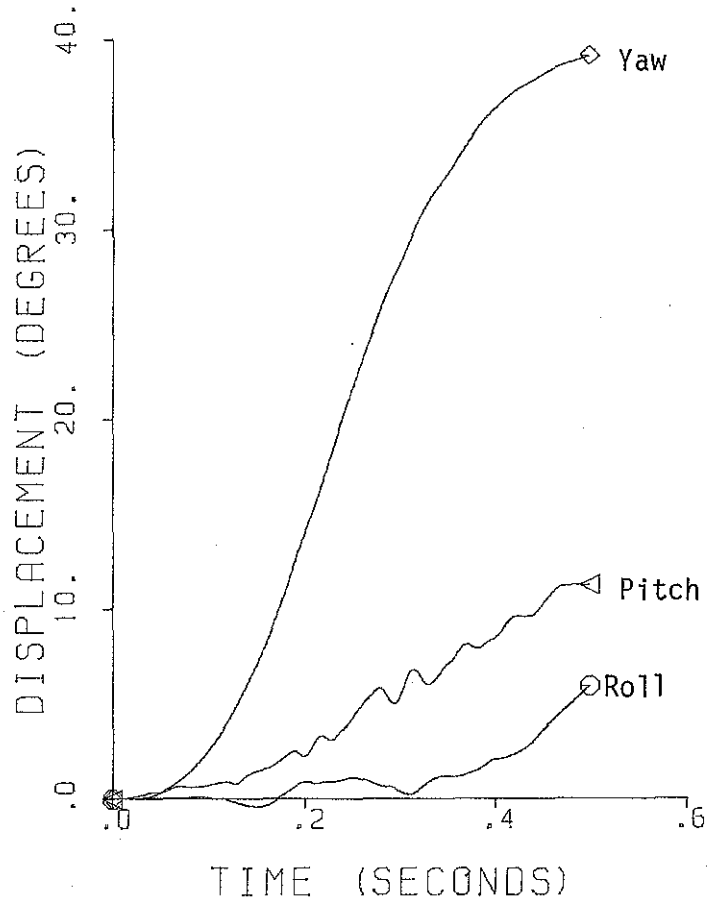

FIGURE E-6. VEHICLE ANGULAR DISPLACEMENT FOR TEST 3

APPENDIX F

CONSTRUCTION DRAWINGS FOR RECOMMENDED RETROFIT TRANSITION INSTALLATION

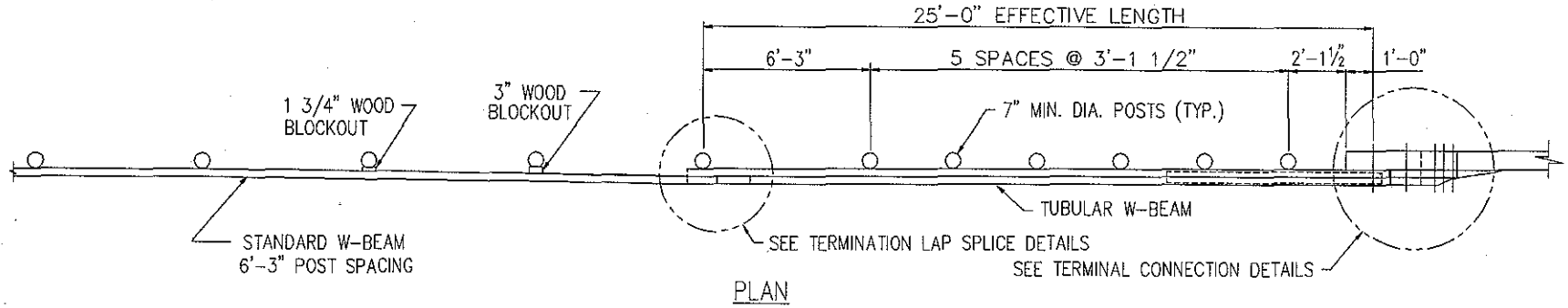

PLAN

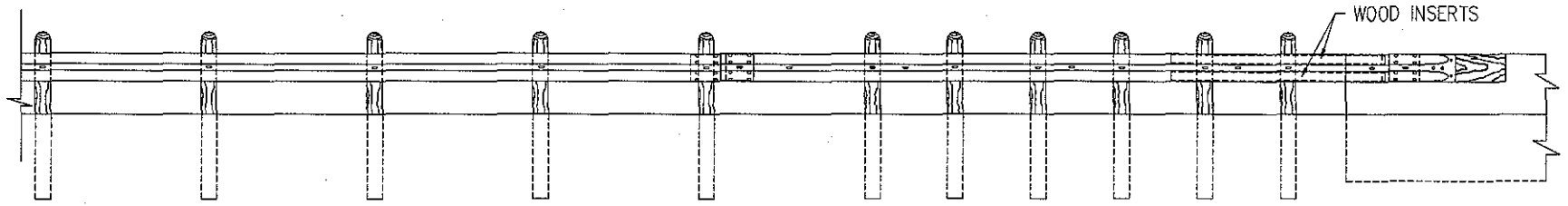

ELEVATION

FIGURE F-1. RECOMMENDED RETROFIT TRANSITION DESIGN

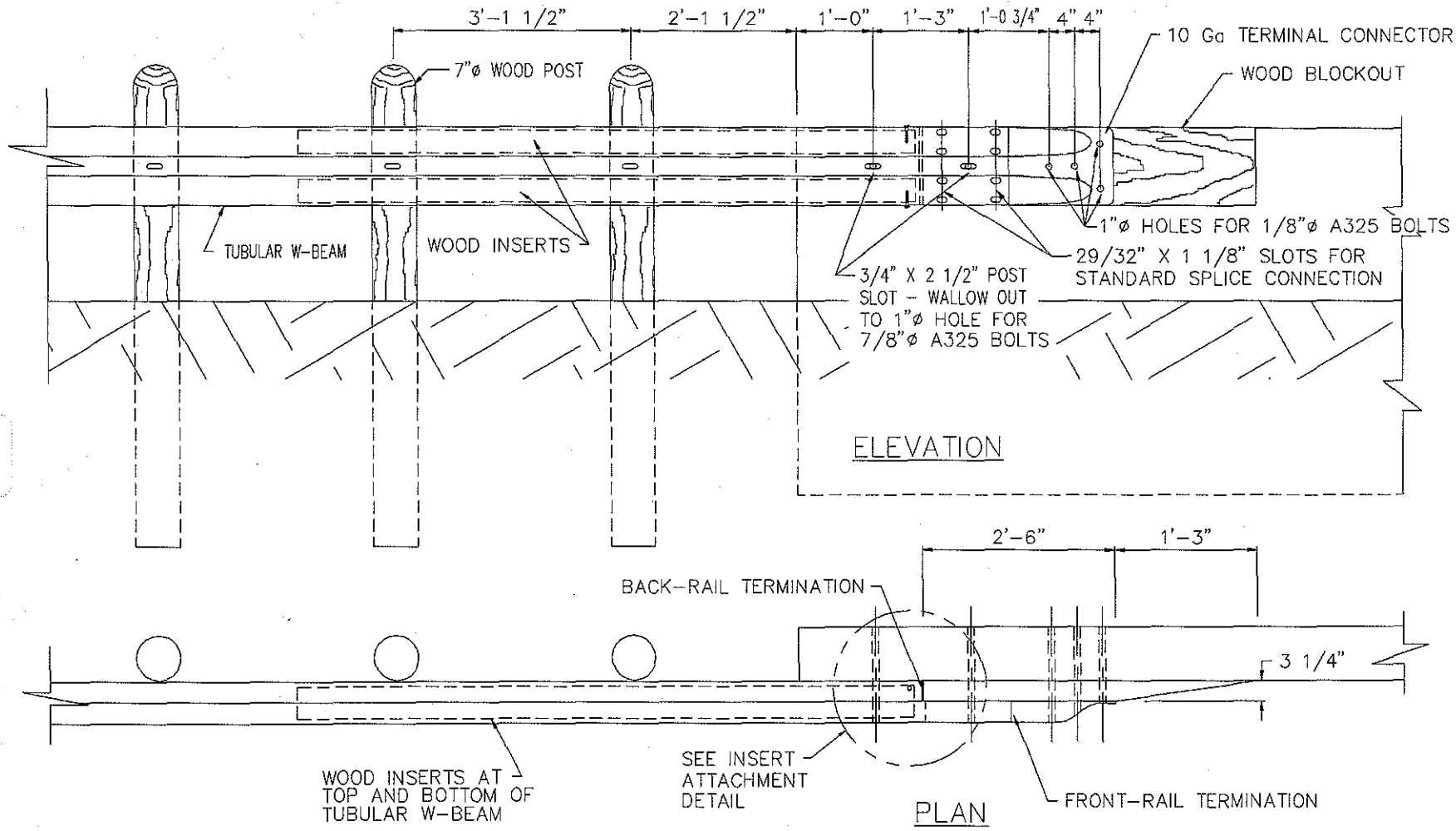

FIGURE F-2. TUBULAR W-BEAM CONNECTION TO VERTICAL WALL FOR RETROFIT INSTALLATION

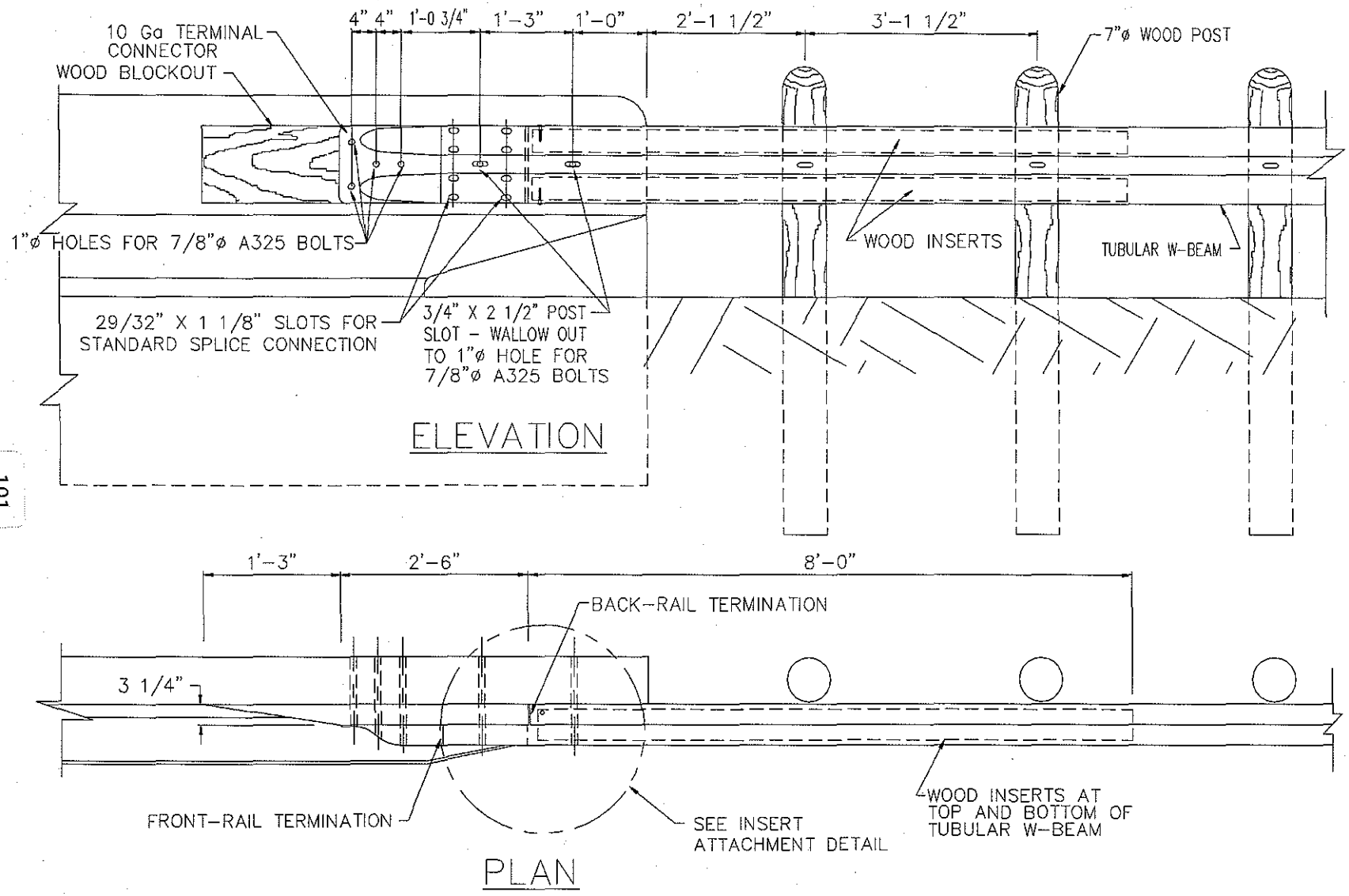

FIGURE F-3. TUBULAR W-BEAM CONNECTION TO SAFETY SHAPE FOR RETROFIT INSTALLATION

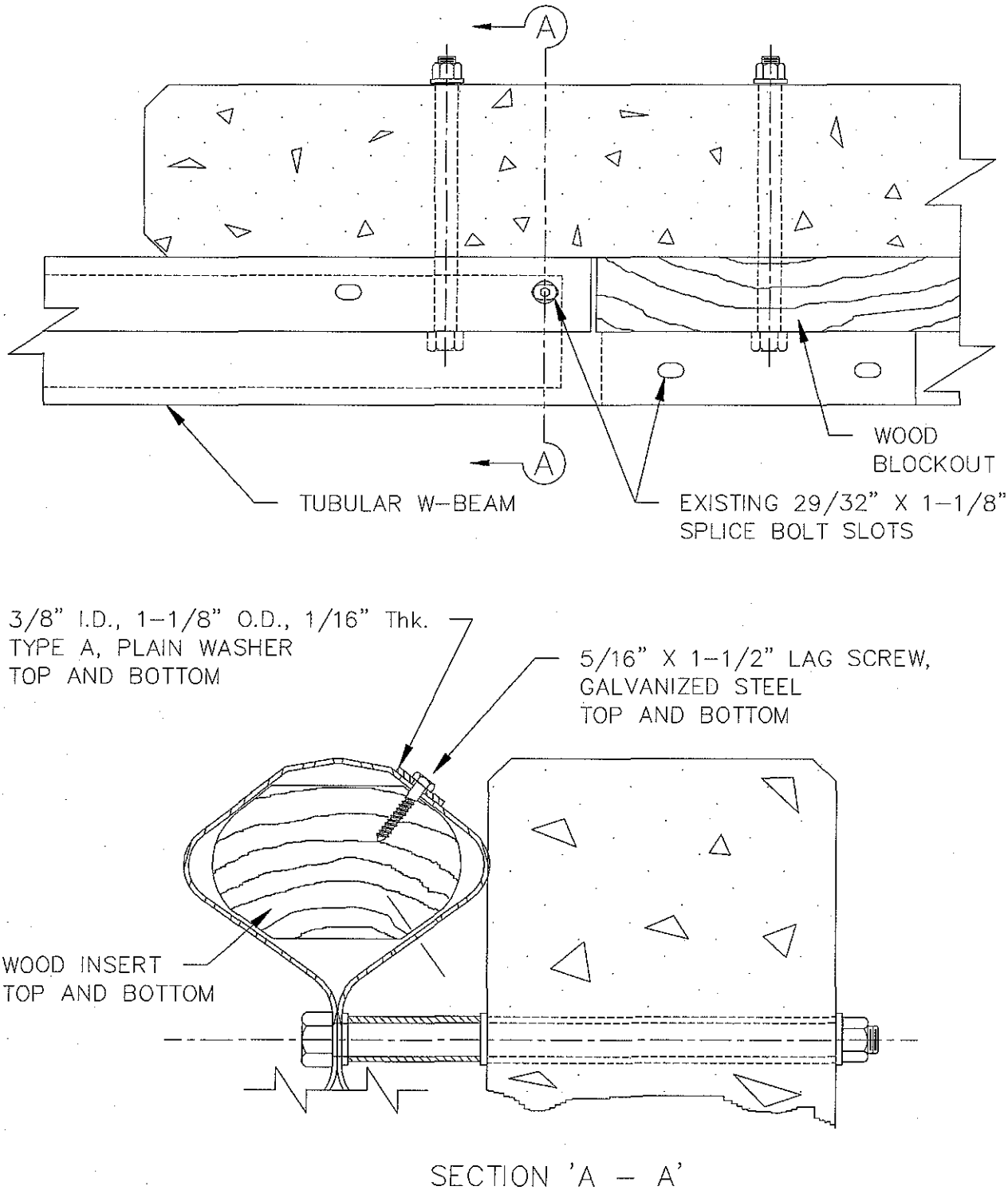

FIGURE F-4. WOOD INSERT ATTACHMENT DETAILS FOR RETROFIT INSTALLATION

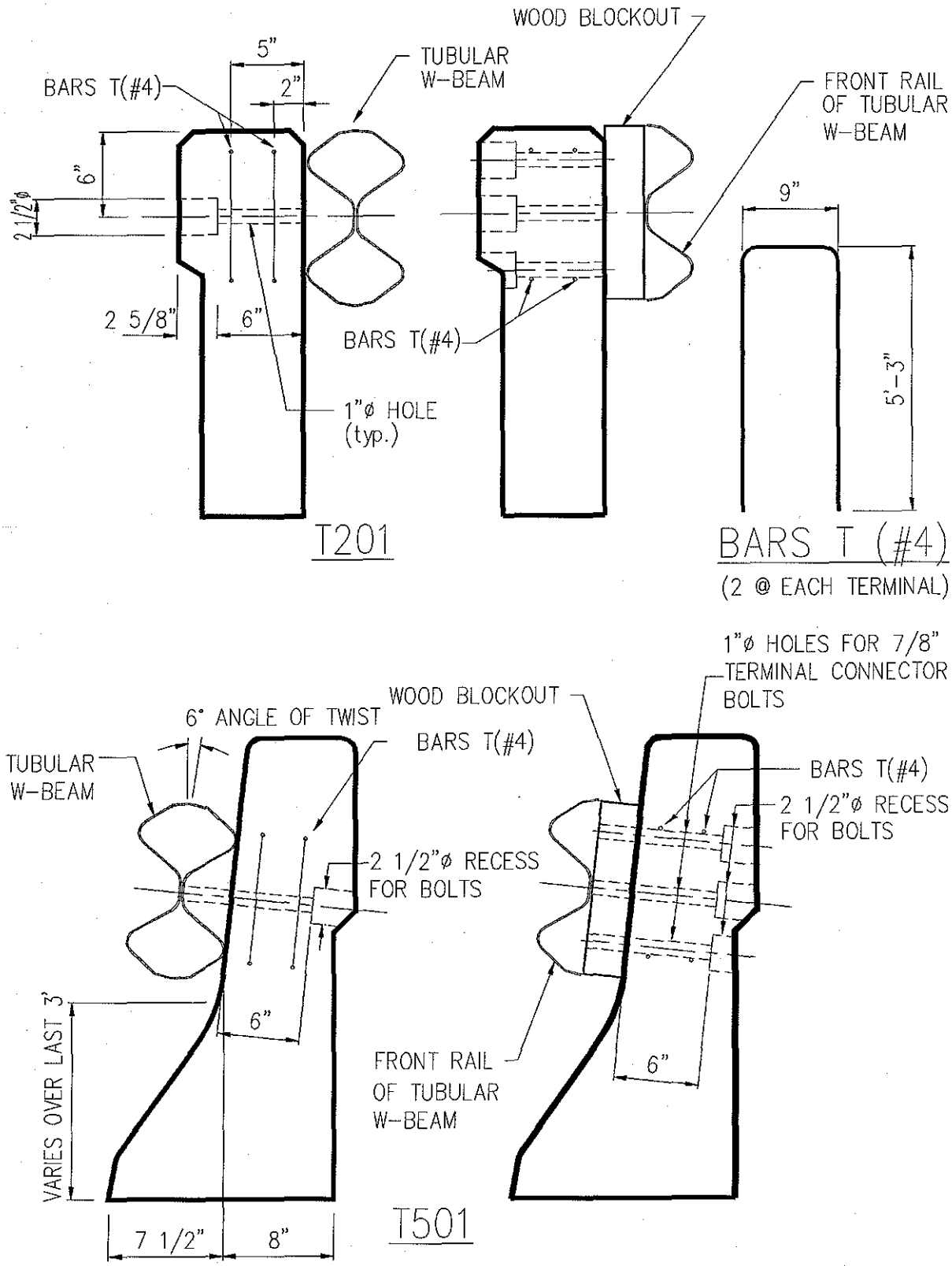

FIGURE F-5. TERMINAL CONNECTION DETAILS FOR RETROFIT INSTALLATION

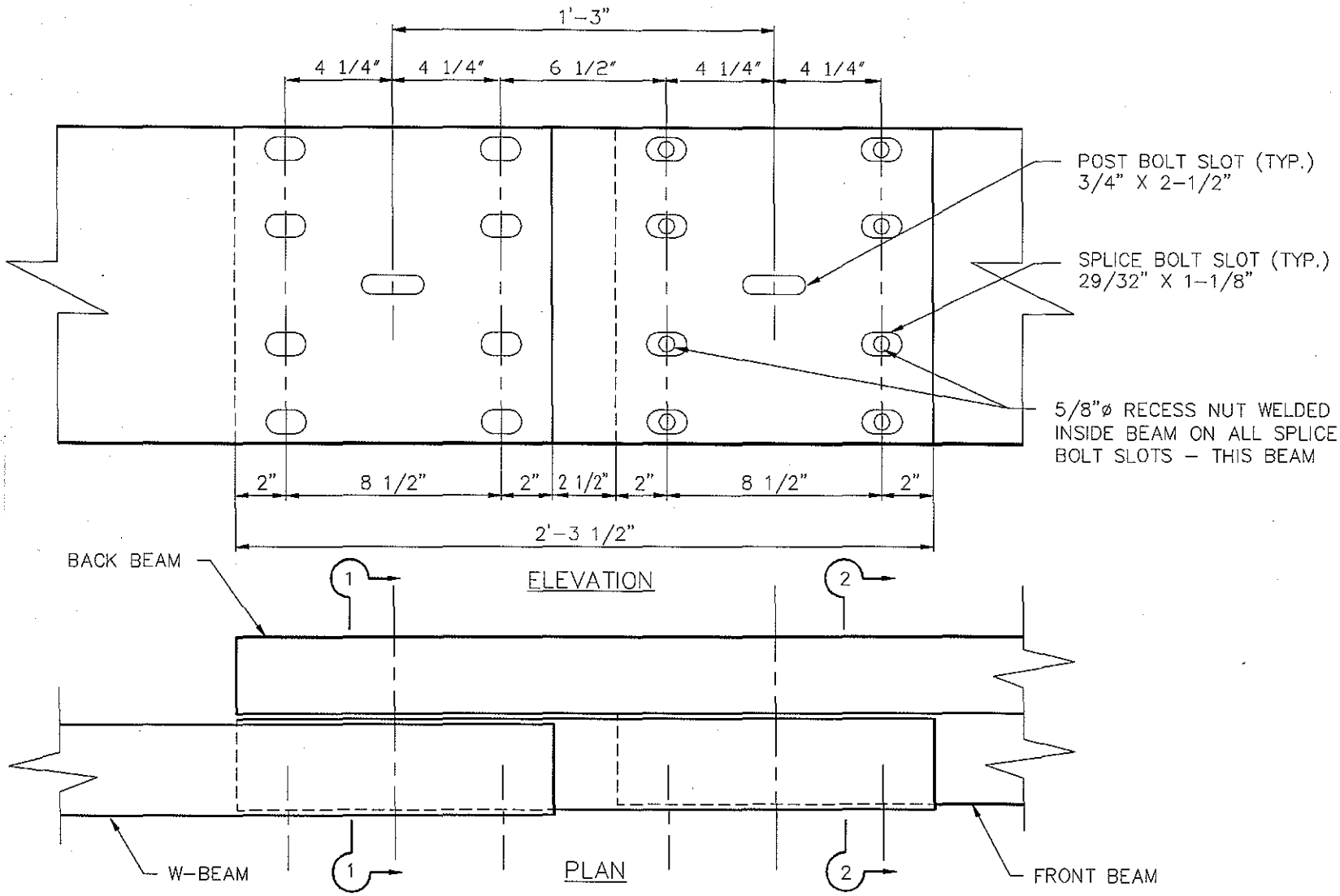

FIGURE F-6. LAP SPLICE DETAILS FOR RETROFIT INSTALLATION

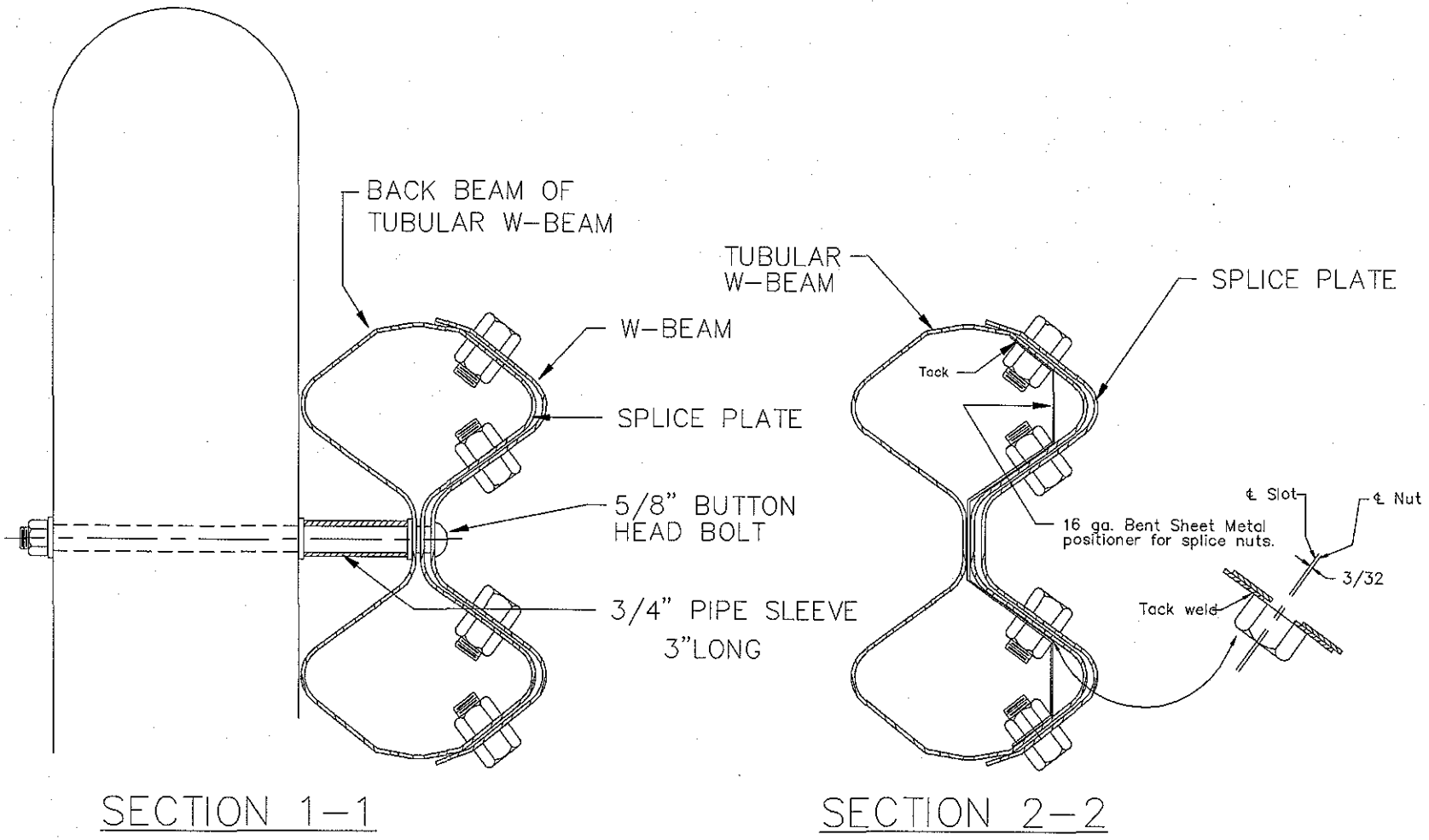

FIGURE F-6. CONTINUED

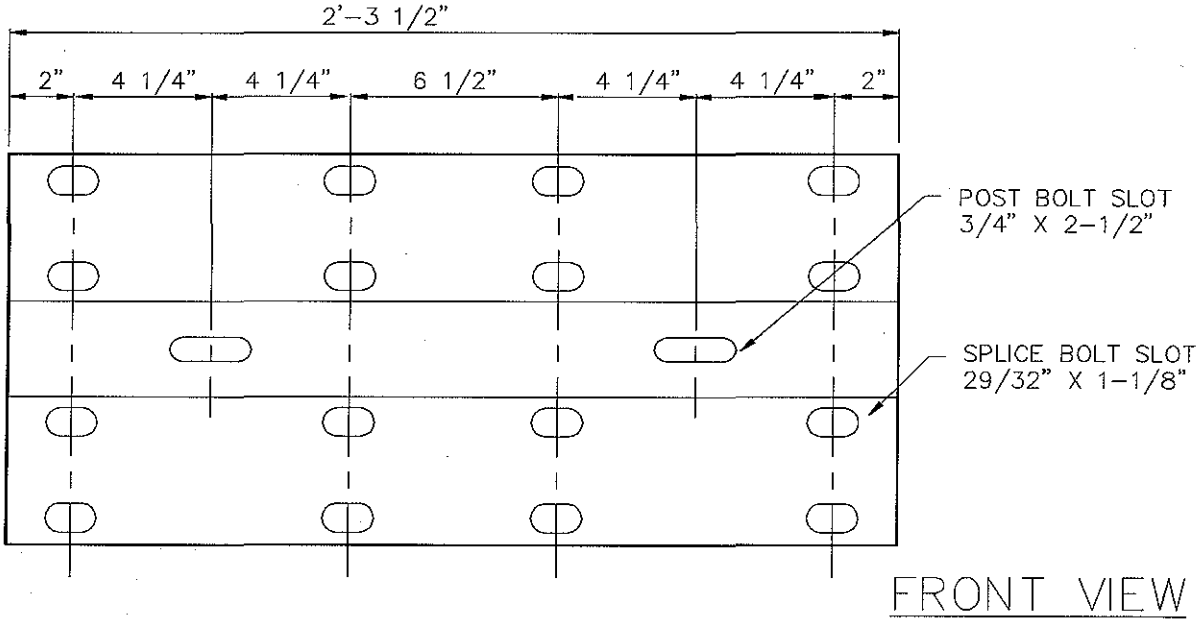

FRONT VIEW

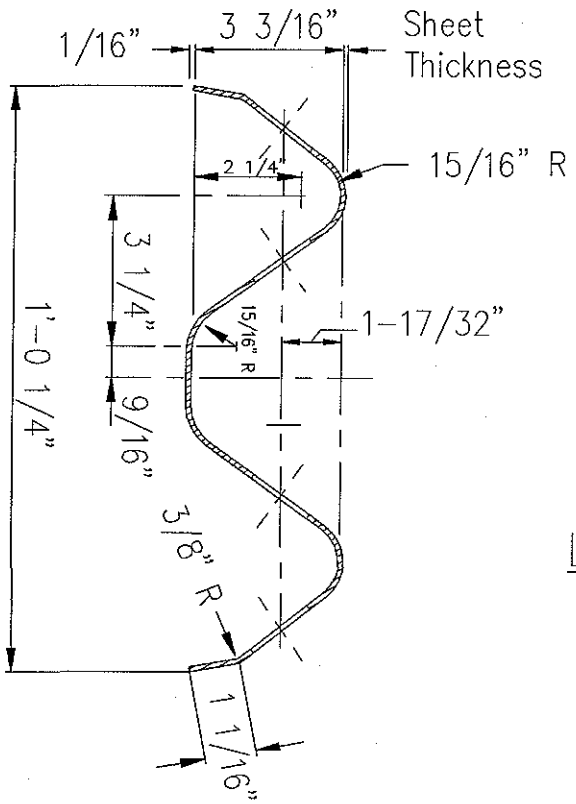

LEFT SIDE VIEW

FIGURE F-6. CONTINUED

APPENDIX G

CONSTRUCTION DRAWINGS FOR NEW CONSTRUCTION TRANSITION INSTALLATION

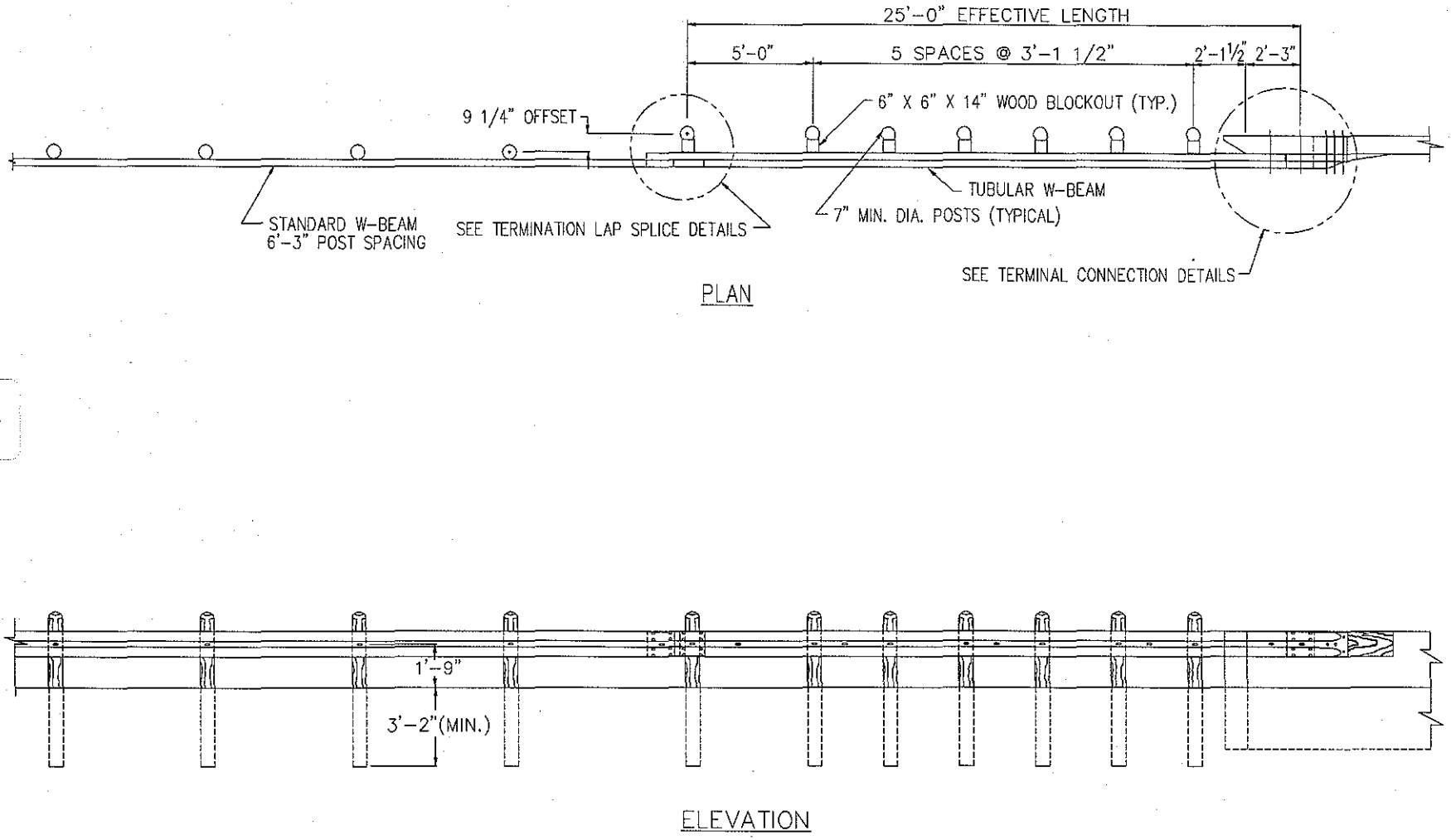

FIGURE G-1. TUBULAR W-BEAM TRANSITION FOR NEW CONSTRUCTION INSTALLATIONS

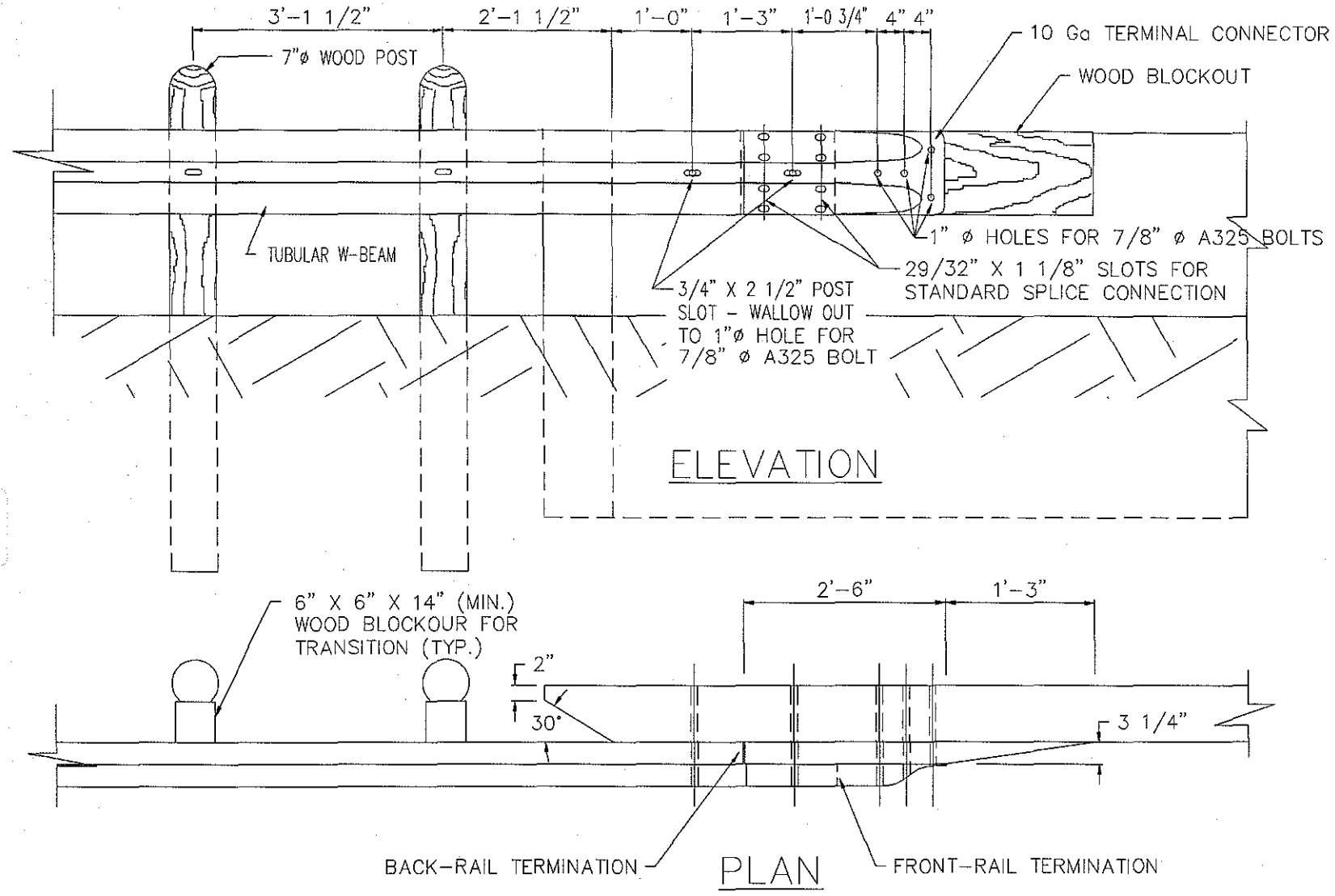

FIGURE G-2. TUBULAR W-BEAM CONNECTION TO VERTICAL WALL FOR NEW CONSTRUCTION INSTALLATIONS

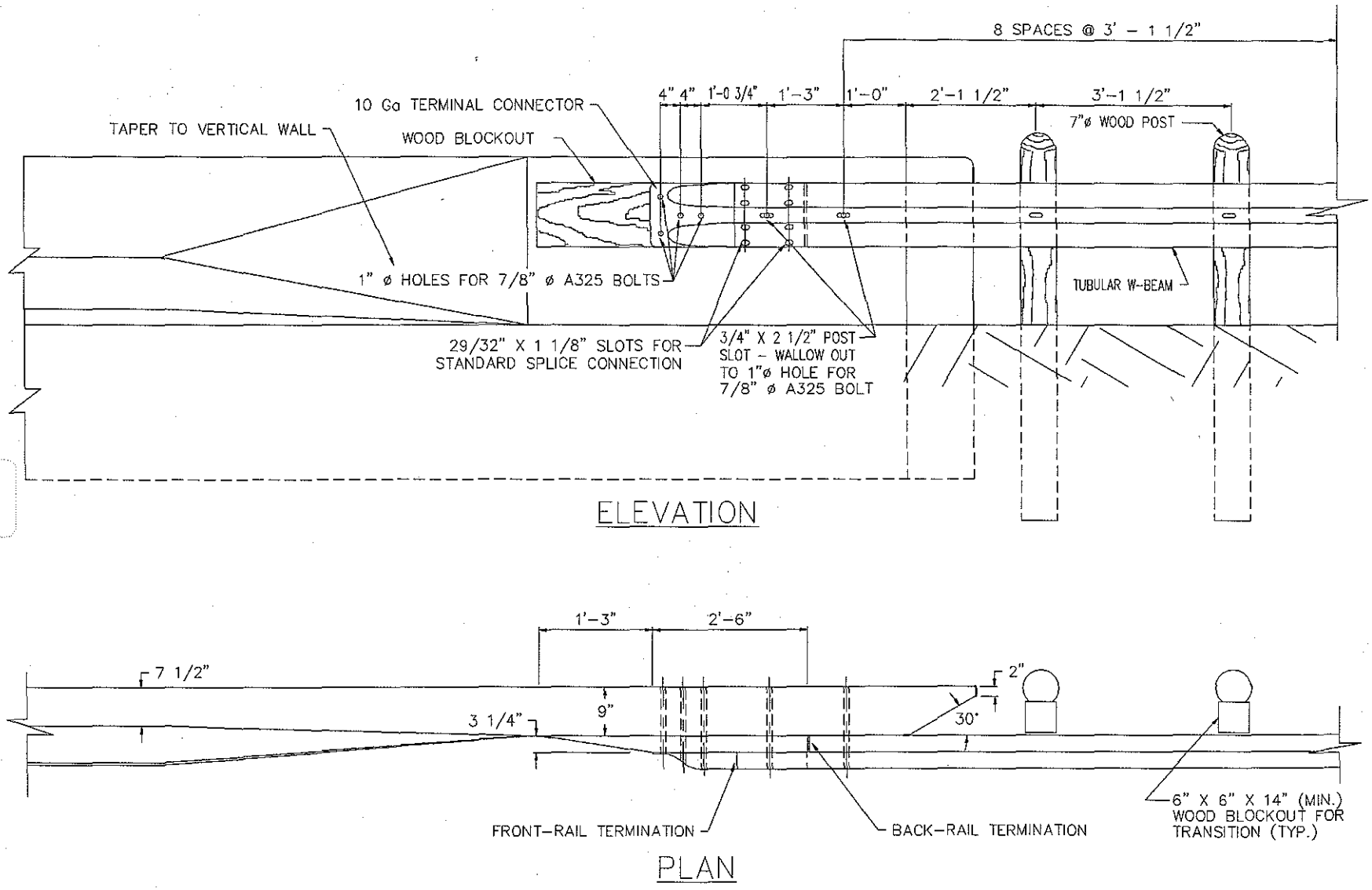

FIGURE G-3. TUBULAR W-BEAM CONNECTION TO SAFETY SHAPE FOR NEW CONSTRUCTION INSTALLATIONS

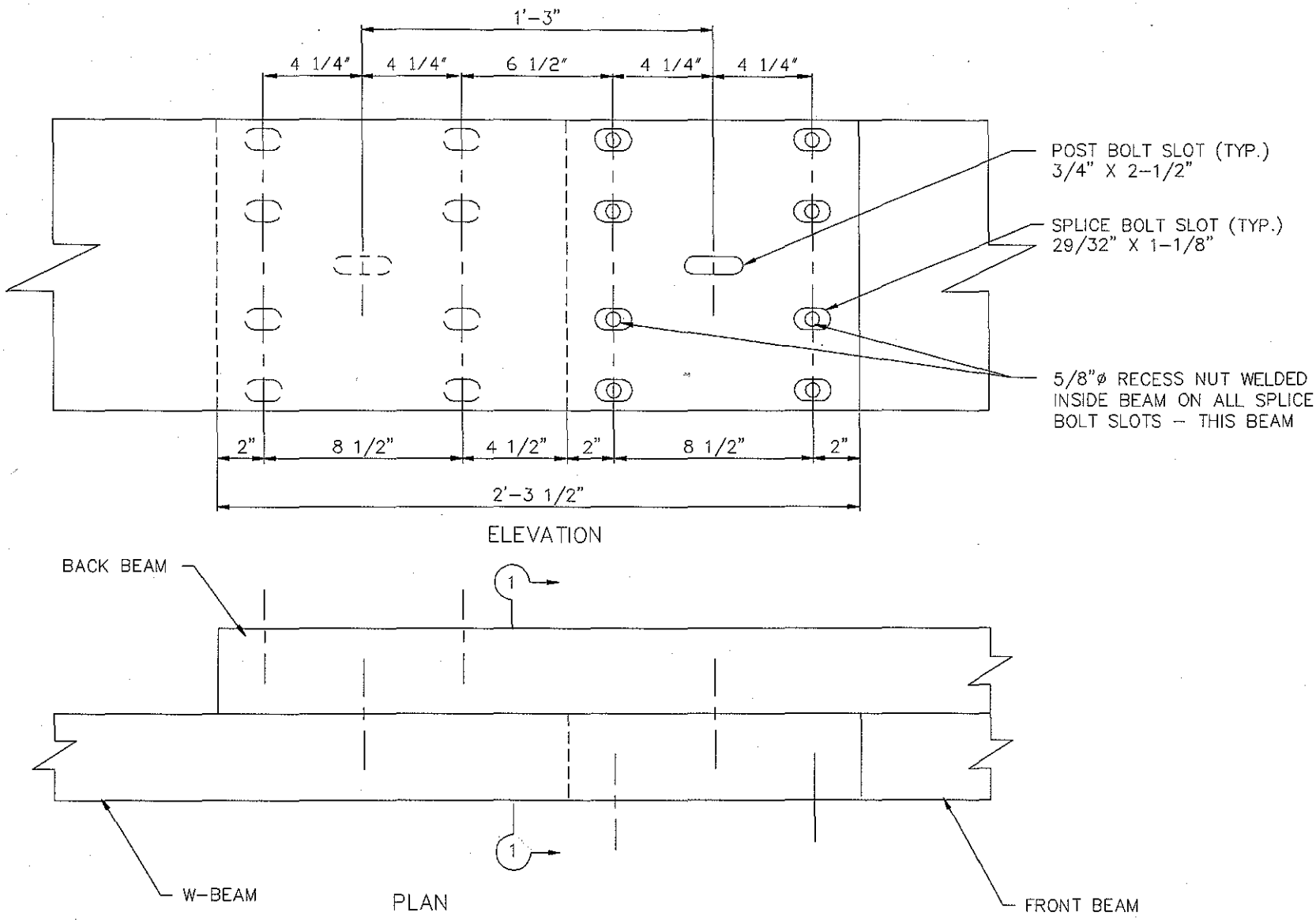

FIGURE G-4. LAP SPLICE DETAILS FOR NEW CONSTRUCTION INSTALLATIONS

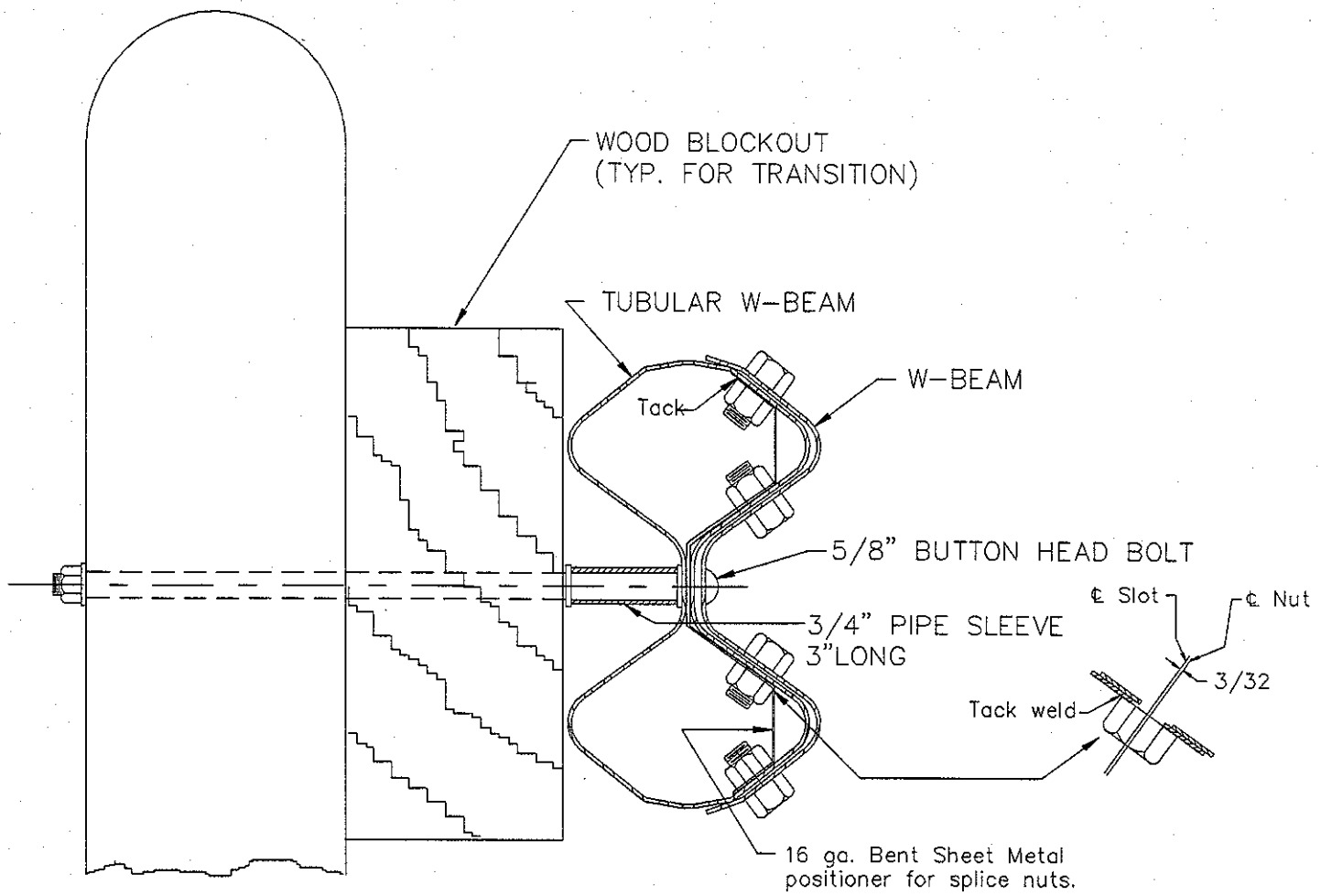

SECTION 1 – 1

FIGURE G-4. CONTINUED

APPENDIX H

DRAWINGS FOR SHORT-RADIUS GUARDRAIL TREATMENT

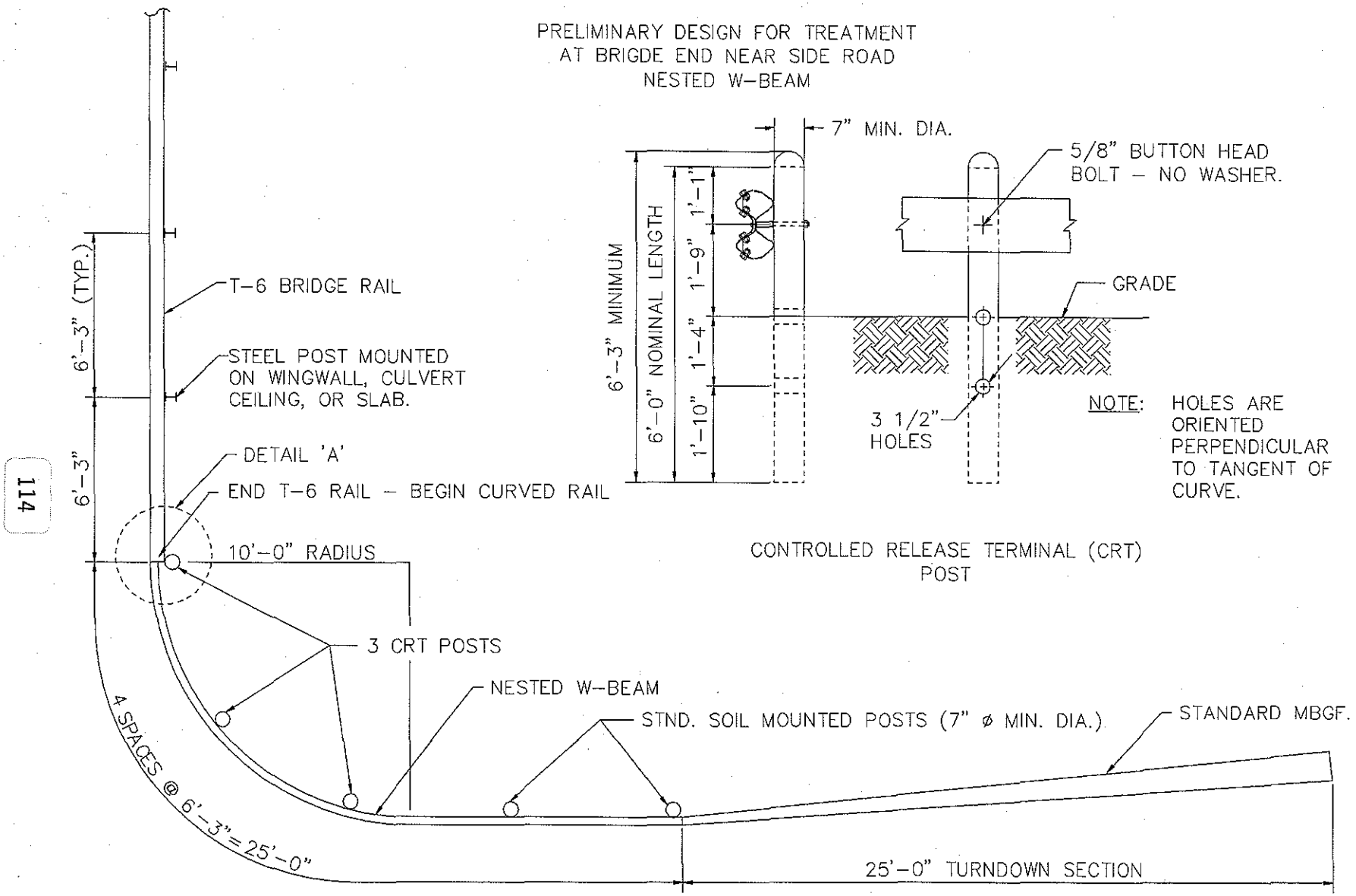

FIGURE H-1. SHORT-RADIUS GUARDRAIL TREATMENT, NESTED W-BEAM

DETAIL 'A'
TUBULAR W-BEAM TO NESTED W-BEAM CONNECTION

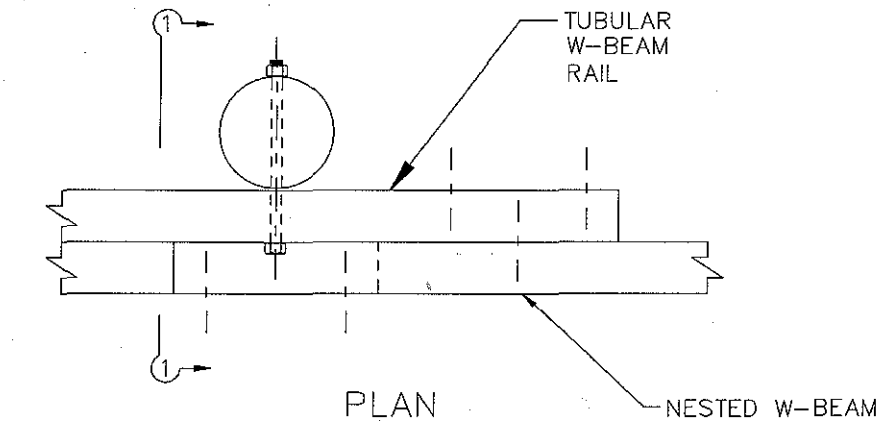

PLAN

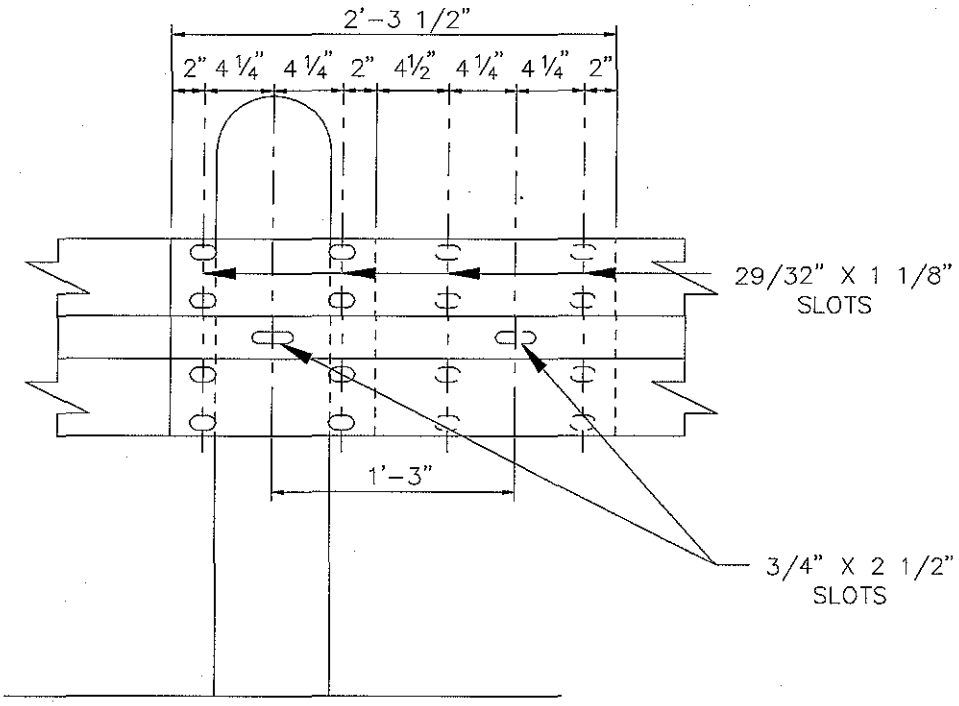

ELEVATION

NOTE: LAP BEAMS IN DIRECTION OF TRAFFIC.

FIGURE H-2. TUBULAR W-BEAM TO NESTED W-BEAM CONNECTION

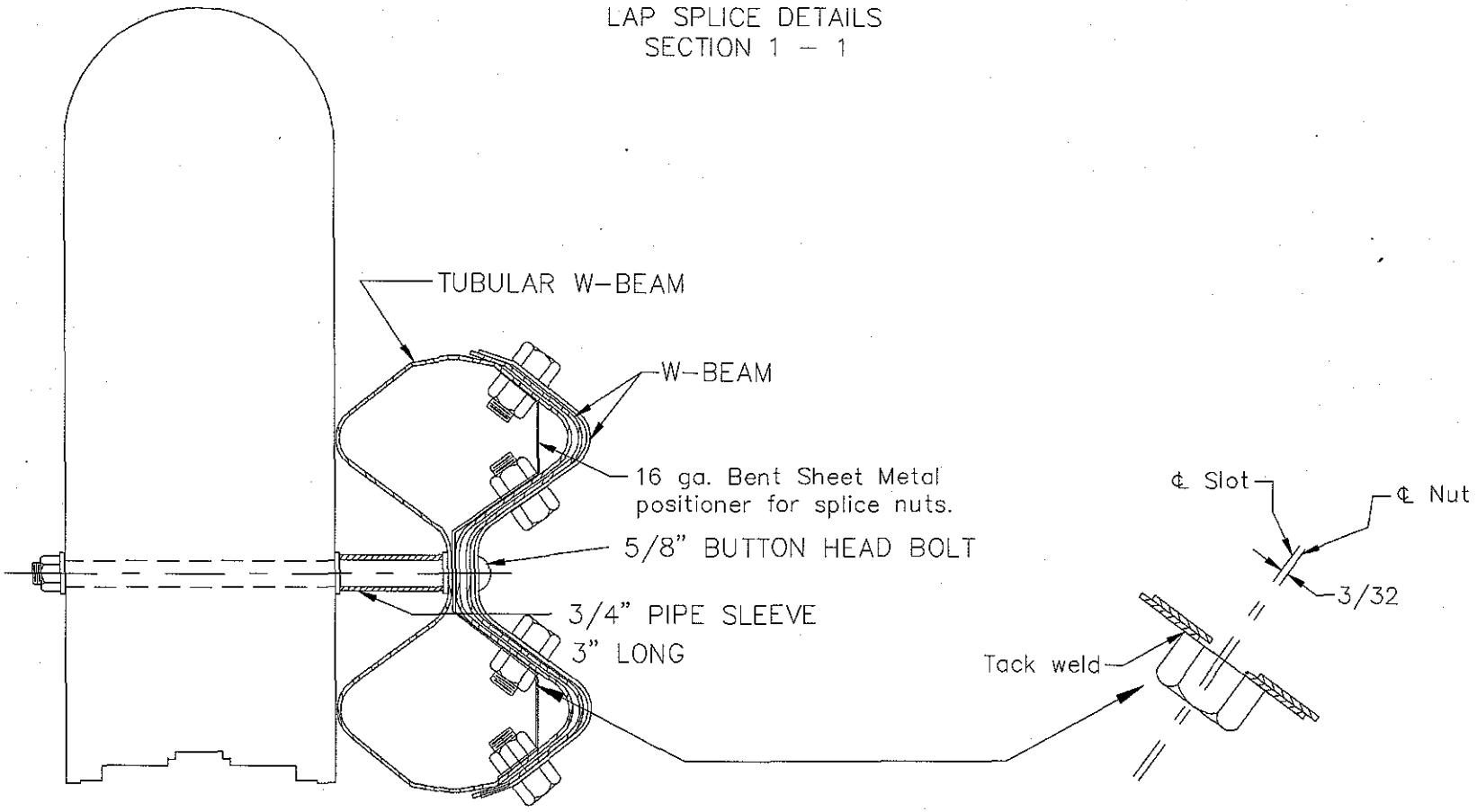

NOTE: 8~5/8" Splice nuts shall be tacked inside front rail of Tubular W–Beam. The nuts must be tacked approx. 3/32" off the center of the bolt slot toward the outside of the tube. Optionally, the nuts may be tacked to a bent sheet metal positioner as shown. Other suitable positioning methods or devices may be substituted. The complete splice shall have 8 bolts

FIGURE H-2. CONTINUED

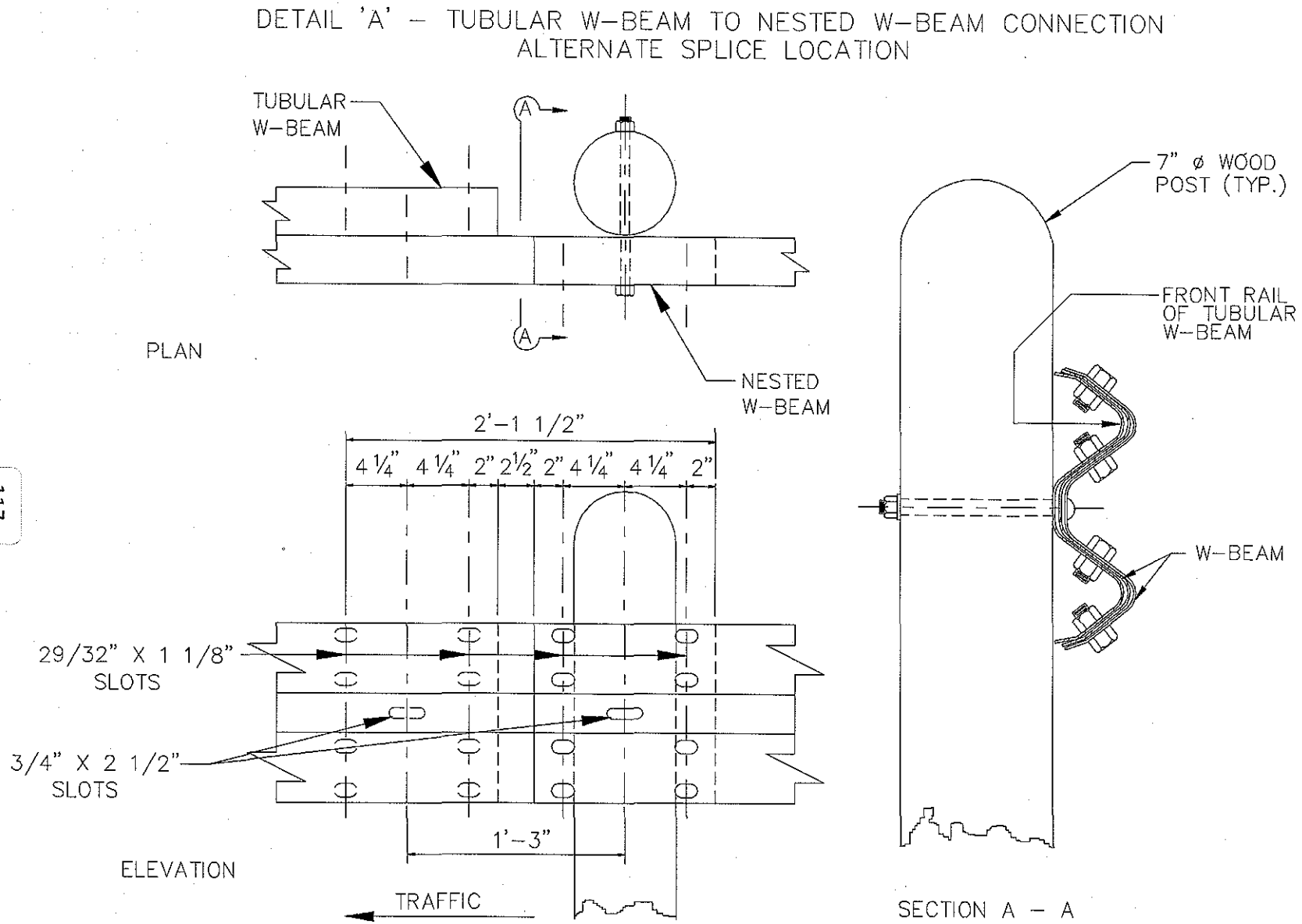

FIGURE H-3. ALTERNATE TUBULAR W-BEAM TO NESTED W-BEAM SPLICE CONNECTION

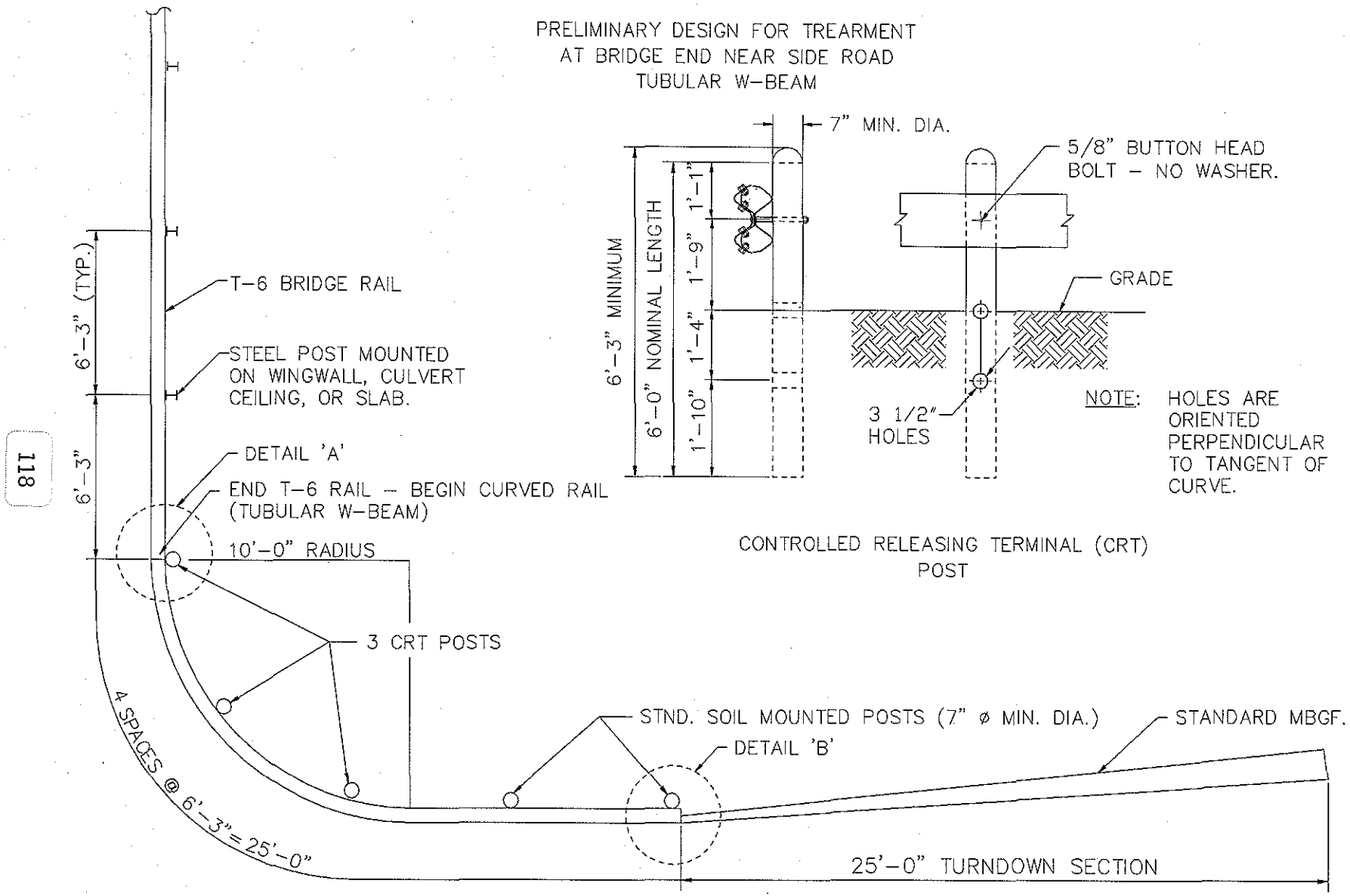

FIGURE H-4. SHORT-RADIUS GUARDRAIL TREATMENT, TUBULAR W-BEAM

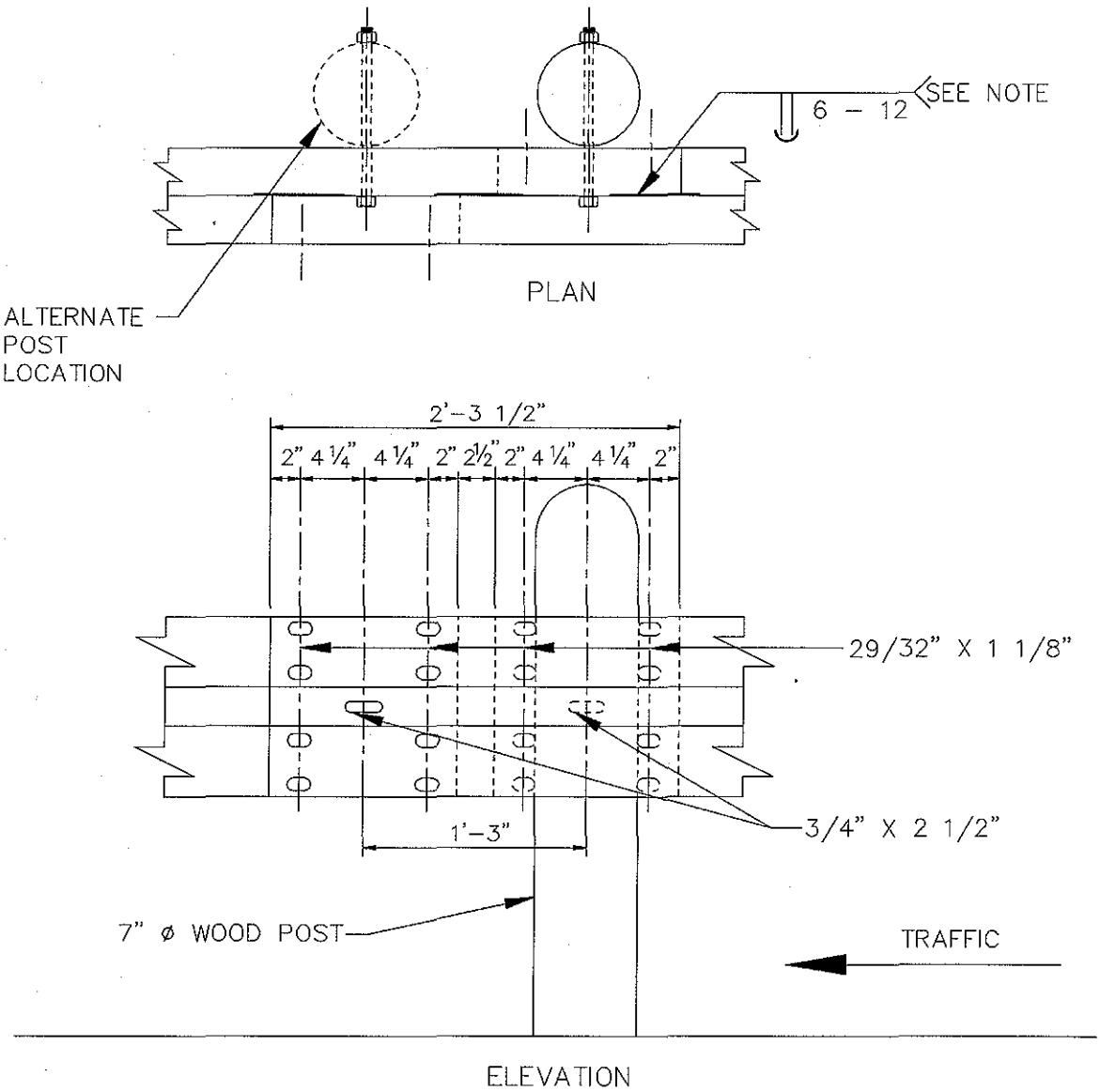

NOTE: Tubular W–Beam Rail Member is to be fabricated from standard 25' Nominal W–Beam sections. Additional post mounting slots are to be made in each member 15" from the standard slots at 6'–3" centers. Top and bottom seams shall be butt welded 6" at 12" spacing. Continuous seam welding is also acceptable.

FIGURE H-5. TUBULAR W-BEAM LAP SPLICE

DETAIL 'B'
TUBULAR W-BEAM TO W-BEAM CONNECTION

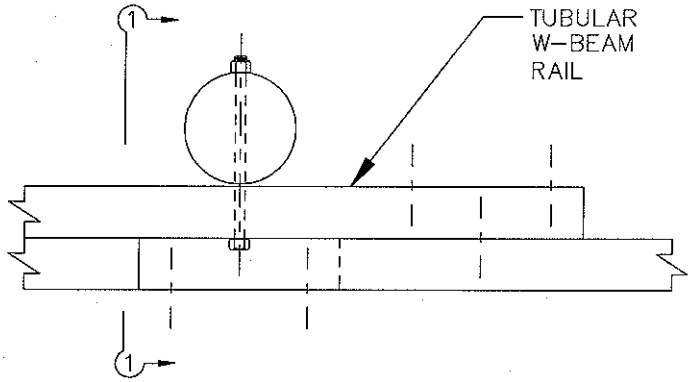

PLAN

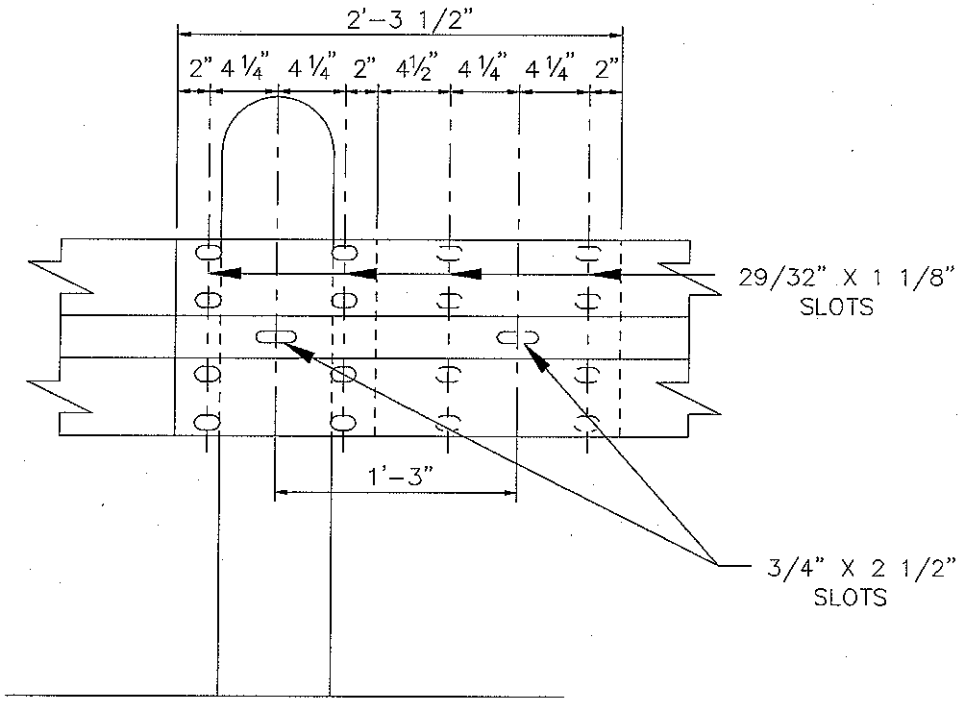

ELEVATION

NOTE: LAP BEAMS IN DIRECTION OF TRAFFIC.

FIGURE H-6. TUBULAR W-BEAM TO W-BEAM CONNECTION

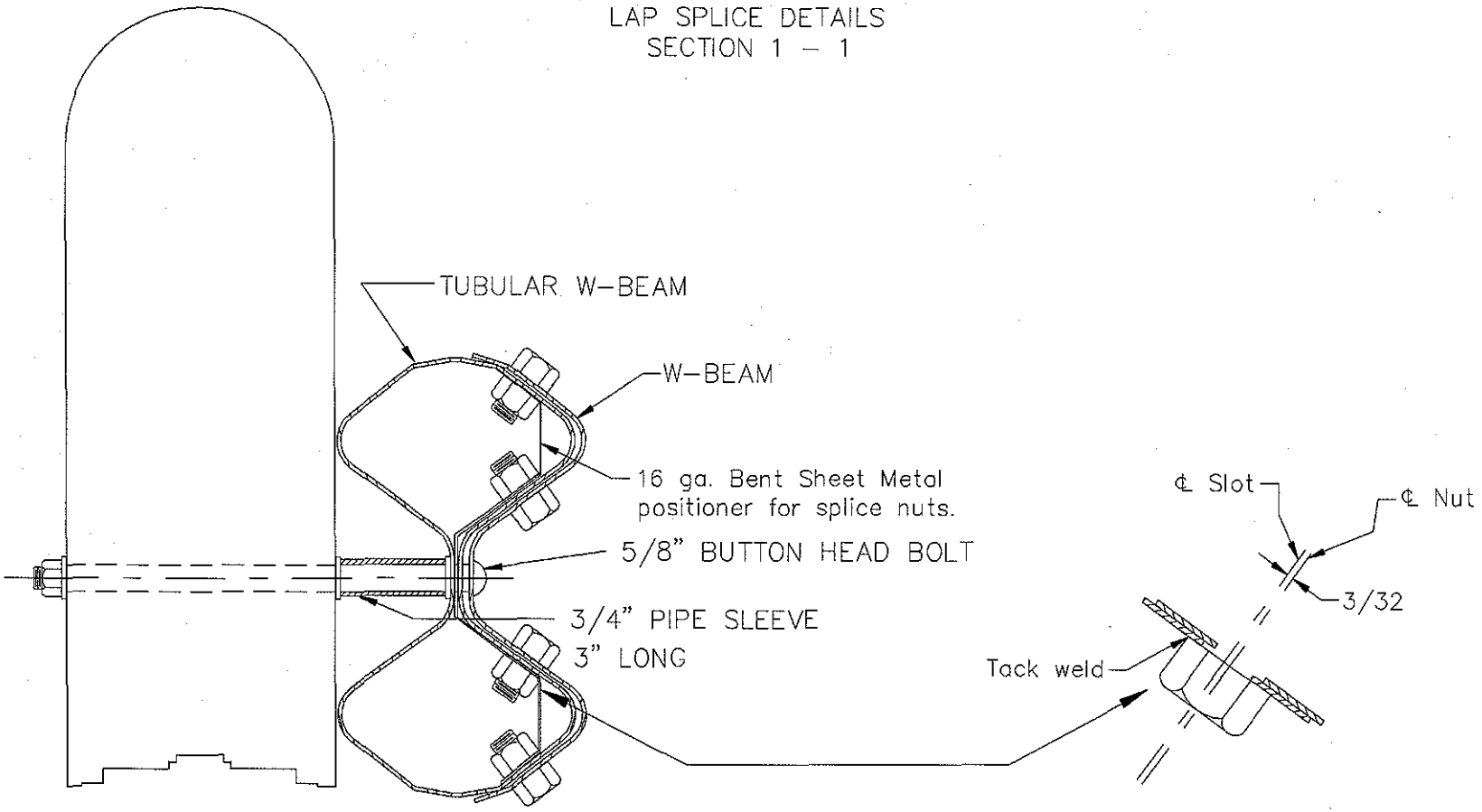

NOTE: 8~5/8" Splice nuts shall be tacked inside front rail of Tubular W–Beam. The nuts must be tacked approx. 3/32" off the center of the bolt slot toward the outside of the tube. Optionally, the nuts may be tacked to a bent sheet metal positioner as shown. Other suitable positioning methods or devices may be substituted. The complete splice shall have 8 bolts

FIGURE H-6. CONTINUED

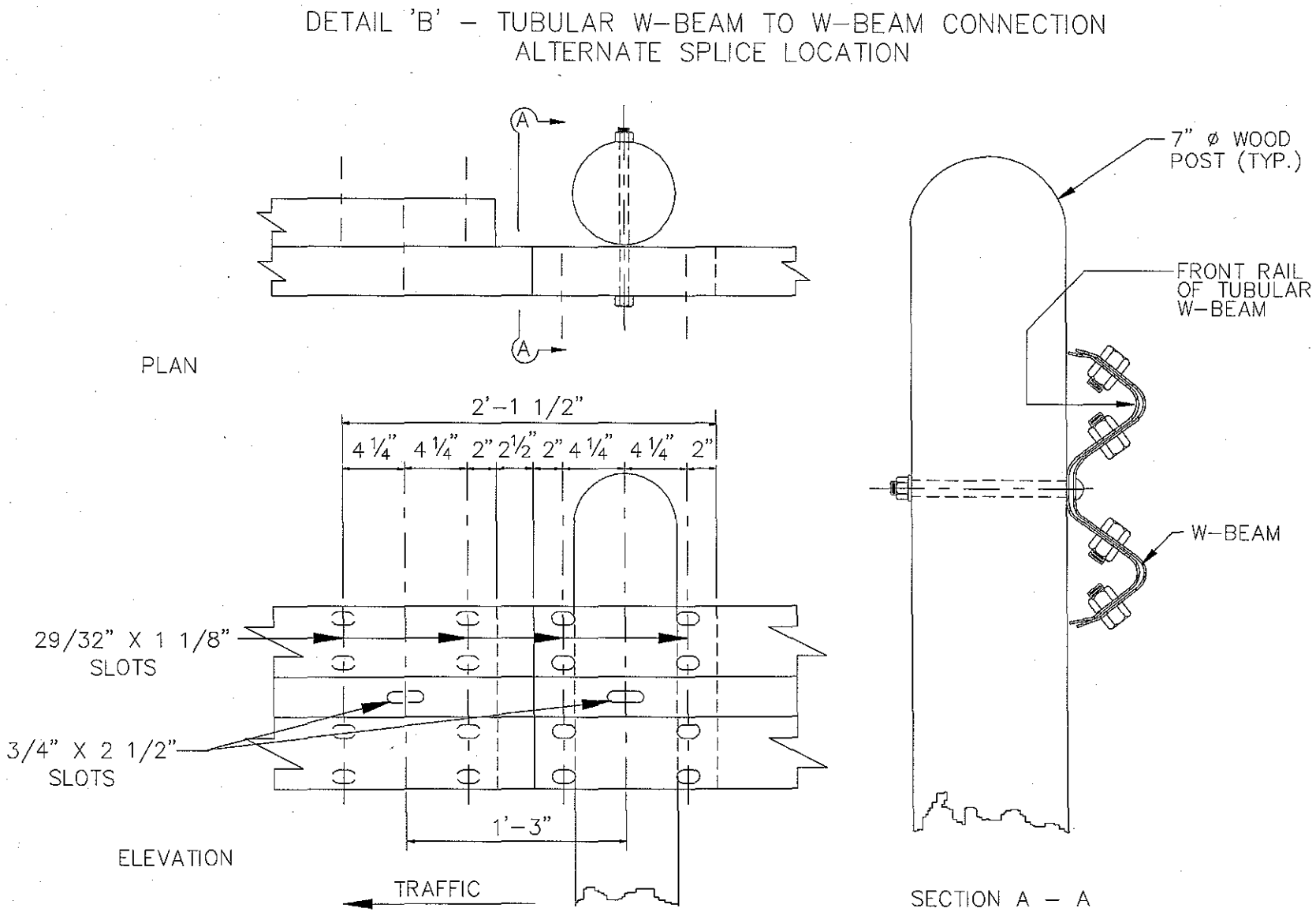

FIGURE H-7. ALTERNATE TUBULAR W-BEAM TO W-BEAM SPLICE CONNECTION